

ANALYSIS OF SLIP TRANSFER IN TI-5AL-2.5 (WT. %) AT TWO TEMPERATURES IN  
COMPARISON TO PURE ALUMINUM

By

Chelsea M. Edge

A THESIS

Submitted to  
Michigan State University  
in partial fulfillment of the requirements  
for the degree of

Material Science and Engineering – Master of Science

2020

## **ABSTRACT**

### **ANALYSIS OF SLIP TRANSFER IN TI-5AL-2.5 (WT. %) AT TWO TEMPERATURES IN COMPARISON TO PURE ALUMINUM**

By

Chelsea M. Edge

Understanding the deformation mechanisms present near grain boundaries in polycrystalline hexagonal alloys will aid in improving modeling methods. Ti-5Al-2.5Sn samples were tensile tested at 296K and 728K, and slip behavior was assessed near grain boundaries. From the EBSD measurements of grain orientations, various metrics related to the slip systems, traces, residual Burgers vectors, and grain boundary misorientation were computed for boundaries showing evidence of slip transfer and boundaries showing no evidence of slip transfer. This work is compared to a similar study of an Aluminum oligo-crystal to aid in understanding the differences in slip behavior near grain boundaries in HCP and FCC crystal structures. Slip transfer in Ti525 was generally observed in less geometrically compatible conditions than Al, and slip transfer occurs at high misorientation angles in Ti-5Al-2.5Sn much more frequently than in Al.

## **AKNOWLEDGEMENTS**

First, I would like to thank my advisor, Dr. Thomas R. Bieler, for his continued support throughout my two years at Michigan State University. He taught me most of what I know about crystallography, and the processes used to further understand how materials behave. His previously developed code in Matlab, was the building block for my research, and his patience in helping me understand it was pivotal to my work. Dr. Bieler created a space for us to have open discussions about science and his approachability made for a great learning environment.

I would also like to thank Dr. Phillip Eisenlohr for his invaluable insights, specifically regarding programming. He provided a critical role in helping me understand dislocations and other crystallographic topics. His detailed technical support and knowledge greatly improved the quality of the work presented.

I would also like to express my gratitude toward my committee member Dr. Carl Boehlert, for his participation in my thesis discussion, and constructive criticism he has provided to complete the work. In addition, Dr. Per Askeland was a great help to me with the completion of EBSD analysis and use of the SEMs.

Additionally, I would like to thank Hongmei Li, whom I have not met, but know through her work on Titanium alloys, which inspired this project.

I would also like to thank the team of graduate students within the metals group that sacrificed their time to help me with my work and understanding of concepts. Specifically, David Hernandez Escobar for his help with EBSD analysis and Harsha Phukan for his help on understanding crystallography.

Finally, I would like to express my deepest gratitude to my family, friends, and Alex, for their constant support and encouragement throughout the course of this endeavor.

# TABLE OF CONTENTS

<b>LIST OF TABLES</b> .....	<b>vii</b>
<b>LIST OF FIGURES</b> .....	<b>viii</b>
<b>KEY TO ABBREVIATIONS</b> .....	<b>xii</b>
<b>Chapter 1: Introduction</b> .....	<b>1</b>
1.1 Rationale and research objective .....	1
<b>Chapter 2: Literature Review</b> .....	<b>3</b>
2.1 Fundamentals of Titanium alloys .....	3
2.1.1 Titanium allotropes .....	3
2.1.2 Dislocations .....	3
2.1.3 Crystal Structure .....	4
2.1.4 Deformation mechanisms .....	5
2.2 Dislocations and slip transfer across grain boundaries .....	6
2.2.1 Slip transmission .....	6
2.2.2 Metrics used to analyze slip transfer .....	8
2.3 Previous work .....	12
2.3.1 Titanium .....	12
2.3.2 Aluminum .....	12
2.3.3 Aluminum and Titanium Crystal structure differences .....	13
<b>Chapter 3: Experimental Procedure</b> .....	<b>15</b>
3.1 Material .....	15
3.2 Mechanical testing .....	15
3.2.1 Sample preparation .....	15
3.2.2 Test set up .....	16
3.2.3 Tensile Test Results .....	17
3.3 Microstructural Observations .....	18
3.3.1 Orientation evaluation .....	19
3.4 Grain pair analysis .....	21
3.4.1 Slip transfer .....	21
3.4.2 Slip transfer analysis .....	30
<b>Chapter 4: Results</b> .....	<b>33</b>
4.1 Misorientation angle histogram .....	33
4.2 Metric combinations .....	35
4.3 Misorientation angle vs. $m'$ .....	37
4.4 $m'$ vs. residual Burgers vector ( $\Delta b$ ) .....	38
4.5 Misorientation angle vs. the sum of the Schmid factors .....	40
4.6 Misorientation angle vs. $m'/\Delta b$ .....	43
4.7 Slip systems present .....	45

<b>Chapter 5: Discussion</b> .....	<b>52</b>
5.1 $m'$ vs. $\Delta b$ .....	52
5.2 Misorientation angle vs. $m'$ .....	55
5.3 Misorientation angle vs. the sum of Schmid factors .....	57
5.4 Misorientation angle vs. $m'/\Delta b$ .....	58
5.5 Slip system analysis .....	60
5.6 Comparison between measured weakly textured grain orientations to random populations .....	62
<b>Chapter 6: Summary and conclusions</b> .....	<b>69</b>
6.1 Summary .....	69
6.2 Conclusions .....	69
6.3 Future work suggestions.....	71
<b>APPENDICES</b> .....	<b>72</b>
APPENDIX A: Matlab hexagonal orientation code (written by Thomas R. Bieler) .....	73
APPENDIX B: Matlab MPR hexagonal grain pair analysis code (written by Thomas R. Bieler) .....	83
APPENDIX C: Sample reconstructed boundary and grain files.....	99
<b>BIBLIOGRAPHY</b> .....	<b>101</b>

## **LIST OF TABLES**

Table 3.1: Measured composition of polycrystal Ti525 (Li, 2013).....	15
Table 3.2: Ti525 tensile properties obtained from room temperature and high temperature tensile tests (Li, 2013). .....	18
Table 3.3: $m'/\Delta b$ table for slip system combinations and associated Schmid factor. High $m'/\Delta b$ values in the upper left-hand corner of the table indicates the slip system pair that is most likely transmitting slip. ....	25
Table 3.4: Comparison of random poll of data from each sample, and the number/percentages of the fully analyzed GBs used in the analysis.....	31
Table 5.1: Percentages of “slip transfer” and “no slip transfer” inside and outside of boundaries, respectively. RT and HT Ti5252 relationships are flipped with high percentage of “no slip transfer” outside of the box in RT and high percentage of “slip transfer” inside the box for HT. ....	53
Table 5.2: Temperature comparison for Al and Ti525. RT Al and HT Ti525 have similar homologous temperatures. ....	54
Table 5.3: Compensated Strengths and values used to obtain them. The pure aluminum compensated strength is much lower than the Titanium alloy (Aluminum 1100-O and Li 2013). .....	55

## LIST OF FIGURES

Figure 1.1: Schematic of a turbo pump showing where Ti525 is commonly used. The highlighted area points toward the part in the turbo pump that is typically Ti525 (Sutton, 2017). .....	2
Figure 2.1: (a) Dislocation present within the Burgers circuit. (b) Burgers vector (purple arrow) from c to b in a perfect crystal. ....	4
Figure 2.2: Hexagonal crystal structure with shaded area indicating different types of slip planes. The purple line represents the $\langle 2110 \rangle$ direction in which prism, basal and pyramidal planes can slip. The orange line represents the $\langle 1213 \rangle$ direction in which pyramidal planes can slip. ....	5
Figure 2.3: Slip traces interacting with a grain boundary. Focusing on case (b), the dislocations are transmitted from grain 1 into grain 2, and a residual part of the dislocation in grain 1 is retained in the grain boundary (Bayerschen, 2016). ....	7
Figure 2.4: Representation of slip planes (in blue and green) and the angles associated with them used to calculate various factors (Abuzaid, 2016). ....	8
Figure 2.5: Representation of slip in a cylindrical crystal and the associated angles describing the slip plane and slip direction used to compute the Schmid factor. ....	10
Figure 3.1: Geometry of tensile samples electro-discharge machined out of Ti525 (Li, 2013). ..	16
Figure 3.2: Tensile test set up within the Tescan Mira3 SEM (Li, 2013). ....	17
Figure 3.3: Stress vs. displacement curve for the room temperature (296K) and high temperature (728K) samples. Load drops are stress relaxation points when the test was paused for imaging (Li, 2013). ....	18
Figure 3.4: SEM image showing the microstructure of (a) the 296K and (b) the 728K tensile tested Ti525 sample with fiduciary mark. ....	19
Figure 3.5: EBSD IPF map of the deformed Ti525 tensile samples. The intentional scratch is the fiduciary mark, which is visible in the IPF map for (b) the 728K sample, and is located out of the frame in (a) the 296K sample (black rectangular areas are eliminated data that have very small grains/questionable indexing). ....	20
Figure 3.6: $\{0001\}$ and $\{1010\}$ pole figures for (a) the 296K and (b) the 728K Ti525 samples. The black curved lines represent the $30^\circ$ cones along the major axis. The material has orientations that are around 3 times random in both samples. (Li, 2013). ....	21

Figure 3.7: Computed slip system possibilities and corresponding slip traces for (a) the left grain and (b) the right grain, drawn in actual orientation present in the grain.....	23
Figure 3.8: Comparison of computed slip traces and observed slip traces in the SEM image.....	24
Figure 3.9: Calculated prisms of each grain drawn relative to each other.....	26
Figure 3.10: Topography at the grain boundary in (a) is small indicating that there is little to no heterogenous strain on either side. Topography at the grain boundary in (b) is large indicating that there is heterogenous strain on both sides.....	27
Figure 3.11: (a) The red arrows indicate an upward step sense in the grain (light slip traces in the lower part of grain 1 and dark traces in grain 2 and the upper corner of grain 1). (b) Sketch of cross section along the orange line showing opposite directional sense of shear (blue arrows). Though slip traces may appear to be correlated, their slip planes are far from parallel, indicating that slip transfer cannot account for the observed slip traces. ....	29
Figure 3.12: (a) Example of a grain boundary that is categorized as slip transfer, meaning that all five criteria are met. (b) Example of a grain boundary that is categorized as no slip transfer, meaning all five criteria for slip transfer were not met.....	30
Figure 3.13: Probability density (the integral is 1) for the Ti525 728K and 296K data, and McKenzie probability distribution data for randomly generated hexagonal crystal orientations.	32
Figure 4.1: Histograms representing the “slip transfer” and “no slip transfer” data for the (a) high temperature (728K) sample and (b) the room temperature (296K) sample, binned by misorientation angle. The slip transfer category for both samples have higher values at lower misorientation angles. ....	34
Figure 4.2: Possible combinations of factors, with correlations of interest including $m'$ and $\Delta b$ , $m'$ and misorientation angle, and $\Delta b$ and misorientation angle.....	36
Figure 4.3: $m'$ vs. misorientation angle for (a) the room temperature (296K) sample and (b) the high temperature (728K) sample. There is a decreasing trend for misorientation angles below $20^\circ$ in both samples. Above $20^\circ$ , the trend is no longer observed.....	38
Figure 4.4: $m'$ vs. the residual Burgers vector for (a) the room temperature (296K) Ti525 sample and (b) the high temperature (728K) sample. The cluster of “slip transfer” points, denoted with dotted lines, have high $m'$ parameters and low residual Burgers vectors. The dashed black lines represent the boundary where the maximum number of “slip transfer” and “no slip transfer” data are inside and outside of the box respectively. ....	40

Figure 4.5: The  $m'(SF_{LG}+SF_{RG})$  parameter vs. misorientation angle for (a) the room temperature (296K) Ti525 sample, and (b) the high temperature (728K) sample. High  $m'(SF_{LG}+SF_{RG})$  is noted for “slip transfer” data in both cases. There is a decreasing trend in “slip transfer” data below 30° misorientation angle. The “no slip transfer” data are mostly present above 30° misorientation angle..... 42

Figure 4.6:  $m'/\Delta b$  vs. misorientation angle for (a) the room temperature (296K) sample and (b) the high temperature (728K) sample. In both samples, a strong decreasing  $m'/\Delta b$  trend for ‘slip transfer’ data below 30° misorientation angle..... 44

Figure 4.7: “Slip transfer”  $m'/\Delta b$  vs. misorientation angle represented with computed slip systems for each grain pair in (a) the room temperature (296K) sample and (a) the high temperature (728K) sample. There is a cluster of prism<a> to prism<a> slip in grain pairs with misorientation angle less than 30° in the high temperature sample and between 15° and 30° in the room temperature sample..... 46

Figure 4.8: “No slip transfer”  $m'/\Delta b$  vs. misorientation angle represented with observed active slip systems for each grain pair for (a) the room temperature (296K) tensile tested sample and for (b) the high temperature (728K) tensile tested sample. Few clusters are observed in both data sets..... 48

Figure 4.9: Representation of slip systems prevalent in the high temperature (728K) and room temperature sample. The most prevalent slip system pair in the room temperature (296K) data is basal to prism. The slip system pair that shows up the least in all the data is pyramidal<c+a> to pyramidal<c+a>..... 50

Figure 5.1:  $m'$  vs.  $\Delta b$  data for the (a) room temperature (296K) and (b) the high temperature (728K) tensile tested Ti525 sample. Green boxes indicate comparable Al oligo-crystal tensile results at room temperature for both (a) and (b). ..... 53

Figure 5.2: Aluminum oligo-crystal “slip transfer” (blue shaded area) and “no slip transfer” (red shaded area) compared to data of the titanium polycrystal “slip transfer” and “no slip transfer” data for (a) the room temperature (296K) sample and (b) the high temperature (728K) sample. Titanium “slip transfer” and “no slip transfer” points do not follow as strict of a trend compared to the aluminum data..... 57

Figure 5.3: Misorientation angle vs.  $m'(SF_{LG}+SF_{RG})$  for the (a) room temperature Ti525 sample and the (b) high temperature Ti525 sample. The aluminum boundaries represented by the green line show the difference between the aluminum data set which has a steep slope and the titanium data set which slope is flatter. .... 58

Figure 5.4: Misorientation vs.  $m'/\Delta b$  for (a) the room temperature (296K) tensile test sample and (b) the high temperature (728K) sample. The red shaded area represents the aluminum oligo-

crystal “no slip transfer” data set. The blue shaded area represents the aluminum oligo-crystal “slip transfer” data set and line up with the slip transfer points in the titanium data sets. .... 60

Figure 5.5: Misorientation angle cumulative percentages for Ti525 and randomly generated data sets separated by type of slip system observed in the grains. Pyramidal slip is behaving counter-intuitively with respect to more restrictive conditions..... 64

Figure 5.6: Overall Ti525 statistics in comparison to a random population. Random population data sets have a high frequency for pyramidal<c+a> to pyramidal<c+a> where experimental results are low for the same category..... 65

Figure 5.7: Relative frequency of data represented as half-circles. Larger area half-circle represents a higher frequency. (a) Comparison of experimental Ti525 at room temperature and high temperature. (b) Comparison of randomly generated data sets ..... 66

Figure 5.8: Randomly generated orientation pairs with the most likely slip systems present that facilitates slip across the grain boundaries. (a) Unmodified Schmid factors. (b) Schmid factor for pyramidal<c+a> is halved. A high frequency is present in slip system pairs with pyramidal slip systems in both cases. .... 68

## KEY TO ABBREVIATIONS

Al	Aluminum
ASTM	American Society for Testing and Materials
BSE	Back scattered electron
CP	Commercially Pure
CPFE	Crystal Plasticity Finite Element Modeling
CRSS	Critically Resolved Shear Stress
EBS	Electron Backscatter Diffraction
EDM	Electro discharge machined
FCC	Face centered cubic
Fe	Iron
GBS	Grain Boundary Sliding
HCP	Hexagonal close-packed
HT	High Temperature
IPF	Inverse Pole Figure
$m'$	Geometric compatibility factor
Ni	Nickel
RT	Room Temperature
SE	Secondary electron
SEM	Scanning Electron Microscopy
SF	Schmid factor
SFLG	Schmid factor left grain
SFRG	Schmid factor right grain

SiC	Silicon Carbon
Sn	Tin
Ti	Titanium
Ti525	Ti-5-Al-2.5Sn
Wt.%	Weight percent
XRD	X-ray Diffraction
Zn	Zinc
$\Delta b$	Residual Burgers vector

## **Chapter 1: Introduction**

### 1.1 Rationale and research objective

The overarching goal of the research is to further understand the deformation mechanisms in titanium alloys, specifically Ti-5Al-2.5Sn (Ti525). Knowledge of the deformation mechanisms can aid in improving the modeling methods of titanium alloys such as crystal plasticity finite element (CPFE) modeling, to enable more predictive ability to model heterogeneous strain near grain boundaries.

Titanium is a good candidate for the aerospace industry for many factors. One of the most important factors are the possibilities for weight reduction in an engine. Since titanium has a high strength-to-weight ratio, components traditionally made of steel or aluminum could be replaced with titanium, depending on the application. Titanium is also corrosion resistant meaning that coatings are not usually required unless it is in contact with an aluminum or a steel component in which galvanic corrosion may occur. Although titanium has many factors that make it appealing, it can cost from 3 to 10 times as much as aluminum or steel (Boyer, 1996).

Ti525 is mainly used in cryogenic applications. It does not exhibit a ductile-to-brittle transition which aids in high ductility and fracture toughness at low temperatures. Ti525 has been used in the space shuttle, on the hydrogen side of the high-pressure fuel turbo-pump (Boyer 1996). Figure 1.1 shows a schematic of a turbo-pump, and the location of where Ti525 is commonly used (Sutton, 2017). At elevated temperatures Ti525 has excellent creep resistance (Boyer, 1996).

Courtesy of Aerojet Rocketdyne.

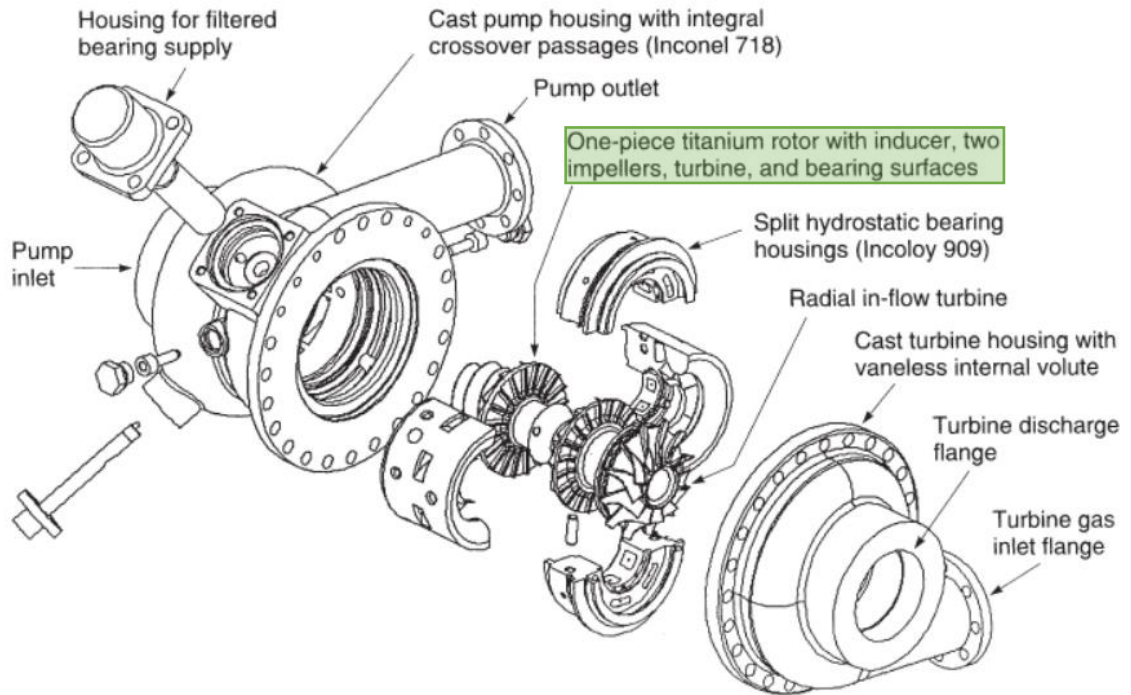


Figure 1.1: Schematic of a turbo pump showing where Ti525 is commonly used. The highlighted area points toward the part in the turbo pump that is typically Ti525 (Sutton, 2017).

## Chapter 2: Literature Review

### 2.1 Fundamentals of Titanium alloys

#### 2.1.1 Titanium allotropes

Titanium has two allotropes,  $\alpha$  and  $\beta$ , the low and high temperature allotropes, respectively. The microstructure of the  $\alpha$  and near- $\alpha$  alloys are mostly  $\alpha$  phase at room temperature, while  $\alpha/\beta$  alloys have more  $\beta$  phase introduced. Alpha alloys are nominally commercially pure titanium, whereas near- $\alpha$  alloys usually have the addition of  $\alpha$ -stabilizers such as Sn, or Al (Li, 2013). For the purposes of this paper, near- $\alpha$  alloys will be the focus. The near- $\alpha$  alloy studied is Ti-5Al-2.5Sn (Ti525).

#### 2.1.2 Dislocations

Two important concepts that need to be understood before moving forward in the paper are the dislocation and Burgers vectors. Dislocations are line defects within a crystal. The Burgers vector describes the relative displacement on the slipped plane. The Burgers circuit is a pathway along atoms, that form a closed loop within which dislocations are located. Figure 2.1 (a) shows the Burgers circuit (a-b-c-d-e) and a defect within the Burgers circuit. When you present the same circuit in a perfect crystal, there is a loop closure failure. In order to complete the circuit, a vector from c to b would be necessary, see Figure 2.1 (b). This vector is the Burgers vector (Hull, 2011).

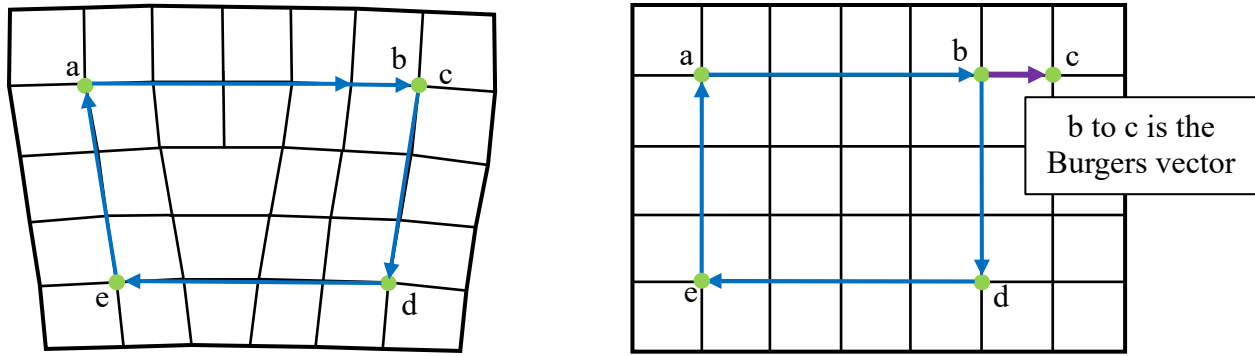


Figure 2.1: (a) Dislocation present within the Burgers circuit. (b) Burgers vector (purple arrow) from c to b in a perfect crystal.

### 2.1.3 Crystal Structure

The crystal structure of the titanium alpha phase is hexagonal close packed (HCP). Figure 2.2 shows the hexagonal structure. The blue shaded area represents the basal planes. The red shaded area represents prism planes. The yellow/green shaded area represents pyramidal planes. The  $a_1$ ,  $a_2$ ,  $a_3$ , and  $c$  directions are represented by black arrows. Slip occurs on close packed planes, in close packed directions. For hexagonal crystal structures slip has been observed in the following directions:  $\langle \bar{2}110 \rangle$  on  $\{0001\}$ ,  $\{10\bar{1}0\}$ , and  $\{10\bar{1}1\}$  planes, and  $\langle 1\bar{2}13 \rangle$  on  $\{10\bar{1}1\}$  plane (Li, 2013 and Bridier, 2005).

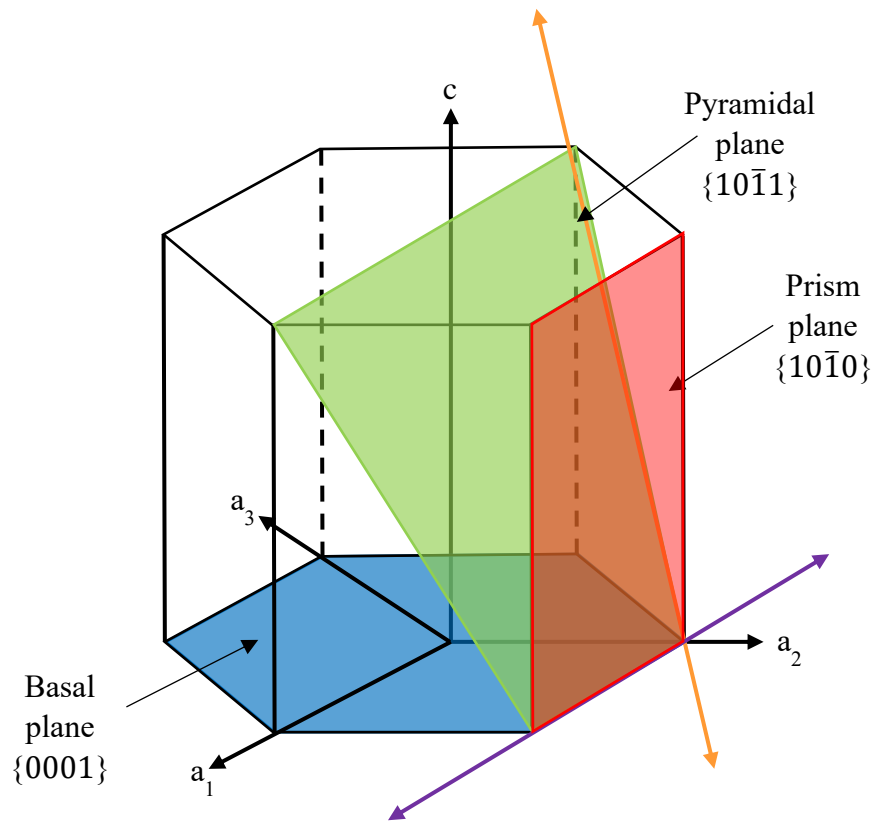


Figure 2.2: Hexagonal crystal structure with shaded area indicating different types of slip planes. The purple line represents the  $\langle \bar{2}110 \rangle$  direction in which prism, basal and pyramidal planes can slip. The orange line represents the  $\langle \bar{1}213 \rangle$  direction in which pyramidal planes can slip.

#### 2.1.4 Deformation mechanisms

The critical resolved shear stress (CRSS) determines the ease of slip on a system. Generally, with a higher CRSS, the ease of movement on that plane decreases. Hongemei et. al. found that at both 296K and 728K for the Ti525 alloy, prismatic slip was more easily activated than all other slip systems, including basal, since prismatic slip was found at low Schmid factors. Basal slip was then considered to be the next slip system easily activated in both samples (Li, 2013).

With different alloys, different slip systems become more active. In near- $\alpha$  alloys, basal slip is more active compared to commercially pure (CP) Ti. This is due to the addition of Al and

Sn, in which both increase the  $c/a$  ratio from 1.587 in CP Ti to about 1.60, towards the ideal  $c/a$  ratio (1.633). With a higher  $c/a$  ratio, a more closely packed basal plane results, which increases the ease of basal slip. In addition, with different temperatures, different slip systems become more active. With Al alloyed Ti, a decrease in the CRSS for both basal and prismatic slip systems is indicated with an increase of temperature. (Li, 2013).

At high temperatures, climb is enabled. Climb is the process in which a dislocation moves out of its slip plane with the aid of diffusion (Hull, 2013). This means that a dislocation can move to another, possibly more favorable slip plane during high temperature deformation.

When dislocations move through the material, in one grain slip is often prevalent on a specific slip system with a specific Burgers vector. If a dislocation moves across a grain boundary into another grain, it travels on another slip system with a different Burgers vector in the neighboring grain. Burgers vectors have a direction and length, depending on if the Burgers vector is an  $\langle a \rangle$  vector,  $\langle c \rangle$  vector or a  $\langle c+a \rangle$  vector, the length will vary. For the purpose of this thesis, only the Burgers vector *directions* were analyzed. That is, the Burgers vectors used are unit vectors.

## 2.2 Dislocations and slip transfer across grain boundaries

### 2.2.1 Slip transmission

One of the goals for this thesis is to identify and analyze slip transfer across grain boundaries. Slip traces interact with grain boundaries in a few different ways in polycrystalline metals. Figure 2.3 depicts possible cases in which slip is transmitted. In case (a) dislocations are stopped by the grain boundary, do not transmit, but pile up at the grain boundary. Case (b) (our focus) is when dislocations are emitted from grain 1 into grain 2 through the grain boundary, and

residual Burgers vector content is left in the boundary. In another example, dislocations can be dissociated into the grain boundary, leaving no dislocations in grain 2 (case (c)). Case (d) shows full transmission of slip. If a full transmission of slip has occurred (i.e. perfect alignment of the slip directions), theory suggests that no residual Burgers vector is left in the grain boundary. Case (e) shows where two dislocations meet at a grain boundary and generate a new dislocation in the grain boundary. Case (f) depicts a reflection of the dislocation in grain 1 back into grain 1 and leaving a dislocation in the grain boundary (Bayerschen, 2016).

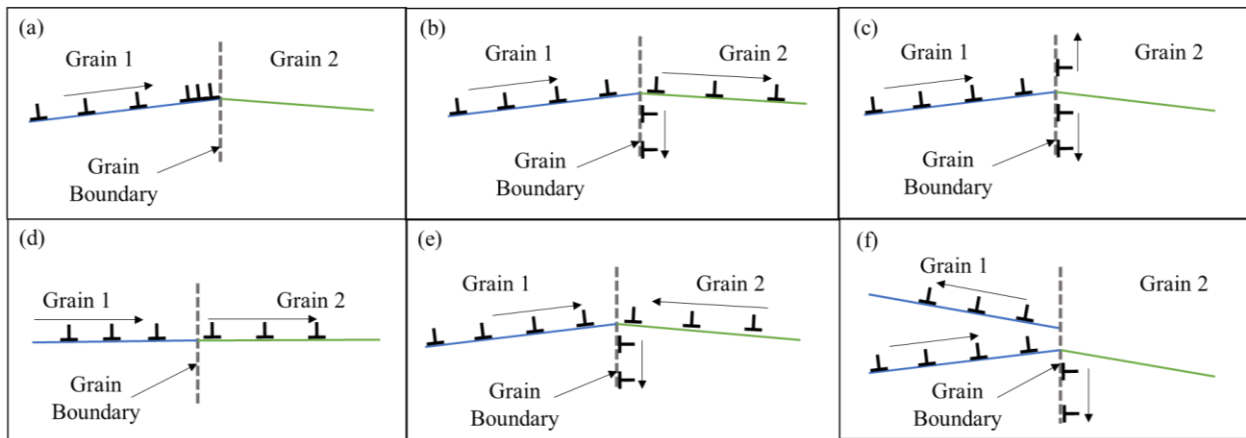


Figure 2.3: Slip traces interacting with a grain boundary. Focusing on case (b), the dislocations are transmitted from grain 1 into grain 2, and a residual part of the dislocation in grain 1 is retained in the grain boundary (Bayerschen, 2016).

The case that will be discussed is case (b) where perfect slip transfer does not occur across the grain boundary, implying that the Burgers vector changes direction from one grain to the next, resulting in some residual Burgers vector ( $\Delta b$ ) left in the grain boundary (see Figure 2.3 (b)). The better the alignment of the slip systems in grain 1 and grain 2, the more likely the transmission of the dislocation into grain 2 will occur, and a smaller residual component of slip would be retained in the grain boundary. This suggests that minimizing the size of the residual

Burgers vector would make a slip transmission event more likely, as observed and argued by Shen et al. (1989) and Lee et al. (1988).

### 2.2.2 Metrics used to analyze slip transfer

The direction and relative size of the residual Burgers vector can be estimated using data obtained from electron backscatter diffraction (EBSD) analysis. Knowing the grain orientation, the Burgers vector of the left grain ( $\vec{b}_1$ ), which we assume to be the initiating slip system, and the right grain Burgers vector ( $\vec{b}_2$ ) is the transmitted slip, the residual Burgers vector,  $\Delta b$  is estimated by the following dislocation reaction equation:

$$\Delta b = \vec{b}_1 - \vec{b}_2 \quad (1)$$

Figure 2.4 shows the Burgers vectors ( $\vec{b}_1$ ) and ( $\vec{b}_2$ ) on two different slip planes, and the angles associated with the transmission.

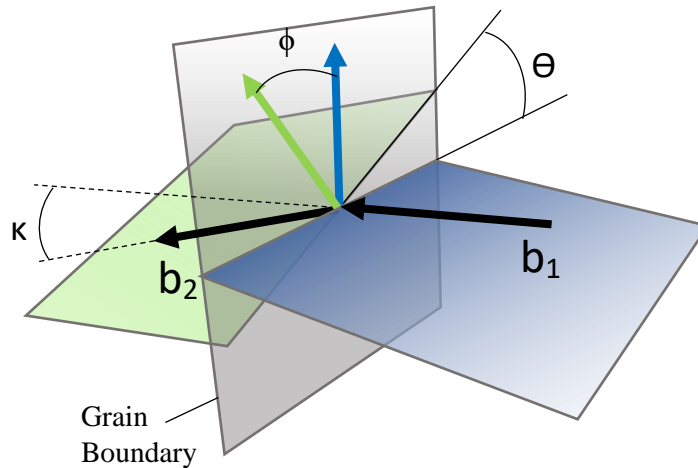


Figure 2.4: Representation of slip planes (in blue and green) and the angles associated with them used to calculate various factors (Abuzaid, 2016).

The geometric compatibility factor,  $m'$ , is used as a criterion to determine if slip transfer is likely to occur. The factor can be calculated from two angles  $\phi$  and  $\kappa$ , the angle between the normal to the slip plane, and the angle between the two slip directions in grains 1 and 2, respectively (see Figure 2.4). Therefore, the factor resolves the strain from the slip on grain 1 onto grain 2. The factor is calculated as follows (Luster, 1994):

$$m' = \cos(\phi) \cdot \cos(\kappa) \quad (2)$$

An  $m'$  value closer to 1 would imply that slip transfer is more likely to occur on the specified slip systems, as they would be nearly collinear, as opposed to a slip system pair that has lower  $m'$  values.

The misorientation angle is determined from the orientations of each grain through EBSD analysis. The misorientation between two grains is computed based upon the crystal orientations of each grain,  $\mathbf{g}_A$  for the crystal orientation of grain 1 and  $\mathbf{g}_B$  for the crystal orientation of grain 2. The misorientation is defined as the rotation needed to bring the orientation of grain A into coincidence with the orientation of grain B. The calculation for misorientation ( $\Delta\mathbf{g}_{AB}$ ) is as follows:

$$\Delta\mathbf{g}_{AB} = \mathbf{g}_B \mathbf{g}_A^{-1} = \mathbf{g}_B \mathbf{g}_A^T$$

This operation produces a 3x3 matrix. From this matrix, a rotation angle ( $\omega$ ) and axis about which the rotation happens ( $[n_1, n_2, n_3]$ ) is calculated, shown below (Kocks, 1998).

$$\cos \omega = \frac{1}{2} (\Delta\mathbf{g}_{11} + \Delta\mathbf{g}_{22} + \Delta\mathbf{g}_{33} - 1)$$

$$[n_1, n_2, n_3] = \frac{[\Delta \mathbf{g}_{23} - \Delta \mathbf{g}_{32}, \Delta \mathbf{g}_{31} - \Delta \mathbf{g}_{13}, \Delta \mathbf{g}_{12} - \Delta \mathbf{g}_{21}]}{\sqrt{(\Delta \mathbf{g}_{23} - \Delta \mathbf{g}_{32})^2 + (\Delta \mathbf{g}_{31} - \Delta \mathbf{g}_{13})^2 + (\Delta \mathbf{g}_{12} - \Delta \mathbf{g}_{21})^2}}$$

For hexagonal crystal structures, there are 12 symmetric orientation matrices. The OIM software, from the above equations, calculates the misorientation angle ( $\omega$ ) and the rotation axis ( $[n_1, n_2, n_3]$ ) for all 12 variants of symmetric rotations axes. The smallest misorientation angle is then chosen as the misorientation angle with the associated rotation axes.

In previous work, the resolved shear stress based upon the global stress tensor was used as a criterion to determine if slip is likely. The Schmid factor is used as a metric to determine the most likely slip systems that are activated in the two neighboring grains. A higher Schmid factor implies that slip is more likely to occur. The Schmid factor is determined by two angles,  $\phi$  and  $\lambda$ , when there is unidirectional stress as described in Figure 2.5 (Hull, 2011).

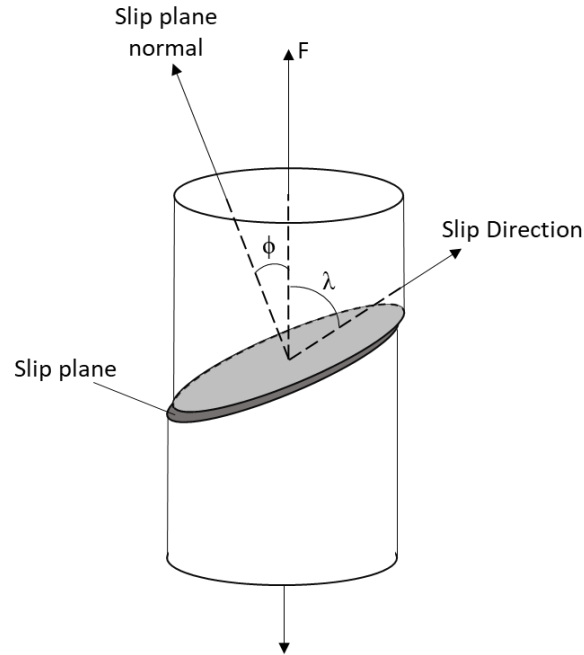


Figure 2.5: Representation of slip in a cylindrical crystal and the associated angles describing the slip plane and slip direction used to compute the Schmid factor.

The Schmid factor is calculated by the following equation, using the angles described in Figure 2.5 (Hull, 2011):

$$\text{Schmid factor} = \cos(\phi) \cos(\lambda) \quad (3)$$

Slip systems with higher Schmid factors will facilitate slip more easily. Since slip will be likely with a high  $m'$  and high Schmid factors based upon another metric worth considering (Bieler, 2019, Alizadeh 2020), given by:

$$m'(SF_{LG} + SF_{RG}) \quad (4)$$

where  $SF_{LG}$  is the Schmid factor in the left grain, and  $SF_{RG}$  is the Schmid factor in the right grain.

Another useful parameter is  $m'/\Delta b$ , as slip transfer is expected to be facilitated with high  $m'$  and low  $\Delta b$ , where  $\Delta b$  is the residual Burgers vector (Alizadeh 2020, Bayerschen 2016, Shen 1988, Lee 1989).

## 2.3 Previous work

### 2.3.1 Titanium

The work done in this thesis is built on the work published by Hongmei Li (2013), “Analysis of the deformation behavior of the hexagonal close-packed alpha phase in titanium and titanium alloys”. Tension and creep samples were tested at low and high temperatures for a variety of alloys. For the purpose of this paper, the interest lies in the Ti525 alloy.

For each sample, distributions of active slip systems in each grain were calculated. Basal and prism slip were found to be dominant in the Ti525 alloy. With the increase in temperature, basal active slip systems increased in frequency. This increase in ease of slip in basal slip systems correlates to a lower CRSS. Prismatic slip systems for Ti-Al  $\alpha$  alloys also have a lower CRSS with high temperature.

Building upon Hongmei Li’s work, further investigation of the tensile tested Ti525 sample at 296K and 728K was considered. The focus was to look at grain pairs and determine if there was slip transfer across the grain boundary. Dividing the grain pairs into slip transfer and no slip transfer categories and using the various parameters that have been discussed, allowed for trends in slip transfer to be uncovered.

### 2.3.2 Aluminum

A similar activity was done by Alizadeh (2020) in “A criterion for slip transfer at grain boundaries in Al”. Alizadeh found that slip transfer usually was associated with high  $m'$  values. Slip transfer is favored by low angle boundaries, which have high  $m'$  values due to the low misorientation geometry. Further, Alizadeh assessed the  $\Delta b$ ,  $m'(SF_{LG}+SF_{RG})$ , and the  $m'/\Delta b$  parameters vs. the misorientation angle to observed trends. Also, Linne and Daly examined a similar specimen of pure Al at 190°C using high resolution differential image correlation (DIC)

(Linne 2020). It is hypothesized that similar trends observed in the Al data sets will be present in the Ti525 data set, with more complicated slip systems. The difference in crystal structure may limit the similarities noticed between the Al face centered cubic (FCC) crystal structure and the Titanium hexagonal close packed (HCP) crystal structure.

### 2.3.3 Aluminum and Titanium Crystal structure differences

Aluminum has face-centered cubic (FCC) crystal structure. Slip occurs on the close-packed planes along the close-packed directions, which in FCC is  $\{111\}$  and  $\langle 110 \rangle$  respectively. Therefore, there are four close packed planes, each with 6  $\langle 110 \rangle$  directions, but positive and negative directional sense are not distinguished, meaning a reduction of a factor of two. Therefore, there are 12 slip systems in FCC crystal structure, all with equal ease of operating (Jackson, 1991). In contrast, titanium has a hexagonal crystal structure, where slip occurs on basal, pyramidal $\langle a \rangle$ , pyramidal $\langle c+a \rangle$  and prism slip systems. There are three slip systems each on basal and prism planes that are easily activated (Li, 2013), but they do not enable changes in crystal dimension in the  $\langle c \rangle$  direction, so easy slip cannot enable needed shape changes in the  $\langle c \rangle$  direction. There are an additional 18 slip systems on pyramidal planes but slip on pyramidal planes is much more difficult to activate, especially in the  $\langle c+a \rangle$  directions, so higher resolved shear stresses are required (Li, 2013). Therefore, titanium alloys have fewer slip systems that facilitate easy slip compared to FCC crystals, even though there are many more slip systems available.

To assess the difference between Al and Ti alloy slip transfer behavior, the methodology developed by Alizadeh et al. is used on a polycrystalline Ti alloy. This work will also examine if this methodology can yield similar statistical information in a standard polycrystal sample rather than an oligo-crystal foil.

The following chapters will explain the experiments done, the results obtained, and the observed trends in the 296K and 728K tensile tested Ti525 samples. Analysis was done on slip transfer data to further the investigation that Hongmei Li presented. The trends observed in the slip transfer data analysis were compared with Alizadeh's results of an aluminum alloy slip transfer data to compare differences in FCC and HCP materials.

## Chapter 3: Experimental Procedure

The description of the material and tensile tests on the Ti-5-Al-2.5Sn alloy is summarized from Hongmei Li's dissertation and related publications.

### 3.1 Material

The Ti-5-Al-2.5Sn (Ti525) alloy was provided by Pratt & Whitney, Rocketdyne. It was forged in the upper half of the  $\alpha+\beta$  phase field. The material was then annealed at 1127K for 1 hour for recrystallization, followed directly by air cooling, followed by a vacuum annealing process at 1033K for 4 hours to reduce the hydrogen content. Table 3.1 denotes the measured bulk composition of the alloy in weight percent (Li, 2013).

Table 3.1: Measured composition of polycrystal Ti525 (Li, 2013)

Element	Al	Sn	Fe	Zn	Ti
Weight %	4.7	2.7	0.2	0.1	balance

### 3.2 Mechanical testing

#### 3.2.1 Sample preparation

Two specimens were prepared by a mechanical polish, using 400, 600, 1200, 2400 and 4000 Silicon Carbide (SiC) grinding papers sequentially for 5 to 10 minutes each. Between each grinding step, the sample was rinsed with water. After grinding, a final polishing step with polishing cloth from Buehler (catalog No. M500-12PS) and five parts colloidal silica with 0.06 $\mu$ m particle size and one part 30% hydrogen peroxide. This step took around an hour to obtain the desired finish. Water was again used to rinse the sample after polishing then

ultrasonically cleaned with acetone and methanol respectively to remove the colloidal silica (Li, 2013).

Multiple dog-bone samples were electro-discharge machined (EDM) from the forging with a gage width of 3mm and 10mm length. Figure 3.1 shows the geometry of the EDM samples.

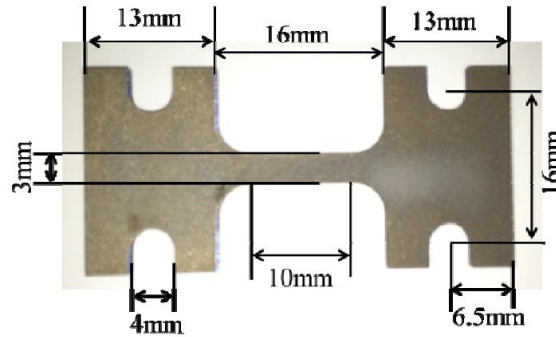


Figure 3.1: Geometry of tensile samples electro-discharge machined out of Ti525 (Li, 2013).

### 3.2.2 Test set up

The samples examined were in-situ tensile tested within the Tescan Mira3 SEM, with a displacement rate of 0.004 mm/s (approximate strain rate of  $10^{-3} \text{ s}^{-1}$ ). The tensile stage was built by Ernest F. Fullam, Incorporated. Displacement time and load data was recorded using the MTESTW (version F 8.83) control software. To obtain the desired temperature of the sample, a 6mm diameter tungsten-based heating unit was used. One sample was tested at 296K and another at 728K. The sample was held at this temperature for 30 minutes prior to loading. During testing, the temperature of the sample was monitored using a thermocouple that was welded to the side of the gage section. Throughout the test, a vacuum below  $2 \times 10^{-6}$  Torr was maintained.

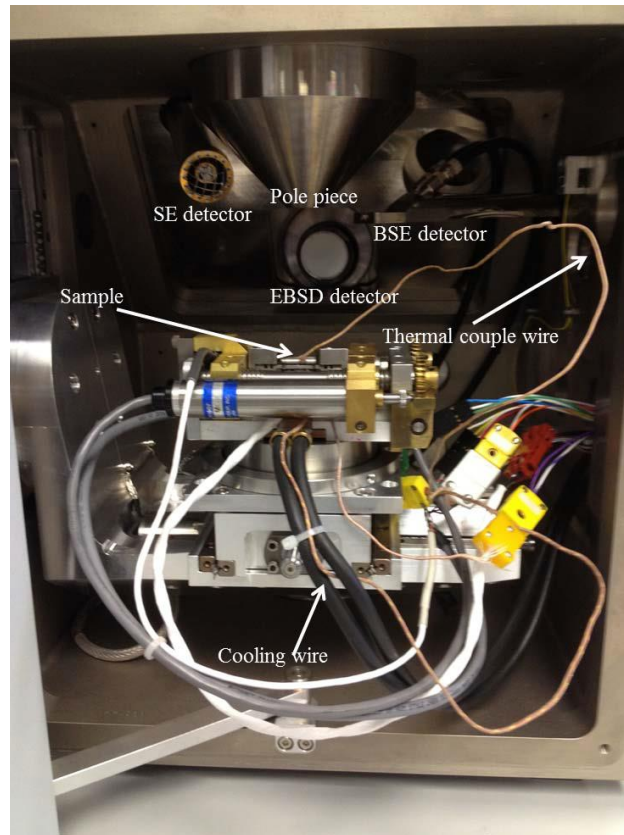


Figure 3.2: Tensile test set up within the Tescan Mira3 SEM (Li, 2013).

### 3.2.3 Tensile Test Results

Figure 3.2 shows the set up within the Tescan Mira3. The stress-displacement curves are presented in Figure 3.3. The load drops shown are due to pausing the test for image acquisitions. Table 3.2 gives the yield strength and maximum stress obtained from the stress displacement curves (Li, 2013).

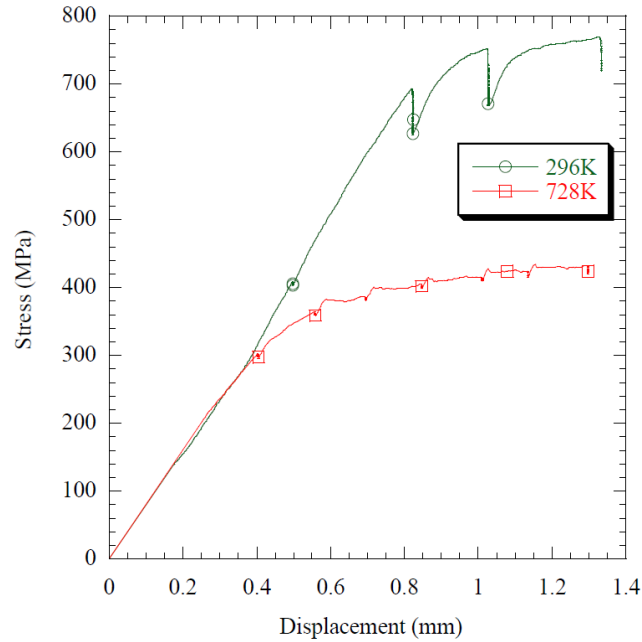


Figure 3.3: Stress vs. displacement curve for the room temperature (296K) and high temperature (728K) samples. Load drops are stress relaxation points when the test was paused for imaging (Li, 2013).

Table 3.2: Ti525 tensile properties obtained from room temperature and high temperature tensile tests (Li, 2013).

Temperature	Yield Strength (MPa)	Max Stress (MPa)
296K	~660	769
728K	~300	434

### 3.3 Microstructural Observations

Figure 3.4 (a) and (b) show representative SE SEM images of the deformed Ti525 in-situ 296K and 728K tensile tested sample. The scratch in the figure is a fiduciary mark so the location of the EBSD analyzed area was easier to find.

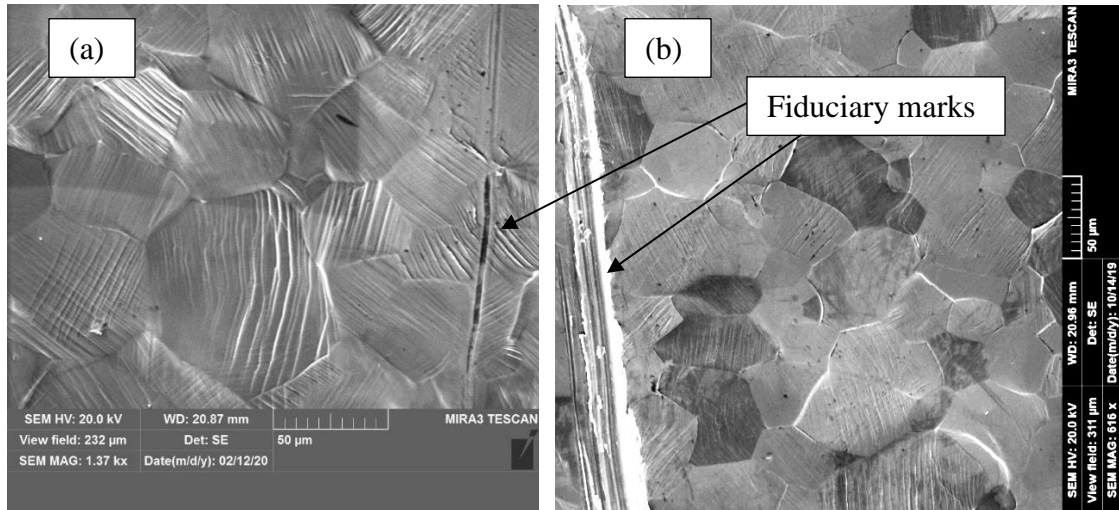


Figure 3.4: SEM image showing the microstructure of (a) the 296K and (b) the 728K tensile tested Ti525 sample with fiduciary mark.

### 3.3.1 Orientation evaluation

After deformation, EBSD orientation maps were created from a portion of the gage section, marked with a fiduciary mark. The maps were obtained using OIM Analysis<sup>TM</sup> Version 7.3.1, by EDAX. Figure 3.5 (a) and (b) show the inverse pole figure (IPF) orientation maps with a variety of colors observed, meaning the samples are not strongly textured. For the room temperature sample, (Figure 3.5 (a)) the fiduciary mark is located just out of the frame to the left of the image and in Figure 3.5 (b), the high temperature sample, the fiduciary mark is cropped out (shown as a black stripe). The black rectangles in the room temperature sample are areas where the EBSD software determined many small grains that were probably artifacts of poor indexing, so they were cropped out of the analysis. Clean-up procedures including one or two rounds of near-neighbor correlation and one round of dilation was used to eliminate small grains from the analysis. This provided a convenient reconstructed boundary file to analyze.

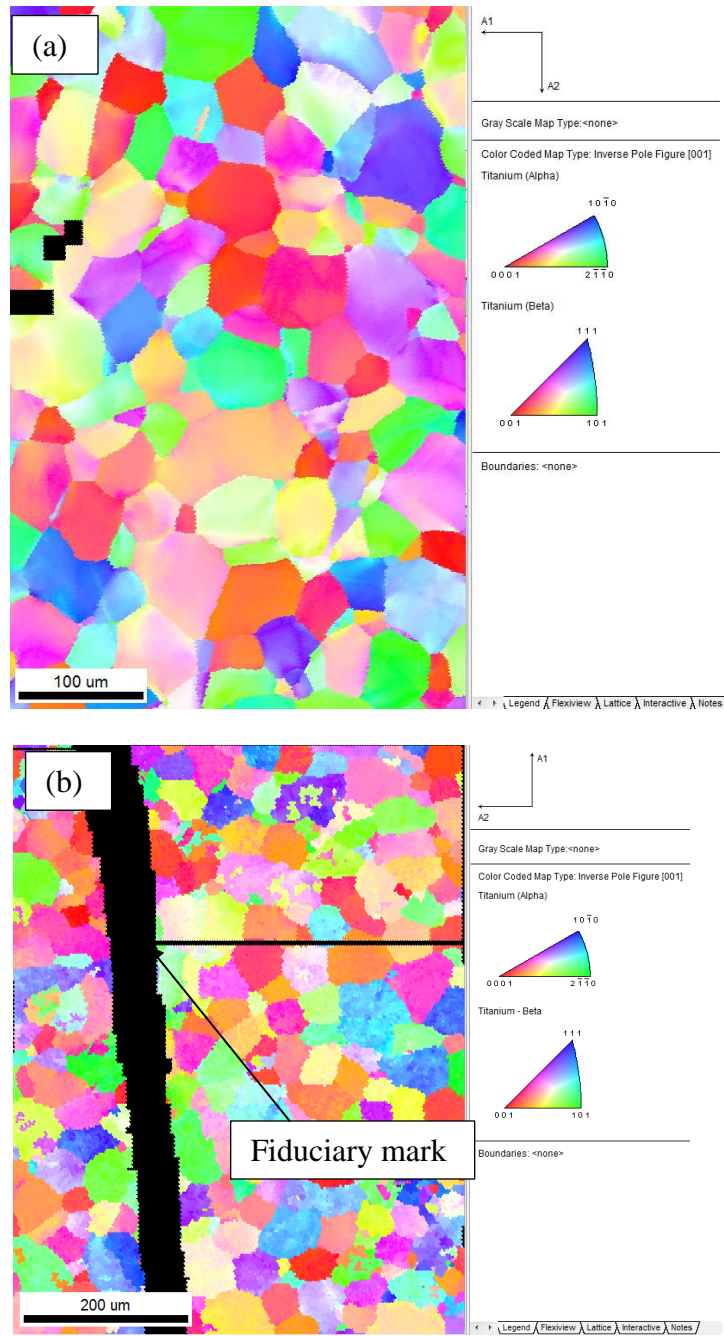


Figure 3.5: EBSD IPF map of the deformed Ti525 tensile samples. The intentional scratch is the fiduciary mark, which is visible in the IPF map for (b) the 728K sample, and is located out of the frame in (a) the 296K sample (black rectangular areas are eliminated data that have very small grains/questionable indexing).

Figure 3.6 (a) and (b) shows the pole figures for both the 296K and 728K data, respectively. The dark lines represent the 30° cones along the major axis. The maximum value in the legend indicates that the orientation of the material after deformation is ~3 times random for both samples.

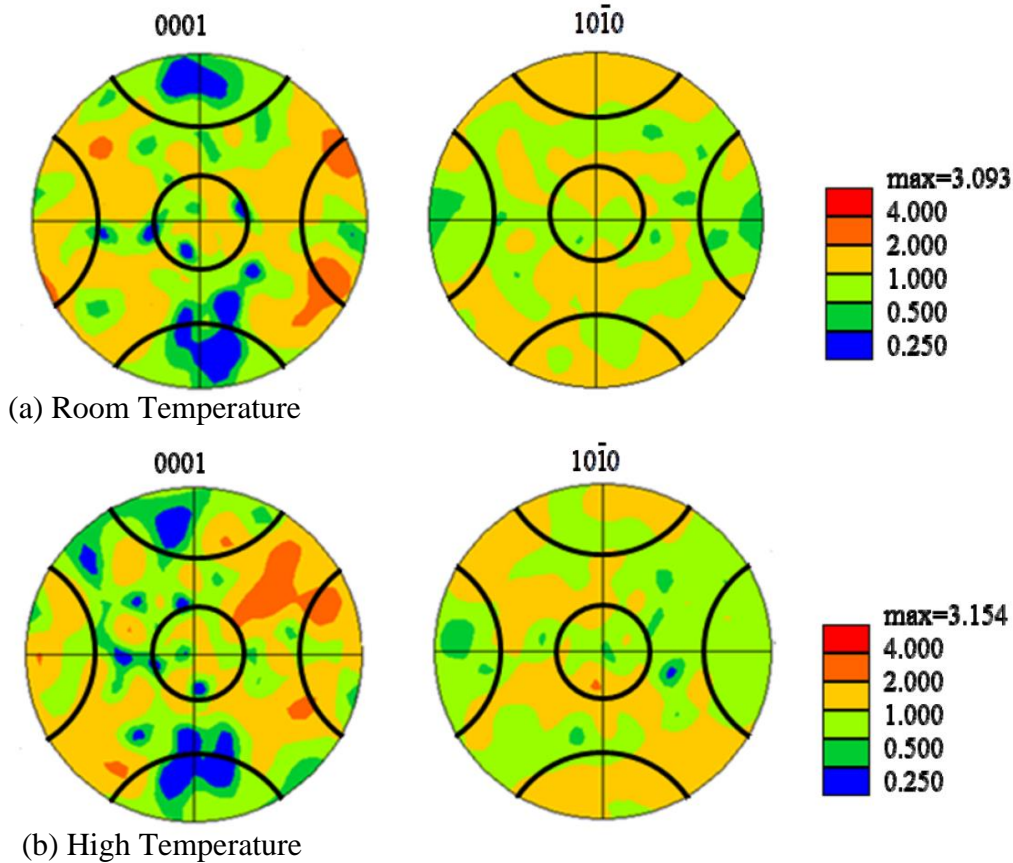


Figure 3.6: {0001} and {10 $\bar{1}$ 0} pole figures for (a) the 296K and (b) the 728K Ti525 samples. The black curved lines represent the 30° cones along the major axis. The material has orientations that are around 3 times random in both samples. (Li, 2013).

### 3.4 Grain pair analysis

#### 3.4.1 Slip transfer

To determine if slip transfer was present through grain boundaries, an in-depth look at slip traces near the grain boundary was necessary. If there were correlated slip traces in one grain

and a neighboring grain, a set of criteria were considered to determine if slip transfer accounted for the correlated slip traces. These criteria are:

**(1) Determination of probable slip systems which would be consistent with observed slip traces.**

**(2) A  $m'$  value associated with the observed correlated slip systems generally larger than 0.7.**

**(3) The residual burgers vector ( $\Delta b$ ) associated with the observed correlated slip systems is generally smaller than 0.5b.**

**(4) The Schmid factor of each slip system is generally larger than 0.25, (5) the topography at the grain boundary is small indicating that the boundary does not lead to heterogenous strain on both sides.**

**(6) The observed slip traces on each side have a topographical directional sense that implies that the slip planes are approximately parallel.**

To determine if probable slip systems are consistent with observed slip traces (criterion (1)), the Euler angles for each grain in a grain pair were entered into a Matlab code (shown in Appendix A: Matlab hexagonal orientation code (written by Thomas R. Bieler)). This code draws the unit cell in the actual orientation that is present in the grain. The unit cell is drawn multiple times with different slip systems in order of decreasing Schmid factor. It also draws the slip trace that would be expected if this slip system was active. Figure 3.7 shows the output of this code for two grains.

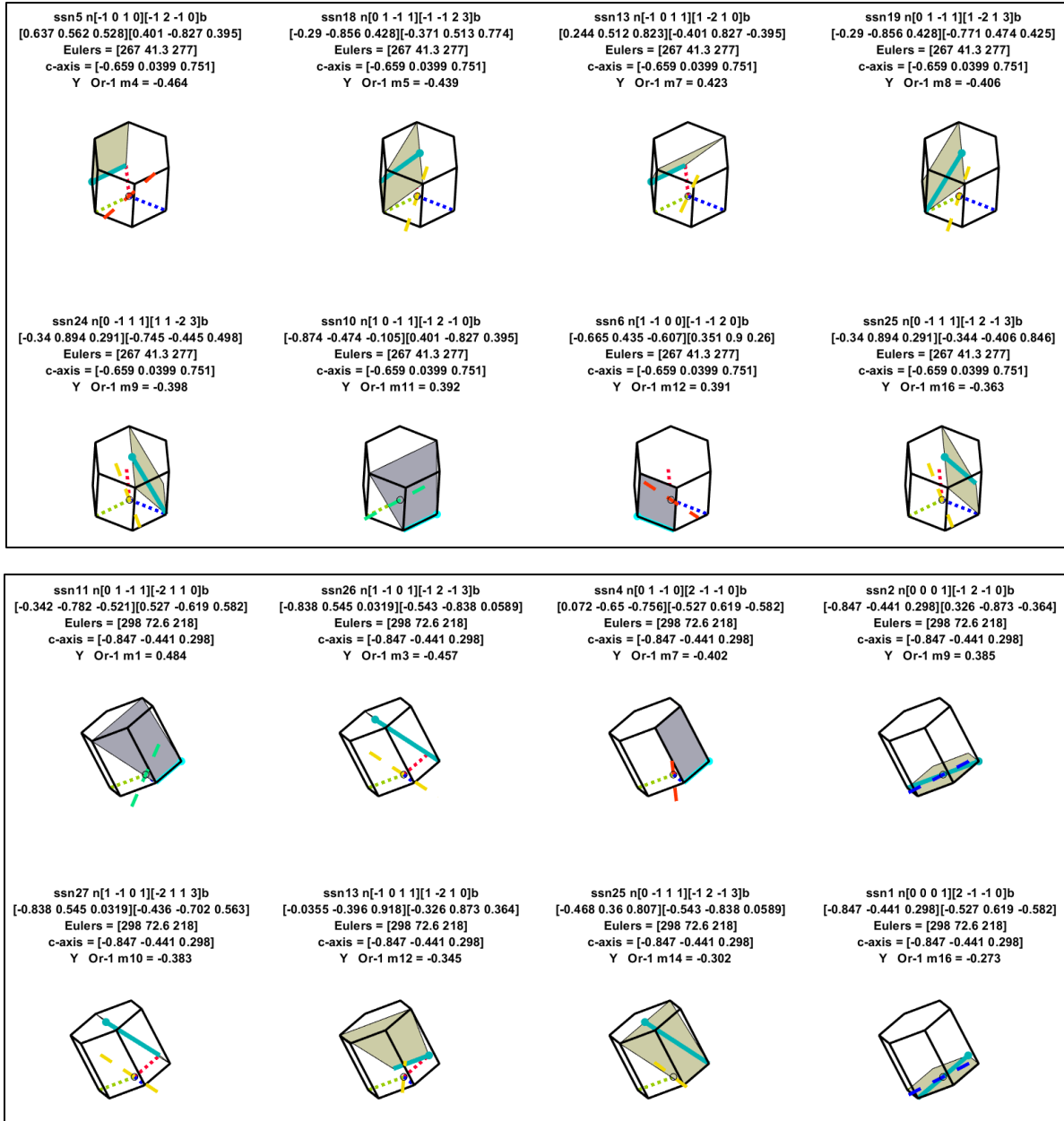


Figure 3.7: Computed slip system possibilities and corresponding slip traces for (a) the left grain and (b) the right grain, drawn in actual orientation present in the grain.

Code generated slip traces are then compared to the SEM image of the grain, to determine what computed slip trace best matches the observed slip trace in the SEM image.

Figure 3.8 shows an example of the comparison, where the trace of slip system number 11

matches closely with the observed slip traces in the left grain and similarly, the trace of slip system number 5 matches the observed slip traces in the right grain. In cases where there are multiple slip systems on the same plane (on pyramidal and basal planes), the slip *direction* with the highest Schmid factor is chosen.

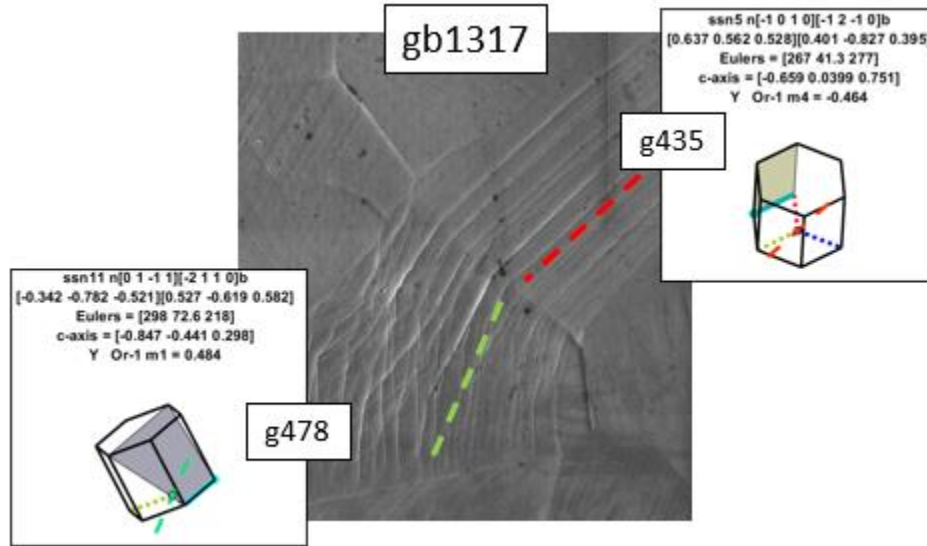


Figure 3.8: Comparison of computed slip traces and observed slip traces in the SEM image.

To determine if criteria (2) (a high  $m'$  value), criteria (3) (high Schmid factor values) and criteria (4) (low residual Burgers vectors) are met, another code was used (also written by Dr. Thomas R. Bieler, shown in Appendix B). The code reads the reconstructed boundary file (which includes the misorientation of each boundary) and grain file generated by the OIM Analysis software. Sample files are shown in Appendix C. The probable slip conditions present and the Schmid factors are determined for each grain. Next, the code computes grain boundary parameters,  $m'$  values and residual Burgers vectors ( $\Delta b$ ) for each slip system pair possibility. Thresholds values are set up to filter out slip system possibilities that are unlikely to be

meaningful, such as Schmid factors lower than 0.2 and  $m'$  values below 0.6. Table 3.3 is then generated for each slip system pair in order of decreasing Schmid factor. The slip system number is shown on the far most left column for the left grain, and upper most row for the right grain. The corresponding number (right or below, respectively) is the corresponding Schmid factor. The values in the middle of the table are the  $m'/\Delta b$  metrics for each corresponding slip system pair, and high values of  $m'/\Delta b$  values are bolded. Values that are bolded, and in the upper left-hand corner of the table, are the best candidates for slip transfer because they have high  $m'$  values, low  $\Delta b$  values, and high Schmid factors. As with the other code, prisms of each grain are drawn in their relative positions to each other, and slip systems are illustrated for slip system pairs in order of decreasing  $m'/\Delta b$  values, as illustrated for the grain pair in Figure 3.9. If there are multiple slip systems that have slip traces that look like they could be present in the SEM image of the grain, this table is used to determine which one is most likely to account for the observation.

Table 3.3:  $m'/\Delta b$  table for slip system combinations and associated Schmid factor. High  $m'/\Delta b$  values in the upper left-hand corner of the table indicates the slip system pair that is most likely transmitting slip.

gb1317	g435ss	<b>5</b>	8	<b>18</b>	<b>13</b>	<b>19</b>	<b>24</b>	<b>6</b>	9	<b>10</b>	<b>25</b>	<b>15</b>	<b>12</b>
g478ss	$m'/rbv$	<b>0.46</b>	0.46	<b>0.44</b>	<b>0.42</b>	<b>0.41</b>	<b>0.40</b>	<b>0.39</b>	0.39	<b>0.39</b>	<b>0.36</b>	<b>0.36</b>	<b>0.33</b>
<b>11</b>	<b>0.48</b>	<b>2.881</b>	-0.076	0.024	<b>2.823</b>	0.235	0.098	-0.035	<b>4.058</b>	<b>2.237</b>	0.443	-0.015	-0.048
<b>26</b>	<b>0.46</b>	-0.105	0.925	0.030	0.050	-0.007	1.013	1.909	0.006	-0.235	0.491	<b>2.379</b>	0.973
<b>4</b>	<b>0.40</b>	<b>2.222</b>	-0.067	0.009	<b>2.900</b>	0.092	0.111	-0.022	<b>3.200</b>	1.002	0.498	0.034	-0.073
7	0.40	-0.066	0.912	1.798	-0.065	0.542	-0.060	1.055	-0.021	-0.051	-0.206	0.893	0.961
<b>2</b>	<b>0.38</b>	0.584	0.066	1.163	0.173	1.025	-0.001	-0.212	0.208	0.852	-0.001	-0.593	0.221
<b>27</b>	<b>0.38</b>	-0.154	0.259	-0.040	0.073	-0.041	1.759	0.582	0.064	-0.344	1.697	0.725	0.297
<b>13</b>	<b>0.34</b>	-0.224	0.312	1.148	-0.506	1.013	-0.002	0.786	0.044	0.113	-0.004	0.318	1.062
<b>25</b>	<b>0.30</b>	0.164	0.200	-0.025	0.366	0.006	0.929	-0.050	0.011	-0.077	0.450	1.049	-1.137
<b>1</b>	<b>0.27</b>	1.944	-0.036	0.033	0.577	0.324	0.003	-0.033	<b>2.607</b>	<b>2.838</b>	0.012	-0.093	0.035

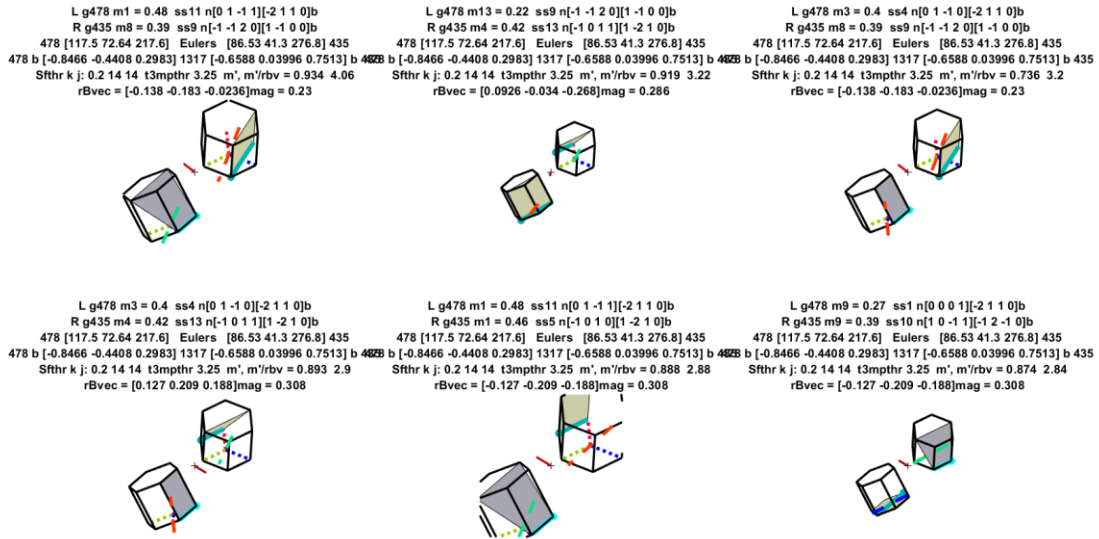


Figure 3.9: Calculated prisms of each grain drawn relative to each other.

To determine if criterion (5) was met, further observations of the grain boundary were made to determine if a large ledge (indicated by topographic contrast) or small ledge was present. Figure 3.10 (a) shows an example of a small (or non-observable) ledge at the grain boundary, while Figure 3.10 (b) shows an example of a larger ledge at the grain boundary that indicates that heterogeneous strain occurred on both sides.

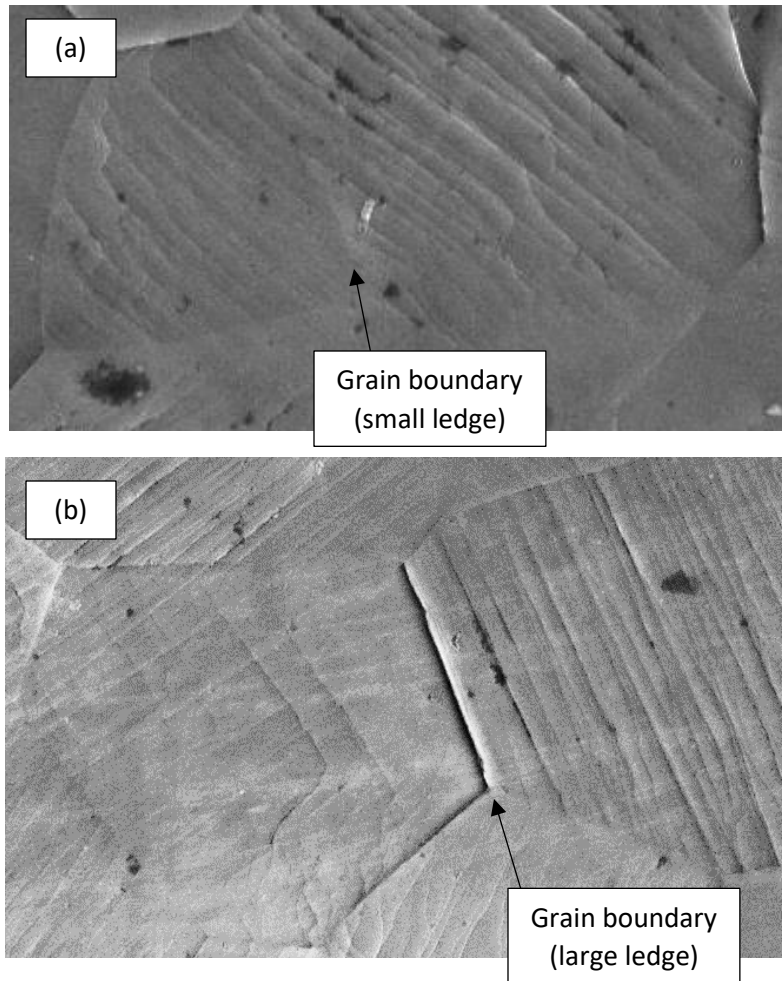


Figure 3.10: Topography at the grain boundary in (a) is small indicating that there is little to no heterogeneous strain on either side. Topography at the grain boundary in (b) is large indicating that there is heterogeneous strain on both sides.

To determine if the observed slip traces on each side have a topographical directional sense that implies that the slip planes are nearly parallel (criteria (6)), the surface topography of the neighboring grains was assessed further. By considering surface topography, from the sense of which direction the ‘light source’ was coming from<sup>1</sup>, the topographic shape of the slip steps was identified in each grain. If the slip steps did not appear parallel, leading to contrasting dark

<sup>1</sup> Specifically, the position of the secondary electron detector is considered as a ‘light source’ for the image.

and light steps on either side of the boundary, the likelihood of slip transfer was low because the sense of shear is in different directions as illustrated in Figure 3.11 (a) and (b), and therefore this criteria was not met. Figure 3.11 (a) shows the top view of two grains, as seen in the SEM. The red lines indicate the upward direction of steps. The orange line shows where a cross section is depicted in Figure 3.11 (b), where the same red arrows show upward steps. It also shows the sense of shear in each grain which are far from parallel. If the slip steps were generally parallel, the criteria would be met.

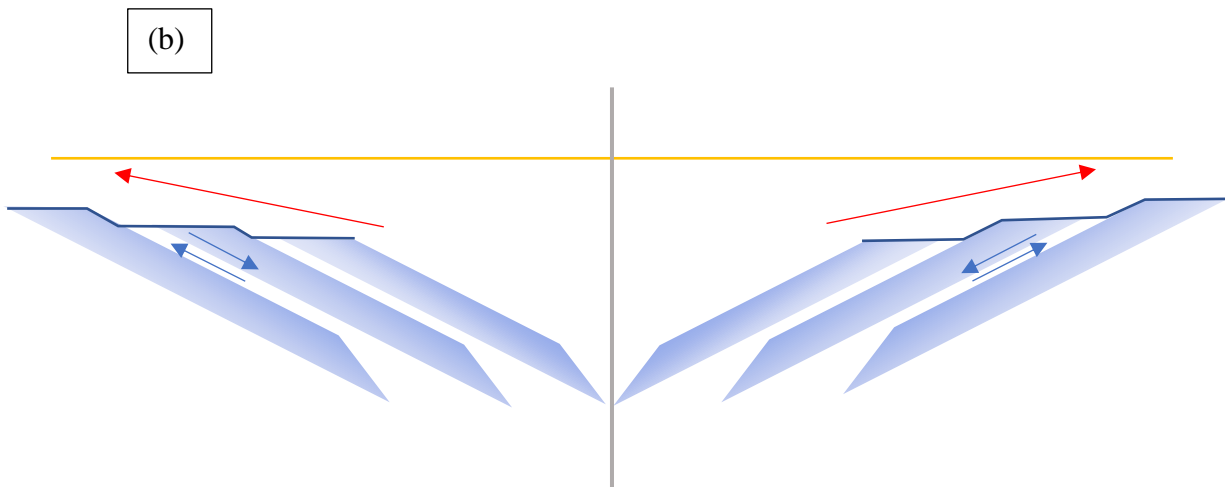
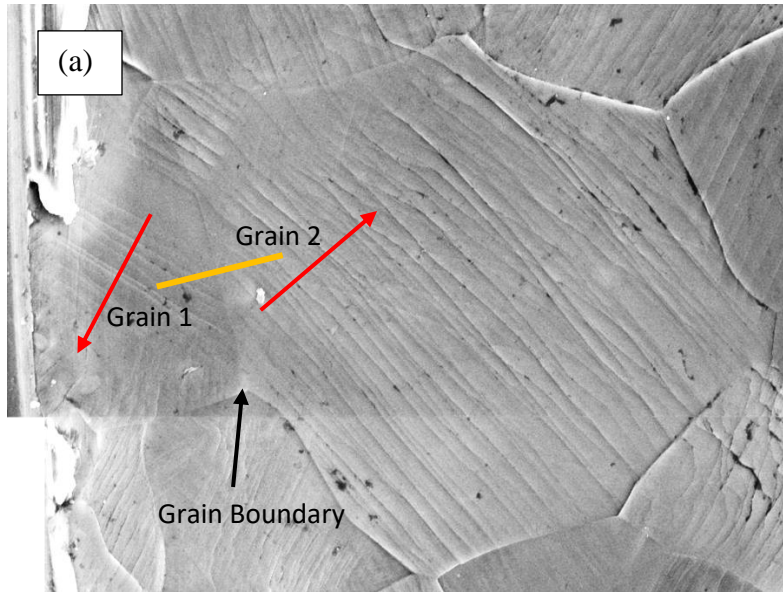


Figure 3.11: (a) The red arrows indicate an upward step sense in the grain (light slip traces in the lower part of grain 1 and dark traces in grain 2 and the upper corner of grain 1). (b) Sketch of cross section along the orange line showing opposite directional sense of shear (blue arrows). Though slip traces may appear to be correlated, their slip planes are far from parallel, indicating that slip transfer cannot account for the observed slip traces.

**If all five criteria were met, the grain boundary was categorized as a case of slip transfer. If one or two criteria were not met, the boundary was categorized as possible slip transfer, or if more criteria were not met, the grain boundary was categorized as a case of no slip transfer.** An example of a case of slip transfer is shown in Figure 3.12 (a). Figure 3.12 (b) shows an example of a boundary where all five criteria are not met, therefore it is categorized as a case of no slip transfer.

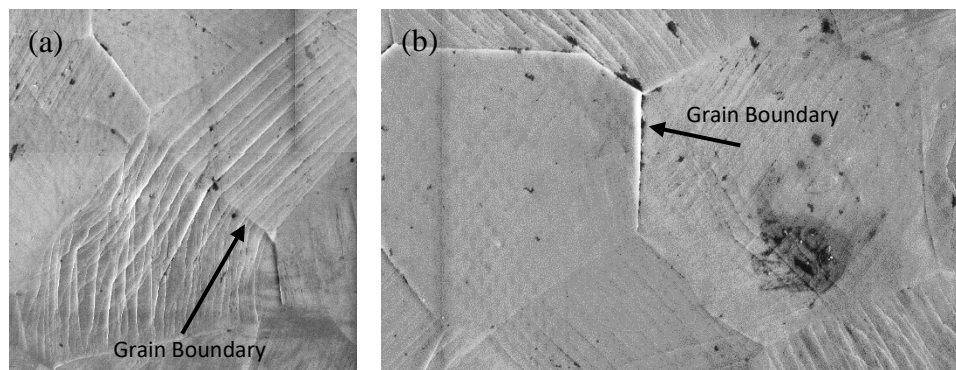


Figure 3.12: (a) Example of a grain boundary that is categorized as slip transfer, meaning that all five criteria are met. (b) Example of a grain boundary that is categorized as no slip transfer, meaning all five criteria for slip transfer were not met.

### 3.4.2 Slip transfer analysis

To obtain a representative set of data from the samples, it was necessary to understand what types of grain boundaries were present in each sample. 50 random grain boundaries were chosen and identified as “slip transfer”, “not slip transfer”, and “maybe slip transfer” as explained in section 3.4: Grain pair analysis. Of these, 8% was determined to fall into the “maybe slip transfer” category for both the room temperature and high temperature samples. The percentages of the random poll of grain boundaries is shown in Table 3.4. Grain boundaries were fully analyzed until the percentages matched the random sampling data, to ensure that the analyzed grain boundaries were representative of the whole sample.

In the room temperature sample, 146 grains were analyzed and divided into the three groups, “slip transfer”, “not slip transfer”, and “maybe slip transfer”. The “maybe slip transferred” category of grain boundaries was not used further in the study and consisted of 10 grain boundaries. 73 grain boundaries were identified as slip transfer. The not slip transfer group consisted of around 68 grain boundaries.

In the high temperature sample, around 173 grain boundaries were analyzed and divided into the three groups. The “slip transferred” grain boundary group consisted of 93 grain boundaries. The “slip not transferred” grain boundary group consisted of 78 grain boundaries. The rest of the grains in the “maybe slip transferred” category was not used in the data analysis.

Table 3.4: Comparison of random poll of data from each sample, and the number/percentages of the fully analyzed GBs used in the analysis.

	Slip transfer GBs	Slip transfer GBs (%)	Not slip transfer GBs	Not slip transfer GBs (%)
RT Random Poll from Ti525	24	52%	22	48%
RT Ti525 fully analyzed	73	52%	68	48%
HT Random Poll from Ti525	25	54%	21	46%
HT Ti525 fully analyzed	93	54%	78	46%

Figure 3.13 shows a probability of the misorientation angles collected from the Ti525 high temperature and room temperature data. In addition, random orientations likely for hexagonal crystal structure were generated and plotted against the Ti525 data. There are some differences, specifically in misorientation angles less than 40°, with the Ti525 data having a higher probability.

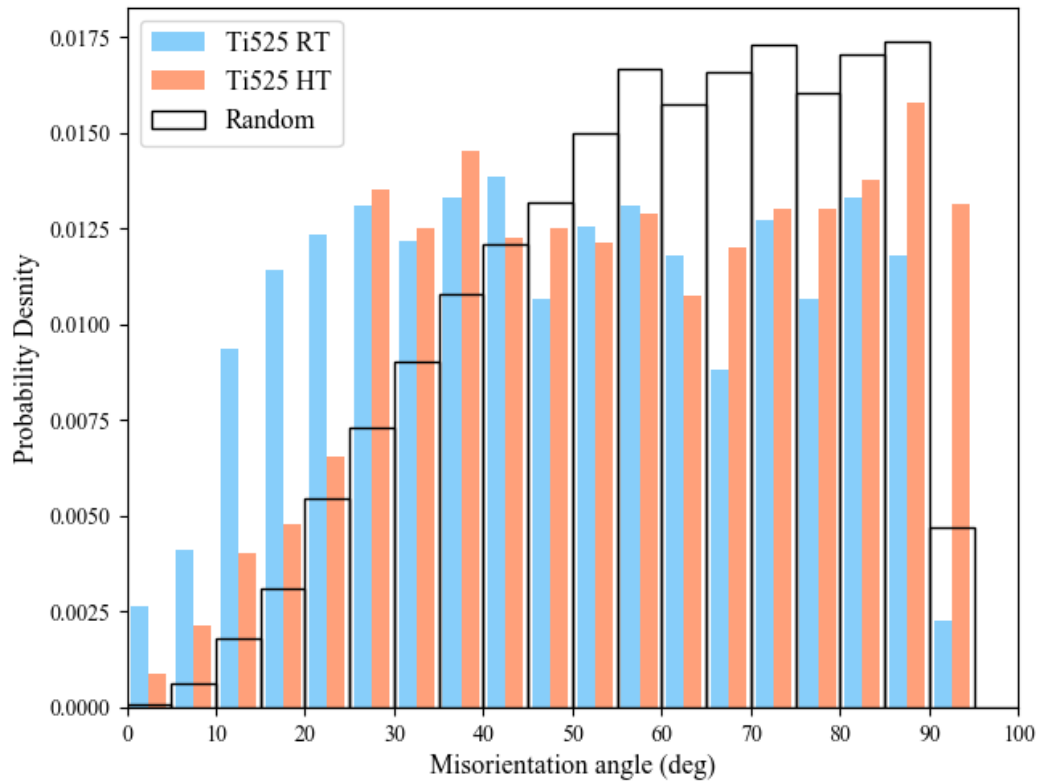


Figure 3.13: Probability density (the integral is 1) for the Ti525 728K and 296K data, and McKenzie probability distribution data for randomly generated hexagonal crystal orientations.

## Chapter 4: Results

This chapter presents the data from the grain boundaries that were fully analyzed, including metrics discussed in the Chapter 2: Literature Review.

### 4.1 Misorientation angle histogram

This section presents the data collected from the room temperature (296K) tensile tested sample and the high temperature (728K) tensile tested sample. From the orientation maps, the misorientation angles,  $m'$  values, Schmid factors, and residual Burgers vectors ( $\Delta b$ ) for the grain pairs were extracted as explained in Chapter 3: Experimental Procedure. Each grain boundary was sorted to either “slip transfer” or “no slip transfer” categories.

Figure 4.1 shows a histogram of the “slip transfer” and “no slip transfer” points plotted with respect to the misorientation angle between grains for (a) the room temperature Ti525 sample, and (b) the high temperature sample. Below 30° misorientation, “slip transfer” data are significantly higher than “no slip transfer” data in both samples. The cumulative percentage lines show the disparity between “slip transfer” and “no slip transfer” data at low misorientation angles.

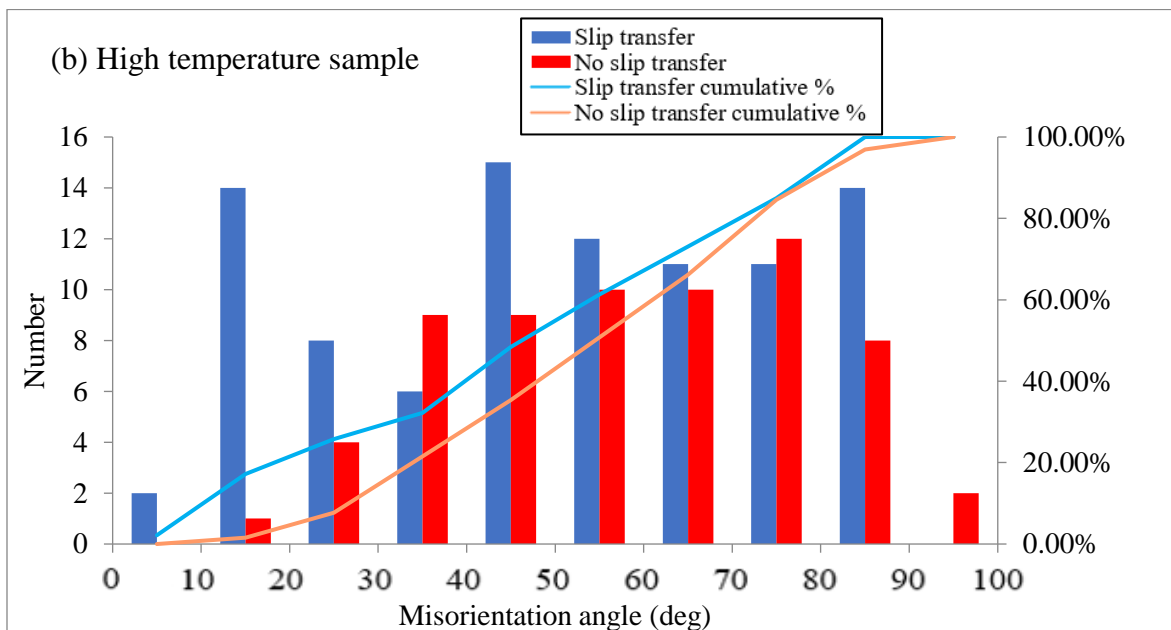
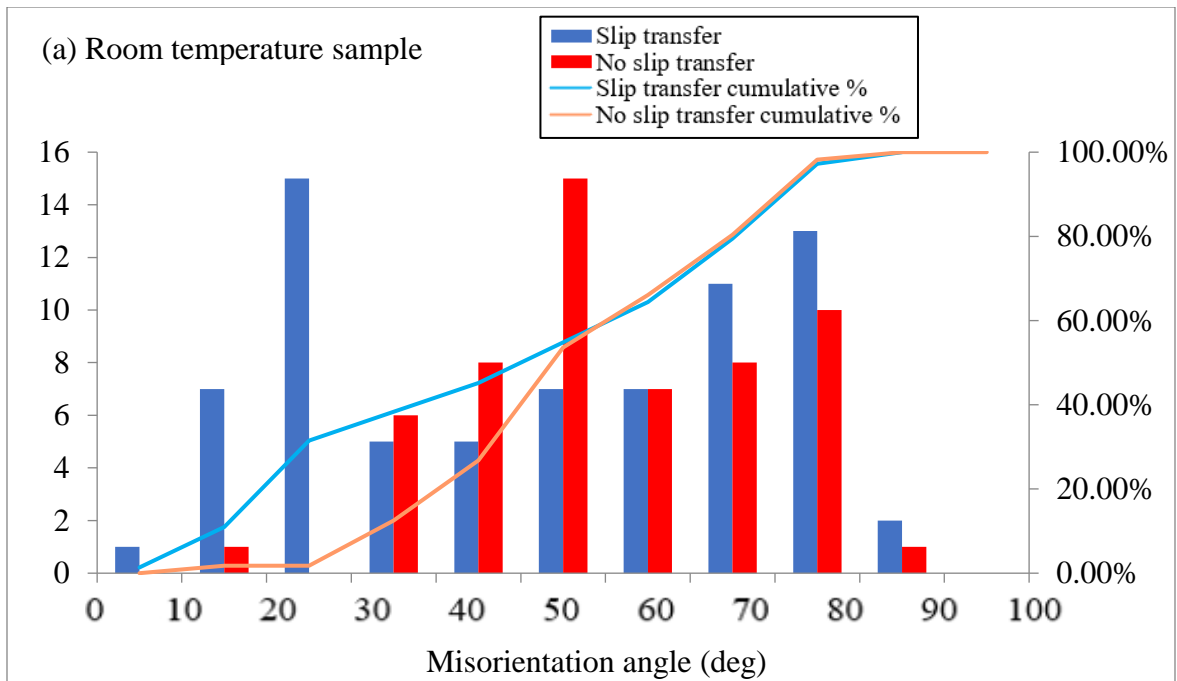


Figure 4.1: Histograms representing the “slip transfer” and “no slip transfer” data for the (a) high temperature (728K) sample and (b) the room temperature (296K) sample, binned by misorientation angle. The slip transfer category for both samples have higher values at lower misorientation angles.

## 4.2 Metric combinations

To determine which metric combinations were of interest, a matrix of all the combinations was created. Figure 4.2 shows a matrix with the possible correlations for (a) the room temperature Ti525 sample, and (b) the high temperature sample. In both matrices, metric pairs with interesting trends include  $m'$  vs.  $\Delta b$ ,  $m'$  vs. misorientation angle, and  $\Delta b$  vs. misorientation angle.

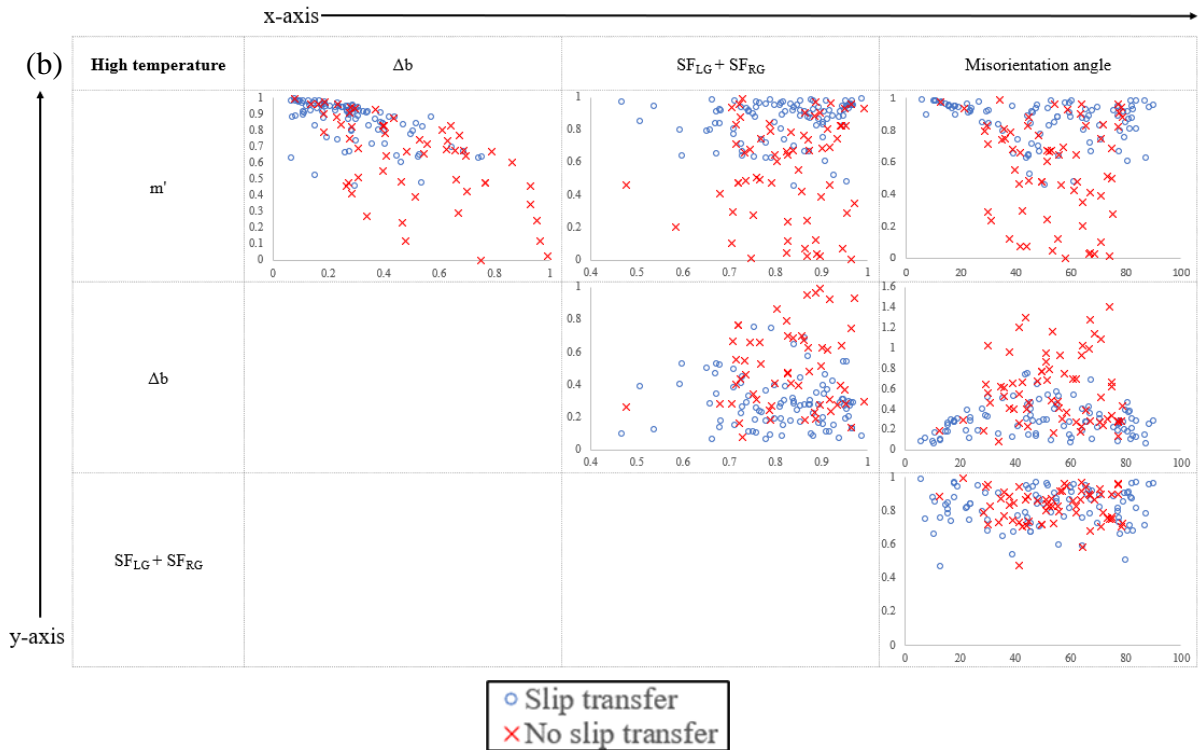
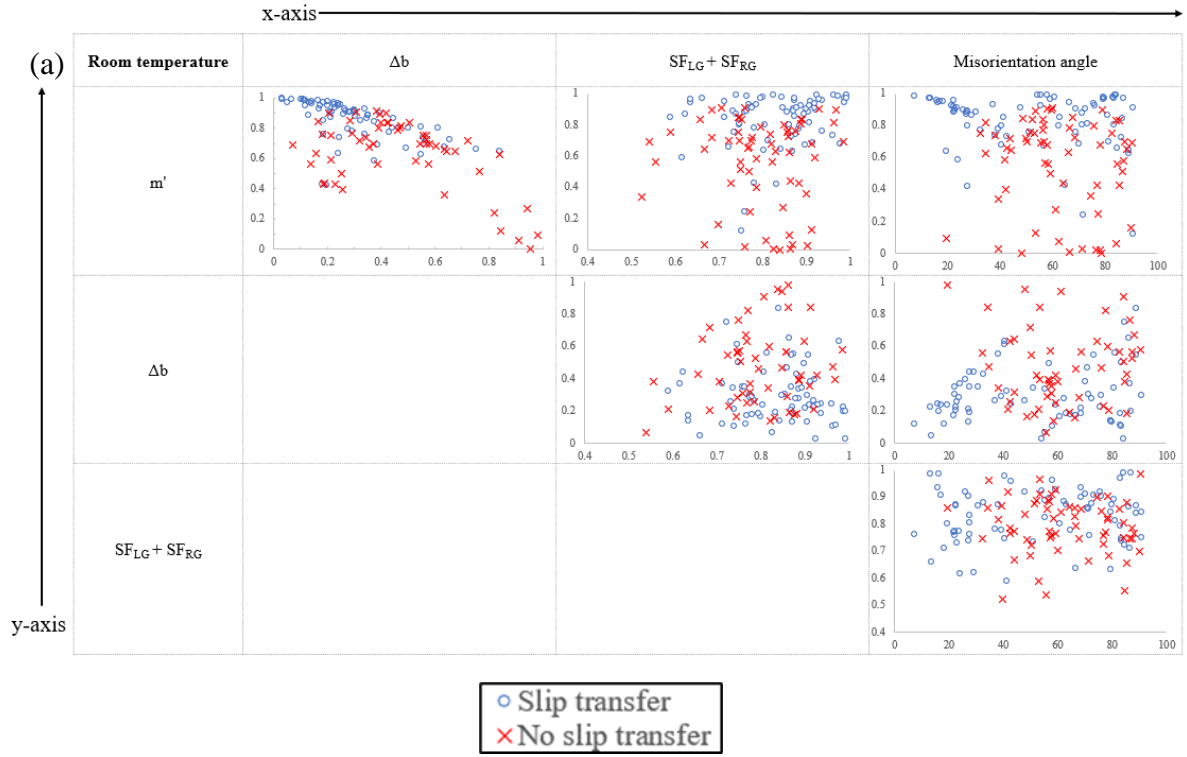


Figure 4.2: Possible combinations of factors, with correlations of interest including  $m'$  and  $\Delta b$ ,  $m'$  and misorientation angle, and  $\Delta b$  and misorientation angle.

### 4.3 Misorientation angle vs. $m'$

Figure 4.3 shows the trend of the “slip transfer” and “no slip transfer” data for misorientation vs. the geometric compatibility factor ( $m'$ ), for (a) the room temperature (296K) sample and (b) the high temperature (728K) sample. Below 20° misorientation angle in both the room temperature and high temperature sample, there is a trend of high  $m'$  values that slopes downward as the misorientation angle increases. Above 20°, the points begin to spread out, and the downward sloping trend is no longer noticeable. The room temperature sample has 3 points with a misorientation angle less than 30° and with  $m'$  values less than 0.7, indicating that the sample does not have as strong of a trend compared to the high temperature data. Most of the “no slip transfer” data lies above 30° misorientation angle in both samples. There is no observed trend in the “no slip transfer” data otherwise.

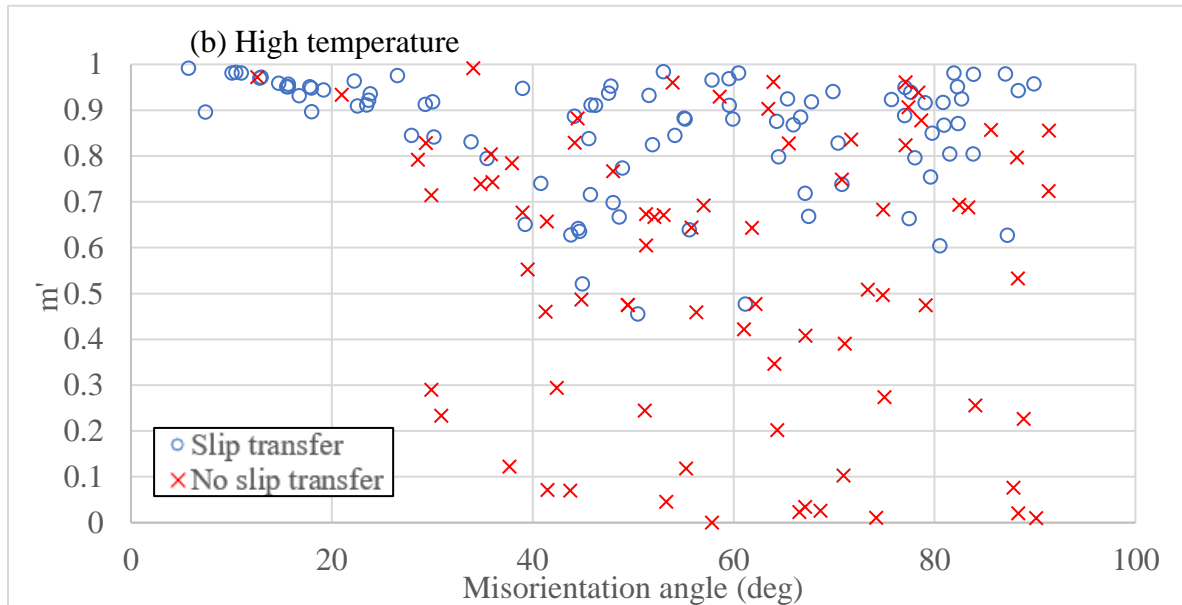
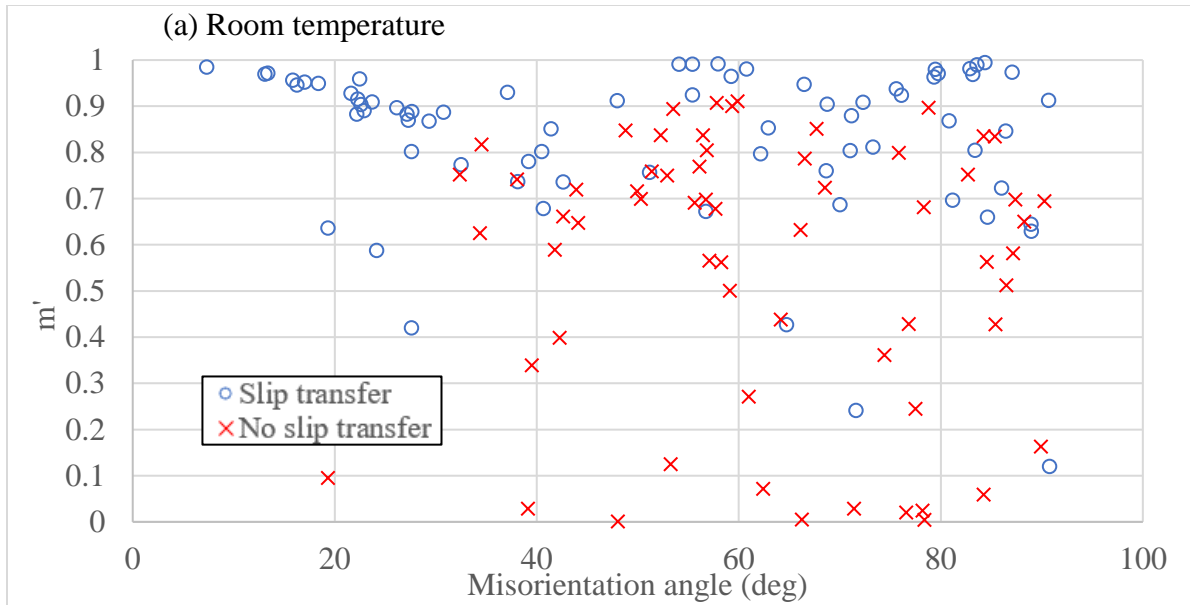


Figure 4.3:  $m'$  vs. misorientation angle for (a) the room temperature (296K) sample and (b) the high temperature (728K) sample. There is a decreasing trend for misorientation angles below  $20^\circ$  in both samples. Above  $20^\circ$ , the trend is no longer observed.

#### 4.4 $m'$ vs. residual Burgers vector ( $\Delta b$ )

The Luster-Morris parameter ( $m'$ ) vs. the residual Burgers vector ( $\Delta b$ ) is plotted in Figure 4.4 for (a) the room temperature (296K) sample and (b) the high temperature (728K) sample.

The black dotted lines are plotted such that the maximum number of “slip transfer” points are inside the box and the maximum number of “no slip transfer” points are outside the box. For the room temperature sample, 64% of the “slip transfer” points are located inside the black dashed box, and 94% of the “no slip transfer” points are outside the dashed box. For the high temperature sample, 91% of the “slip transfer” points are located inside the black dashed box, and 68% of the “no slip transfer” points are outside the dashed box. The high temperature data shows a much larger black dotted box compared to the room temperature data, and the relative percentages of the two populations inside and outside the box are reversed. The “slip transfer” data are clustered in the lower right-hand corner of the graph, i.e. at high  $m'$  and low residual Burgers vector values. The “no slip transfer” points are spread out, and there are many points within the lower right box for the high temperature data. This indicates that the slip transfer happens more frequently with lower  $m'$  and higher residual Burger vectors in the high temperature sample.

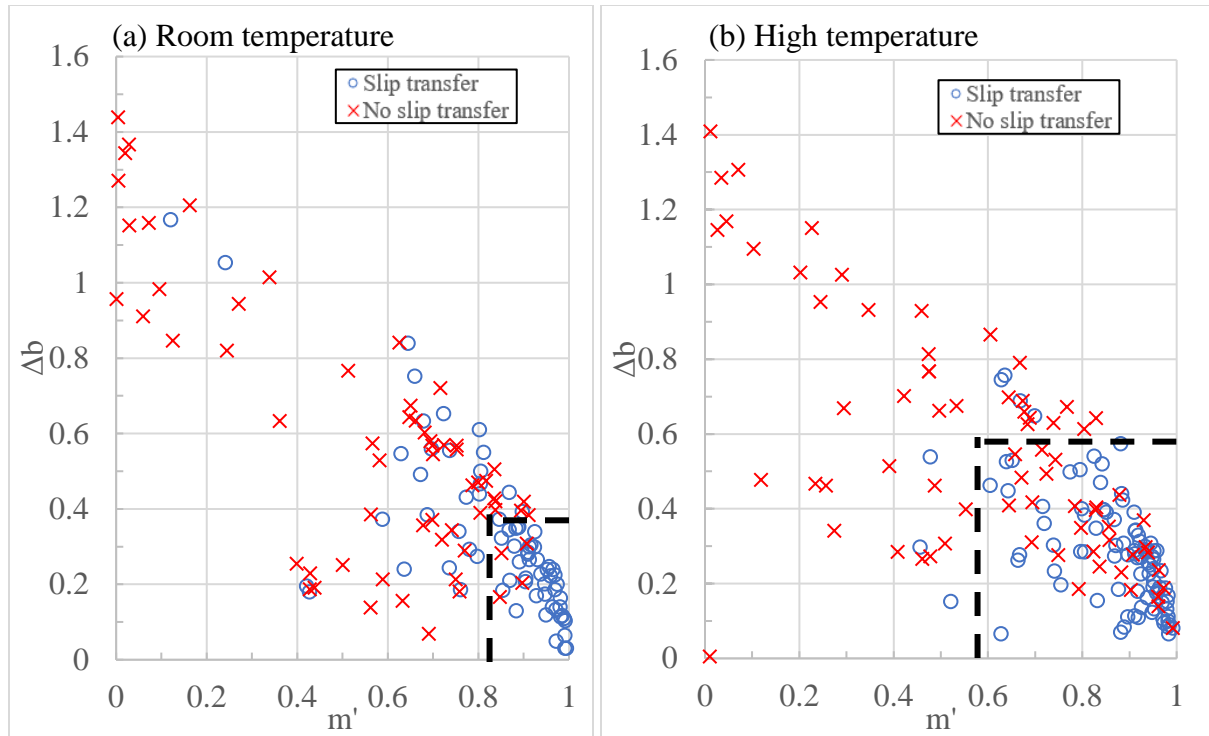


Figure 4.4:  $m'$  vs. the residual Burgers vector for (a) the room temperature (296K) Ti525 sample and (b) the high temperature (728K) sample. The cluster of “slip transfer” points, denoted with dotted lines, have high  $m'$  parameters and low residual Burgers vectors. The dashed black lines represent the boundary where the maximum number of “slip transfer” and “no slip transfer” data are inside and outside of the box respectively.

#### 4.5 Misorientation angle vs. the sum of the Schmid factors

As described in Chapter 2: Literature Review, at high  $m'$  and high Schmid factors, slip transfer is likely to occur. The sum of the two Schmid factors times the corresponding  $m'$  value ( $m'(SF_{LG}+SF_{RG})$ ) is plotted against the misorientation angle in Figure 4.5 (a) the room temperature (296K) data and (b) the high temperature (728K) data, where  $SF_{LG}$  and  $SF_{RG}$  is the Schmid factor of the left grain and right grain respectively. In the room temperature sample above the purple line lies the maximum “slip transfer” data (~75%) and below lies the maximum “no slip transfer” data (~82%). In the high temperature sample above the purple solid line lies the maximum “slip transfer” data (~94%) and below lies the maximum “no slip transfer” data

(~56%). Both thresholds in the high temperature and room temperature sample are increasing lines, lying between 0.4 and 0.8  $m'(SF_{LG}+SF_{RG})$  values. The “no slip transfer” data have a larger spread of  $m'(SF_{LG}+SF_{RG})$ , while the “slip transfer” data have a  $m'(SF_{LG}+SF_{RG})$  closer to 1 for both data sets. In the high temperature data set, there is a cluster of “slip transfer” points between 35° and 50° misorientation that have a  $m'(SF_{LG}+SF_{RG})$  value below 0.6. This cluster is not present in the room temperature data.

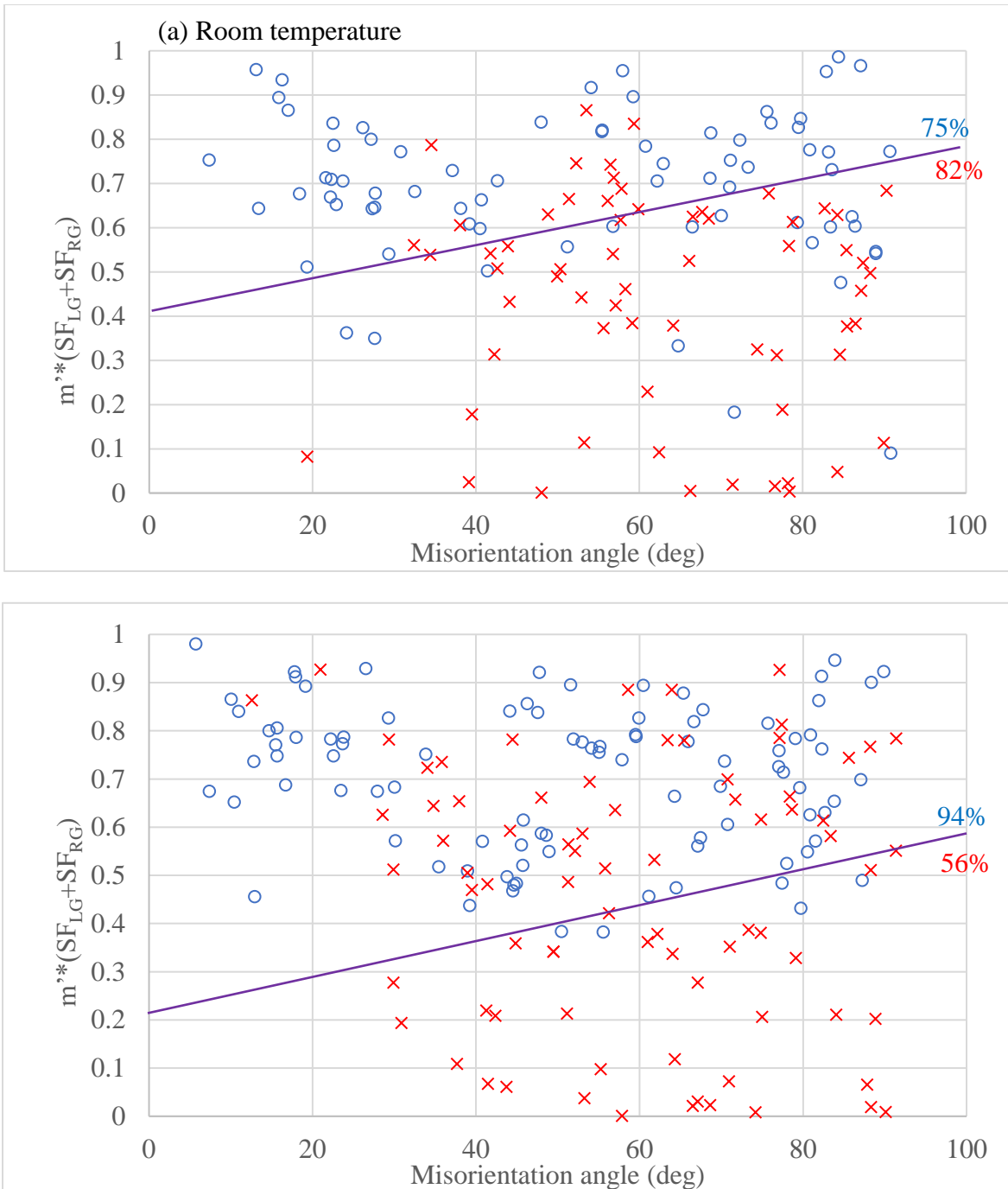


Figure 4.5: The  $m'*(SF_{LG}+SF_{RG})$  parameter vs. misorientation angle for (a) the room temperature (296K) Ti525 sample, and (b) the high temperature (728K) sample. High  $m'*(SF_{LG}+SF_{RG})$  is noted for “slip transfer” data in both cases. There is a decreasing trend in “slip transfer” data below 30° misorientation angle. The “no slip transfer” data are mostly present above 30° misorientation angle.

#### 4.6 Misorientation angle vs. $m'/\Delta b$

Chapter 3 identifies another factor worth looking at graphically,  $m'/\Delta b$ , where  $\Delta b$  is the residual Burgers vector. Figure 4.6 shows the relationship between misorientation angle and  $m'/\Delta b$ . In Figure 4.6 (a) the room temperature (296K) sample, above the purple line (which is constructed to have maximum “slip transfer” points above, and maximum “no slip transfer” points below) is 90% of the “slip transfer” data, and below to which has 60% of the “no slip transfer” data. Figure 4.6 (b), the high temperature (728K) sample, above the purple solid line is 63% of the “slip transfer” data, and below the purple solid line is 84% of the “no slip transfer” data. There is a decreasing  $m'/\Delta b$  trend for “slip transfer” data below the 30° misorientation angle for both the high temperature (728K) data and the room temperature (295K) data. The high temperature data set is observed to have a stronger trend in this region, as the data is more closely packed. Above 30° misorientation angle, both “no slip transfer” and “slip transfer” data have a larger spread but there appears to be a threshold for the “slip transfer” data (above  $m'/\Delta b = 1$ ), while the “no slip transfer” data are scattered over a wider range. Both the “no slip transfer” and “slip transfer” data for the room temperature sample has a larger spread compared to the high temperature data.

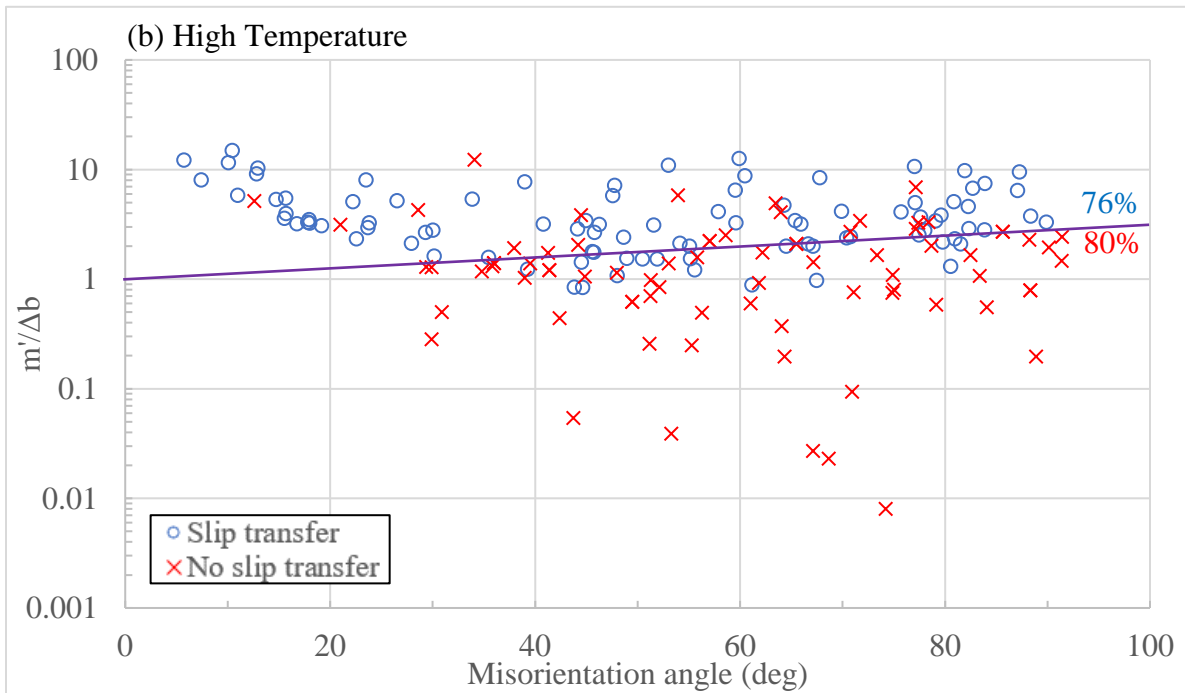
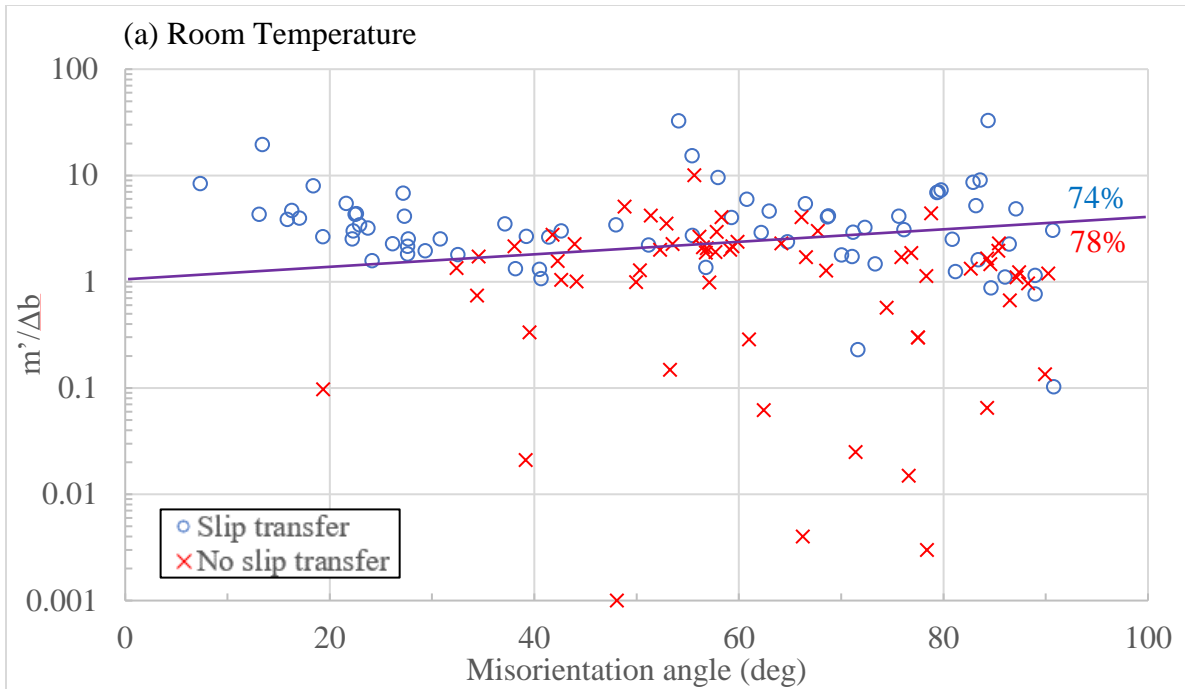


Figure 4.6:  $m'/\Delta b$  vs. misorientation angle for (a) the room temperature (296K) sample and (b) the high temperature (728K) sample. In both samples, a strong decreasing  $m'/\Delta b$  trend for ‘slip transfer’ data below  $30^\circ$  misorientation angle.

#### 4.7 Slip systems present

Each datum point presented thus far has two grains associated with it, each with its own favored/active slip systems. Figure 4.7 and Figure 4.8 represents the same data presented in Figure 4.6 but with the slip systems computed to be present distinguished by color and shape. In Figure 4.7 (a), the “slip transfer” data for the room temperature (296K) sample, there is a cluster of prism<a> to prism<a> slip transfer between 15° and 30° misorientation angle is noted. A cluster of prism<a> to basal slip above 80° misorientation angle is also noted. Basal to basal favored slip is common at lower misorientation angles. In Figure 4.7 (b), the “slip transfer” for the high temperature (728K) sample, there is a cluster of prism<a> to prism<a> slip transfer in grain pairs with misorientation angle less than 45°. There is an observed cluster of prism<a> to pyramidal<a> slip transfer between 20° and 30° misorientation angle. Around 45° misorientation angle there is another cluster of prism<a> to pyramidal<a>. A cluster of basal to pyramidal<a> between misorientation angles 45° to 60° is also observed.

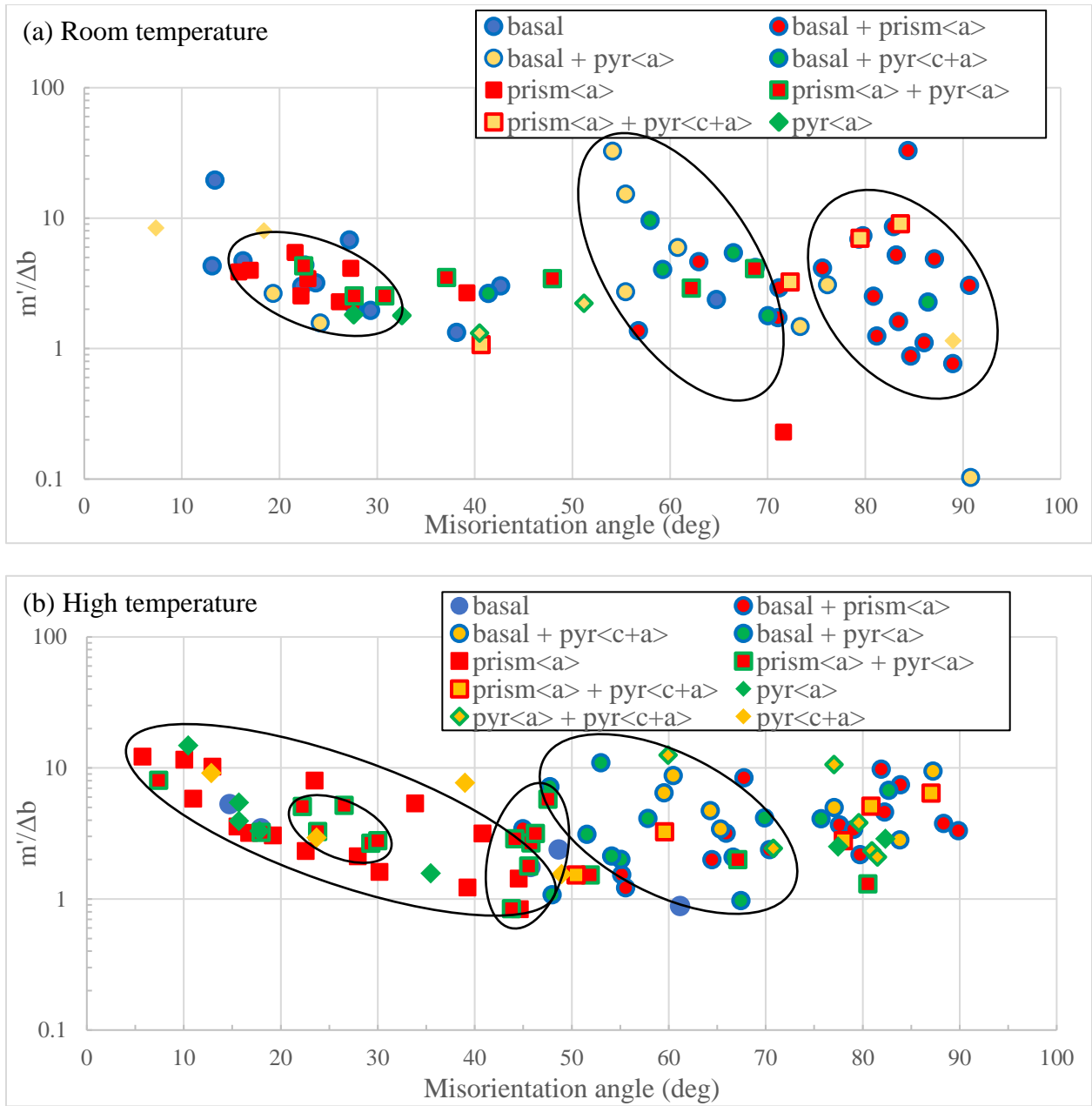


Figure 4.7: “Slip transfer”  $m'/\Delta b$  vs. misorientation angle represented with computed slip systems for each grain pair in (a) the room temperature (296K) sample and (a) the high temperature (728K) sample. There is a cluster of prism<a> to prism<a> slip in grain pairs with misorientation angle less than  $30^\circ$  in the high temperature sample and between  $15^\circ$  and  $30^\circ$  in the room temperature sample.

Figure 4.8 presents the “no slip transfer” data with colors and shapes representing observed slip systems in the two grains for (a) the room temperature (296K) sample, and (b) the high temperature (728K) sample. For the room temperature sample Figure 4.8 (a), there is a cluster of pyramidal<c+a> slip systems between 40° and 50° misorientation angle. There are two clusters of prism<a> + pyramidal<c+a> between 50° and 60° misorientation angle and 75° to 90° misorientation angle. In the high temperature sample Figure 4.8 (b), below 25° misorientation angle, both points are prism <a> to prism <a> slip. There is no other trend observed in the data, as the data are sporadic above 25° misorientation angle.

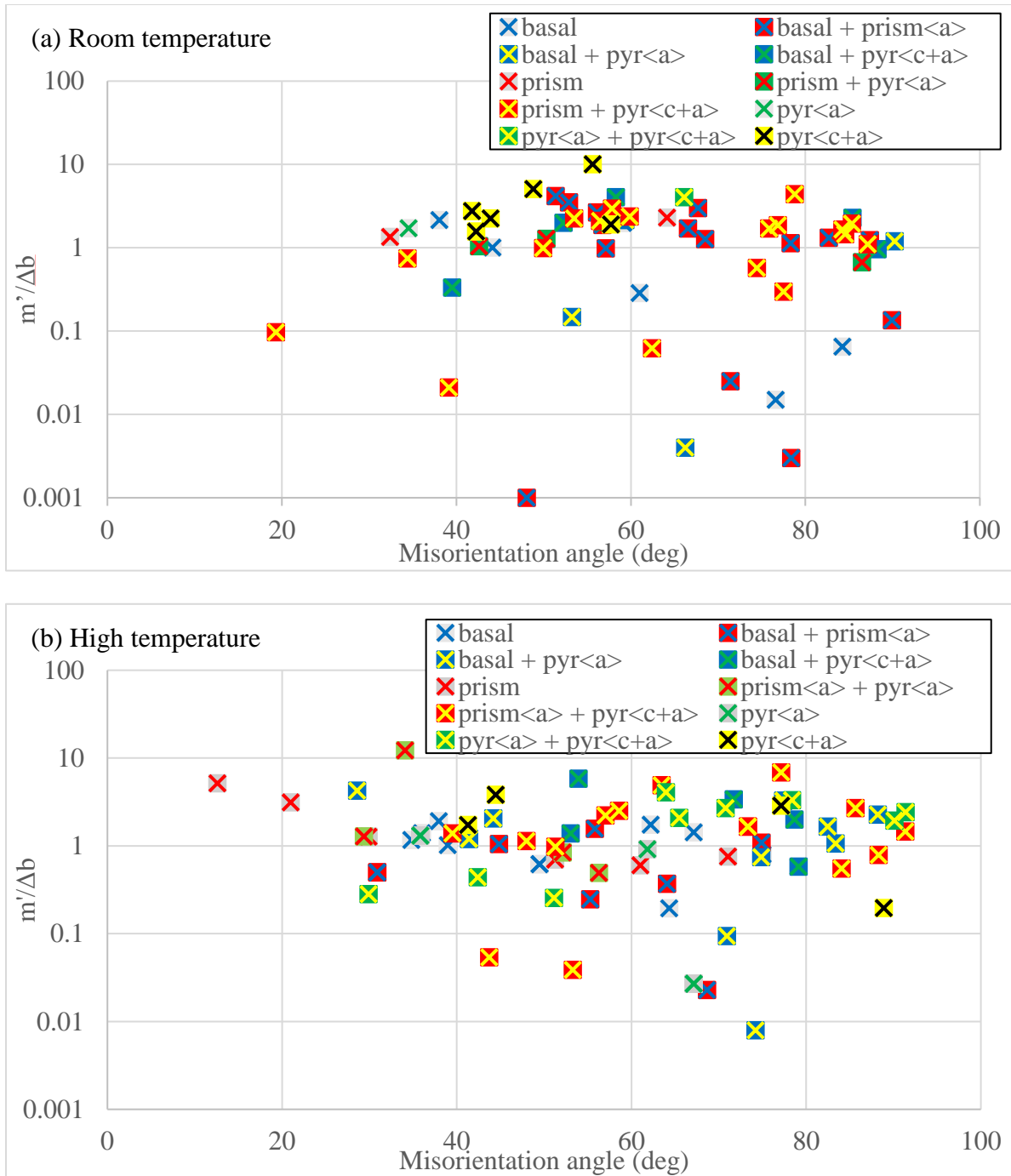
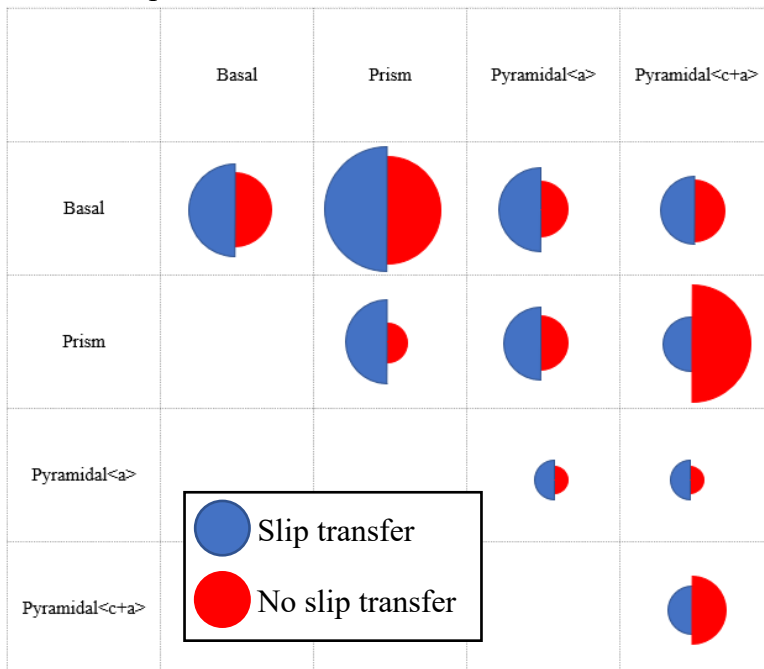


Figure 4.8: “No slip transfer”  $m'/\Delta b$  vs. misorientation angle represented with observed active slip systems for each grain pair for (a) the room temperature (296K) tensile tested sample and for (b) the high temperature (728K) tensile tested sample. Few clusters are observed in both data sets.

Figure 4.9 presents statistics comparing prevalent slip systems for “slip transfer” and “no slip transfer” data in the (a) room temperature (296K) sample and (b) high temperature (728K) samples. The relative area of the half circle represents the frequency of that slip system pair. For the room temperature sample, in both the “slip transfer” and “no slip transfer” data sets, basal to prism has the highest frequency. For the high temperature “slip transfer” data set, prism to prism and prism to pyramidal<a> are both the most prevalent. In the high temperature “no slip transfer” data, prism to pyramidal<c+a> is most prevalent. As a group, the most prevalent slip system pair is basal to prism <a> and the least prevalent slip system pair is pyramidal<c+a> to pyramidal<c+a>. The high temperature sample has a significant increase in pyramidal slip transfer data compared to the room temperature sample.

(a) Room temperature



(b) High temperature

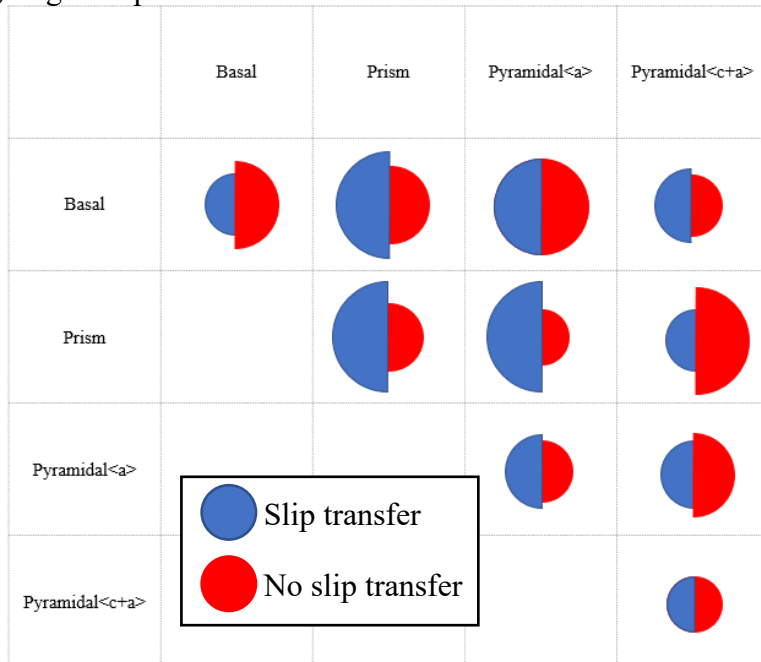


Figure 4.9: Representation of slip systems prevalent in the high temperature (728K) and room temperature sample. The most prevalent slip system pair in the room temperature (296K) data is basal to prism. The slip system pair that shows up the least in all the data is pyramidal<c+a> to pyramidal<c+a>.

The chapter has provided an extensive assessment of slip transfer in the high temperature and room temperature tensile tested Ti525 alloy. Using parameters such as the misorientation angle ( $m'$ ), Schmid factor, and residual Burgers vector ( $\Delta b$ ), the “slip transfer” and “no slip transfer” data were compared. Low  $\Delta b$ , and high  $m'$  grain pairs are more likely to have slip transfer present. The  $m'$  parameter vs. the misorientation angle shows a strong decreasing trend for “slip transfer” data below 30° misorientation angle. The trends found in this section have some differences from room temperature to high temperature tensile testing, which includes the high temperature sample having a general larger spread of data.

## Chapter 5: Discussion

This chapter provides an analysis of the results presented in Chapter 4. This chapter will compare the results of the high temperature tensile tested sample, to the room temperature tensile tested sample. In addition, the results obtained in the Ti525 room temperature tensile (296K) sample and high temperature (728K) sample are especially useful when compared to the results of Alizadeh et al. “A criterion for slip transfer at grain boundaries in Al”. Alizadeh performed an investigation in an aluminum oligo-crystal tensile sample tested at room temperature. Comparison between the two crystal structures will shed new understanding about what facilitates slip transfer.

### 5.1 $m'$ vs. $\Delta b$

Figure 5.1 (a) and (b) compare the  $m'$  vs. residual Burgers vector ( $\Delta b$ ) for the room temperature (296K) sample and high temperature (728K) sample, respectively. The green box identifies the cluster boundary determined by Alizadeh between “slip transfer” and “no slip transfer” for the Aluminum oligo-crystal. Alizadeh maximized the percentage of “slip transfer” points within the box and percentage of “no slip transfer” points outside the box. Within the box lies 93% of “slip transfer” data for the Al sample. Outside the box lies 86% of “no slip transfer” data for the aluminum sample. A similar activity was completed for the Titanium sample, as explained in Chapter 4: Results. A comparison of Al maximized boundaries and Titanium maximized boundaries in Table 5.1. The aluminum sample has a boundary of lower  $\Delta b$  and higher  $m'$  values compared to the high temperature tensile tested sample (Figure 5.1 (b)). In comparing the room temperature Ti525 sample and the room temperature aluminum sample (Figure 5.1 (a)), the boundaries are very similar indicating their data sets are similar. This shows the temperature dependence of the  $m'$  vs.  $\Delta b$  factors. Higher  $\Delta b$  values and lower  $m'$  values

enable slip transfer when the temperature in the material is hotter. In comparing the titanium room temperature sample to the titanium high temperature sample, more points with lower  $m'$  values are observed.

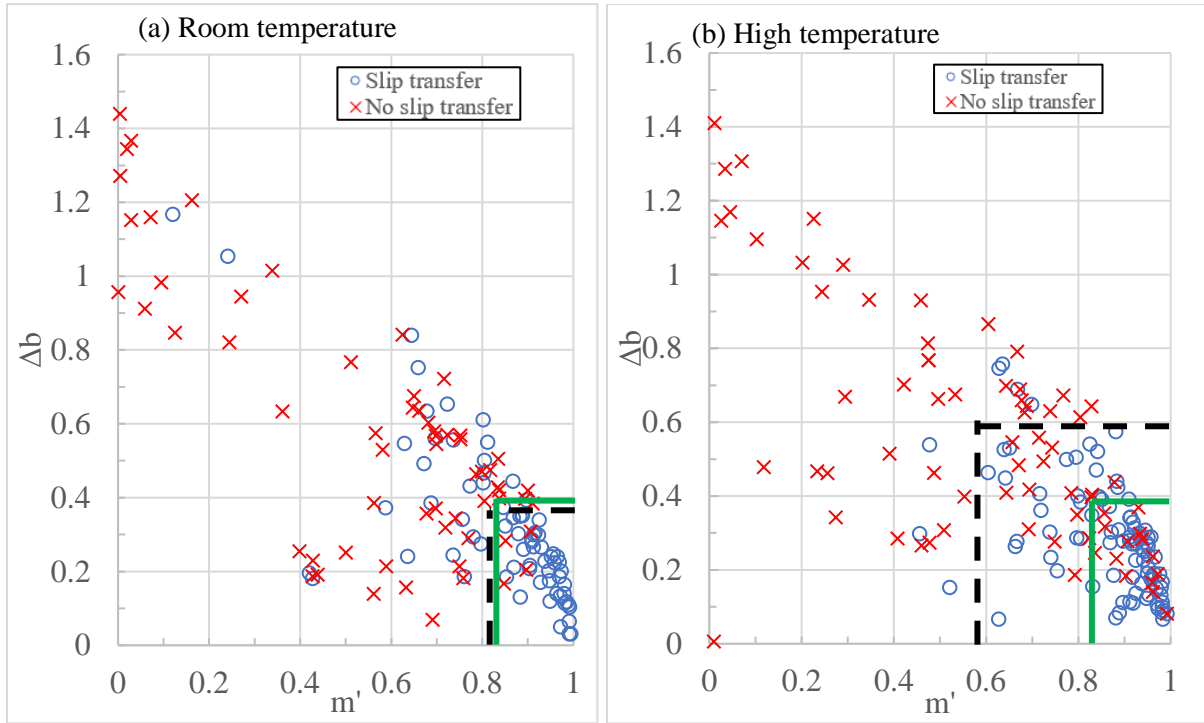


Figure 5.1:  $m'$  vs.  $\Delta b$  data for the (a) room temperature (296K) and (b) the high temperature (728K) tensile tested Ti525 sample. Green boxes indicate comparable Al oligo-crystal tensile results at room temperature for both (a) and (b).

Table 5.1: Percentages of “slip transfer” and “no slip transfer” inside and outside of boundaries, respectively. RT and HT Ti5252 relationships are flipped with high percentage of “no slip transfer” outside of the box in RT and high percentage of “slip transfer” inside the box for HT.

	Slip transfer (Inside)	No slip transfer (Outside)
RT Ti525	64%	94%
HT Ti525	91%	68%
RT Al	93%	86%

Dislocation climb in titanium alloys is facilitated by higher temperatures. If dislocations can climb near the boundary to align themselves with a lower  $m'$  geometry partner, then slip transfer is enabled under less favorable conditions. Higher diffusion rates enable recovery processes to take place near and within grain boundaries, so that residual Burgers vector debris is more easily absorbed.

The homologous temperatures of the two materials are different from each other. The melting temperature for Ti525 is 1863K (1590°C) and the melting temperature for aluminum is 933K (660°C). Room temperature is  $0.16 T_m$  for Ti525 and  $0.32 T_m$  for aluminum. In addition, the high temperature Ti525 experiment was performed at  $0.39 T_m$  (728K) which is equivalent to 364K (90°C) for Al. This fraction is closer to that of the room temperature aluminum homologous temperature. Table 5.2 shows these relations.

Table 5.2: Temperature comparison for Al and Ti525. RT Al and HT Ti525 have similar homologous temperatures.

	Homologous Temperature	Melting Temperature (Kelvin)	Test Temperature (Kelvin)
RT Ti525	$0.16 T_m$	1863	296
RT Al	$0.32 T_m$	933	296
HT Ti525	$0.39 T_m$	1863	728

Given that the slip transfer behavior in aluminum and Ti525 are more similar to each other at room temperature, the effect of alloying elements and/or the much lower CRSS in pure aluminum may lead to less stress assisted climb forces for a similarly high homologous temperature, such that the higher stresses in Ti525 facilitated climb more effectively than in Al. The stiffness normalized strength in Ti525 was 0.006 for the room temperature sample and 0.003

for the high temperature sample while it was 0.00036 in pure Al. Table 5.3 shows the normalized strength and the values used to obtain the metric. The aluminum compensated strength is significantly lower than the Titanium alloy, due to the effects of alloying.

Table 5.3: Compensated Strengths and values used to obtain them. The pure aluminum compensated strength is much lower than the Titanium alloy (Aluminum 1100-O and Li 2013).

	Young's Modulus (GPa)	Yield Strength (MPa)	Compensated Strength (Yield Strength / Young's Modulus)
RT Ti525	110	660	0.006
HT Ti525	110	330	0.003
RT Al	70	25	0.00036

## 5.2 Misorientation angle vs. $m'$

Figure 5.2 shows the misorientation angle vs.  $m'$  for “slip transfer” and “no slip transfer” categories for both the titanium oligo-crystal and the aluminum alloy samples. The room temperature (296K) Ti525 tensile sample (a), and the high temperature (728K) Ti525 tensile sample (b) are overlaid with the shaded areas representing the locus of most of the points in the aluminum polycrystal. Since aluminum has a cubic structure with a maximum disorientations of  $63^\circ$  there is a much larger range of misorientation as well as  $m'$  values for Ti525 slip transfer points. The black box shows the comparable area from the aluminum data. Alizadeh identified a threshold of about  $20^\circ$  that best separated the “slip transfer” and “no slip transfer” categories, which occurred in the middle of the “slip transfer” region (blue region). The titanium alloy shows similar behavior, but the threshold is not as distinct, as most observations are at misorientations larger than  $20^\circ$ . This disparity could arise from the fewer easy slip systems in hexagonal crystal structures that lead to more heterogeneous stress states in titanium. Another possibility is that the aluminum oligo-crystal grains have mostly free surfaces while the Ti525

sample is a polycrystal, where only one side of the grain has a free surface, which makes the stress state more complex.

Also, unlike the Ti alloy, the aluminum oligo-crystal has a strong texture, so that most grains had a more similar stress state and strain response. With fewer easy slip systems available in the Ti525, slip may be required on slip systems that do not facilitate slip easily, leading to a wider variation in the local stress state, which would lead to more spread in the data, as the Schmid factor is based upon the assumption of a uniform uniaxial stress. Furthermore, the “no slip transfer” points are not present in the room temperature titanium sample below  $\sim 30^\circ$  misorientation, while in the aluminum and high temperature Ti525 data sets, they are present at misorientations as low as  $\sim 10^\circ$  in Al and the high temperature Ti525 data. These differences imply that differences in crystal structure and geometrical limitations need to be considered.

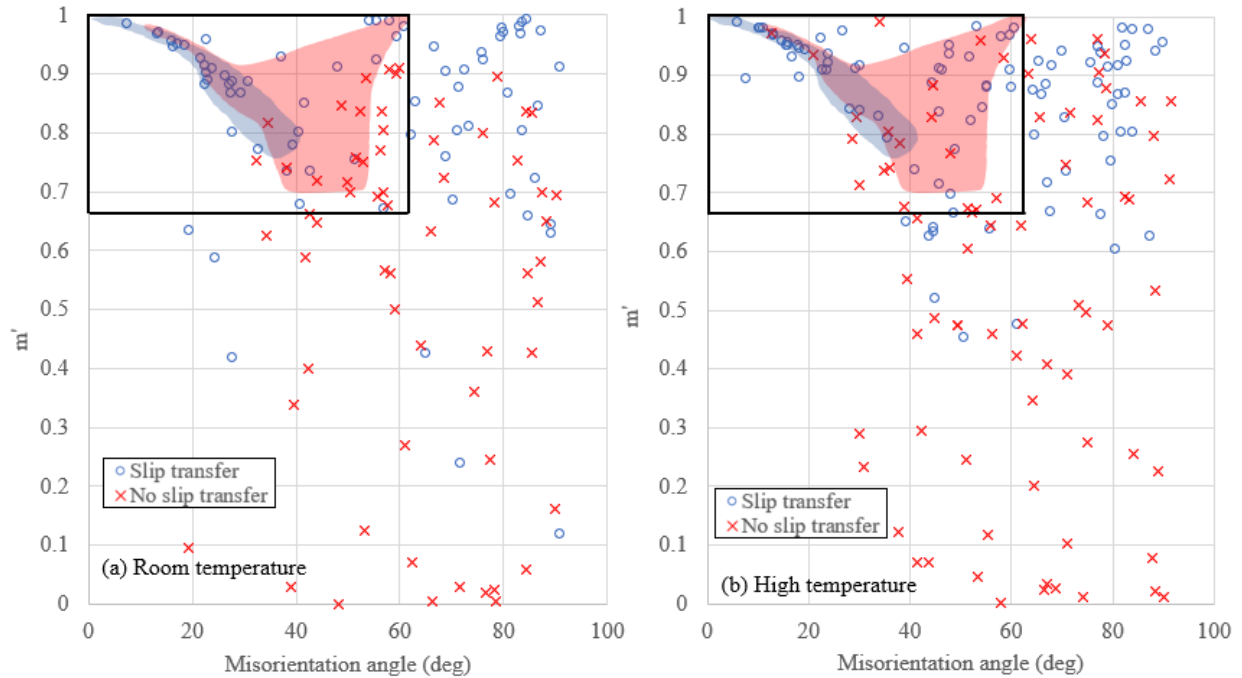


Figure 5.2: Aluminum oligo-crystal “slip transfer” (blue shaded area) and “no slip transfer” (red shaded area) compared to data of the titanium polycrystal “slip transfer” and “no slip transfer” data for (a) the room temperature (296K) sample and (b) the high temperature (728K) sample. Titanium “slip transfer” and “no slip transfer” points do not follow as strict of a trend compared to the aluminum data.

### 5.3 Misorientation angle *vs.* the sum of Schmid factors

Figure 5.3 shows comparison between the misorientation angle *vs.*  $m'(SF_{LG}+SF_{RG})$  for the (a) room temperature Ti525 alloy, (b) high temperature Ti525 alloy. The green solid line represents the thresholds for aluminum, where “slip transfer” points was prevalent above the green line (for strongly textured Al with two different tensile axis directions). The same process done with the titanium data set as described in Chapter 4: Results. The trends between the boundaries of the aluminum and titanium “slip transfer” data are significantly different, in that a shallow positive slope best separates prevalent “slip transfer” and “no slip transfer” populations, and the threshold is much lower threshold than that for Al. The boundaries for the high temperature and room temperature samples in the titanium alloy are very similar, but lower for

high temperature data. This also indicates that a threshold for  $m'(SF_{LG}+SF_{RG})$  vs. misorientation angle is heavily dependent on material and crystal structure. Clearly, the geometrical constraints for slip transfer are much smaller in the hexagonal crystal structure than in Al.

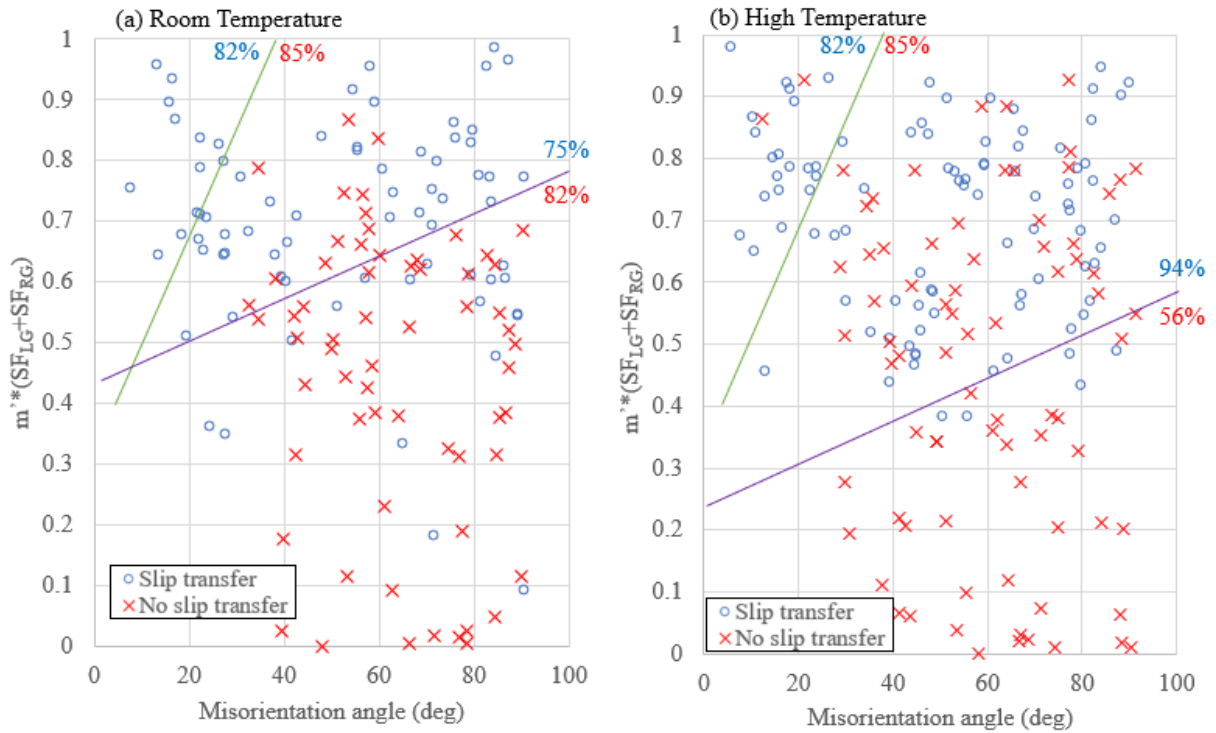


Figure 5.3: Misorientation angle vs.  $m'(SF_{LG}+SF_{RG})$  for the (a) room temperature Ti525 sample and the (b) high temperature Ti525 sample. The aluminum boundaries represented by the green line show the difference between the aluminum data set which has a steep slope and the titanium data set which slope is flatter.

#### 5.4 Misorientation angle vs. $m'/\Delta b$

Figure 5.4 presents the misorientation angle vs.  $m'/\Delta b$  for (a) the room temperature tensile tested sample and (b) the high temperature sample. The shaded areas are approximate representations for misorientation angle vs.  $m'/\Delta b$  for the aluminum oligo-crystal. The blue shaded region for the aluminum oligo-crystal “slip transfer” data and the blue cluster of data

from the titanium alloy below  $30^\circ$  misorientation angle line up well, indicating a strong correlation between the two data sets in this range. The red shaded area representing the aluminum “no slip transfer” data expands greatly below  $m'/\Delta b = 1$ , as do the red x markers representing the titanium “no slip transfer” data. The black rectangle represents the data bounds for the FCC aluminum data set. Figure 5.4 also shows that there are less geometrical constraints for slip transfer in the hexagonal Ti alloy than the Aluminum FCC material. In comparing the 296K to 728K Ti525 data, the boundary lines separating maximum “slip transfer” and “no slip transfer” are nearly the same, but the higher temperature has a slightly smaller slope indicating that temperature does not have a great effect on  $m'/\Delta b$  vs. the misorientation angle.

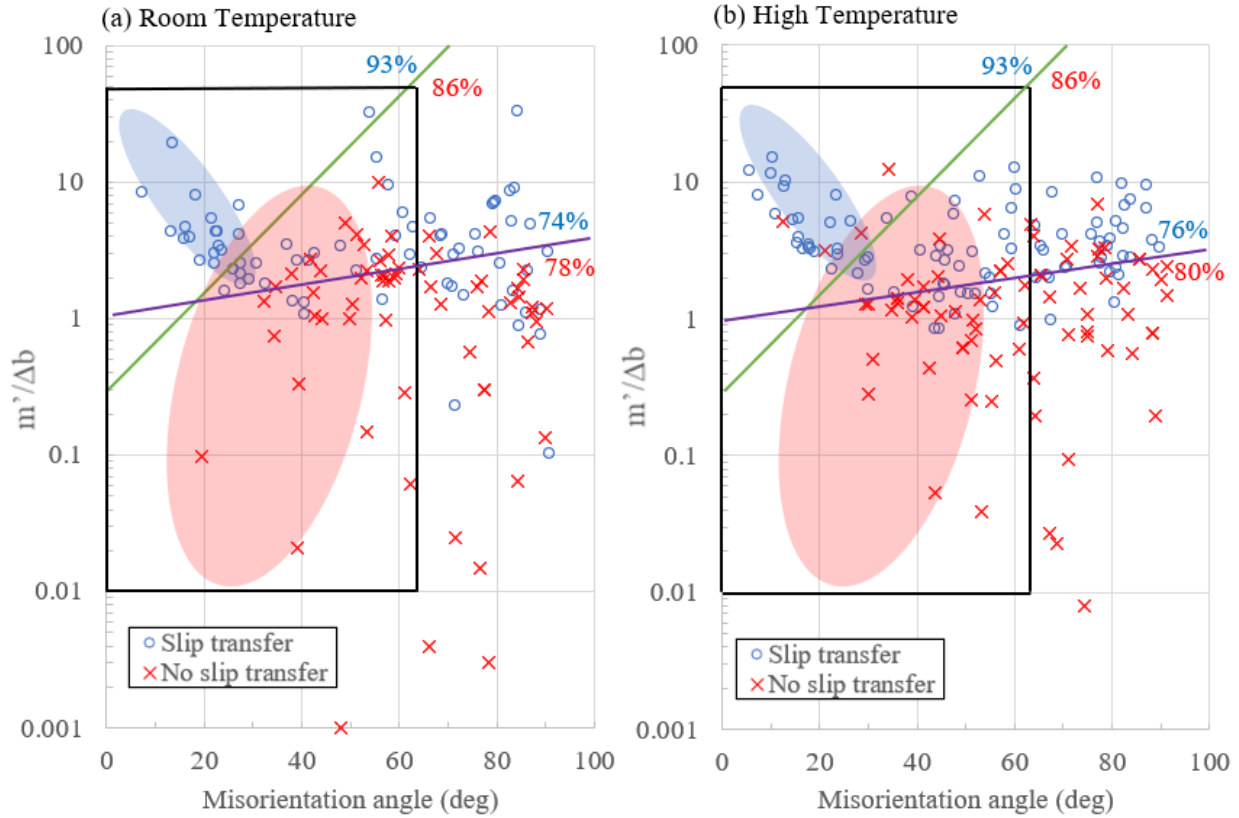


Figure 5.4: Misorientation vs.  $m'/\Delta b$  for (a) the room temperature (296K) tensile test sample and (b) the high temperature (728K) sample. The red shaded area represents the aluminum oligo-crystal “no slip transfer” data set. The blue shaded area represents the aluminum oligo-crystal “slip transfer” data set and line up with the slip transfer points in the titanium data sets.

### 5.5 Slip system analysis

Figure 4.6 shows the favored slip systems for grain pairs that have “slip transfer” in (a) the room temperature (296K) Ti525 sample and in (b) the high temperature (728K) Ti525 sample. The clusters of slip systems described in the section could be attributed to geometric conditions that the hexagonal crystal system imposes on the slip transfer process. At lower misorientation ranges, slip transfer between all slip systems are likely to be favored. The cluster of basal to pyramidal<a> slip transfer between misorientation angles  $45^\circ$  and  $60^\circ$  noted in the “slip transfer” high temperature (728K) sample can be explained by the angle between the two

slip planes. At a misorientation of  $45^\circ$  to  $60^\circ$  the basal plane of one crystal is more likely to be aligned with the pyramidal plane of the second crystal.

Figure 4.7 shows the slip systems in grain pairs that have “no slip transfer” for (a) the room temperature, and (b) the high temperature Ti525 sample. There are no strong trends observed in either graph. This is consistent with that there should be many “no slip transfer” conditions between mismatched slip systems of any family, such that a “shot gun” blast of non-favored slip systems is observed.

Figure 4.8 presents the statistics around the slip systems observed in the “slip transfer” data and “no slip transfer” data. The main slip systems activated are basal and prism, consistent with the fact that these are the most easily activated systems. This is consistent with literature that examines the relative activity of slip systems in  $\alpha$  titanium alloys (Li, 2013).

## 5.6 Comparison between measured weakly textured grain orientations to random populations

5000 orientations pairs for a hexagonal crystal structure were randomly generated. In each pair the probable slip systems for uniaxial tension was determined for each grain. For each grain, the Schmid factors were calculated for each slip system and in each grain pair,  $m'$  was calculated. Two different filters were applied to 5000 randomly generated orientation pairs to obtain two populations. The first (Ran 0.9) collects slip system pairs with an  $m'$  value above the threshold of 0.9 and grain pairs that have Schmid factors of a minimum of 0.3 for each grain. The second data set (Ran 0.8) does the same but with a  $m'$  threshold of 0.8 and a Schmid factor greater than 0.25, yielding a much larger set of nearly 25,000 data.

Figure 5.5 shows the corresponding cumulative misorientation fraction for the experimental and randomly generated data, separated by slip system pair type. In basal to basal slip, all the Ran 0.9 data is below  $\sim 20^\circ$  while all the Ran 0.8 data lies below  $\sim 35^\circ$ . The green arrow indicates which direction the Ran 0.9 data set lies in comparison to the Ran 0.8 data set. It is known that Ran 0.9 is more restrictive than Ran 0.8. As it is hypothesized that the room temperature Ti525 sample (Exp-RT) is more restrictive than the high temperature Ti525 sample (Exp-HT), the hypothesis is supported by the room temperature data being mostly to the left (lower misorientations) of the high temperature observations, but the two cross at the highest misorientations. The arrow is green because the experimental data does follow the same trend (the more restrictive data on the left) compared to the randomly generated data until about  $60^\circ$  in which the Exp-RT and Exp-HT switch. In prism to prism slip, the experimental data sets are much closer to each other, and to the simulation, but contrary to the hypothesis, the higher temperature data appear to be more restricted than lower temperature data (for most of the misorientation range). In pyramidal<a> to pyramidal<a> slip, the high temperature Ti525, Ran

0.9, and Ran 0.8 data all follow a same general trend, and the small number of room temperature observations makes it impossible to compare with the high temperature data, but the simulations show a similar trend. In pyramidal<c+a> to pyramidal<c+a> slip, there are two observed peaks in the randomly generated data, one around 25° misorientation angle, and the other around 75° misorientation angle. Interestingly, the experimental data shows one peak between the randomly generated peaks, at around 45° misorientation angle. The purple arrow depicts this discrepancy.

For the mixed slip system slip transfer, basal to prism slip shows the more restrictive of the random data sets (Ran 0.9) at highest misorientations (on the right), and the hypothesized more restricted of the experimental data (Exp-RT) is also to the right of the higher temperature data. The green arrow depicts this, but the spread of slip transfer misorientations of these two slip systems is much greater in the experimental data. In basal to pyramidal<a> slip, all data sets have a similar trend. In basal to pyramidal<c+a> slip, below 50° the more restrictive of the randomly generated data is on the right, while the hypothesized more restrictive experimental data set (Exp-RT) is on the left. Above 50°, the more restrictive randomly generated data set is now on the left, while the room temperature experimental data is on the right. This is depicted by the red arrows on the graph, indicating trends opposing the hypothesis. In prism to pyramidal<a> slip, Ran 0.9 to the left of Ran 0.8, and Exp-RT to the right of Exp-HT, again contrary to the hypothesis. In prism to pyramidal<c+a> slip, the more restrictive Ran 0.9 to the right of Ran 0.8, and the more restrictive Exp-RT to the left of Exp-HT (except for between 50° and 70°). In pyramidal<c> to pyramidal<c+a> slip there is a relationship opposite of expected when concerning the restrictiveness of the data sets.

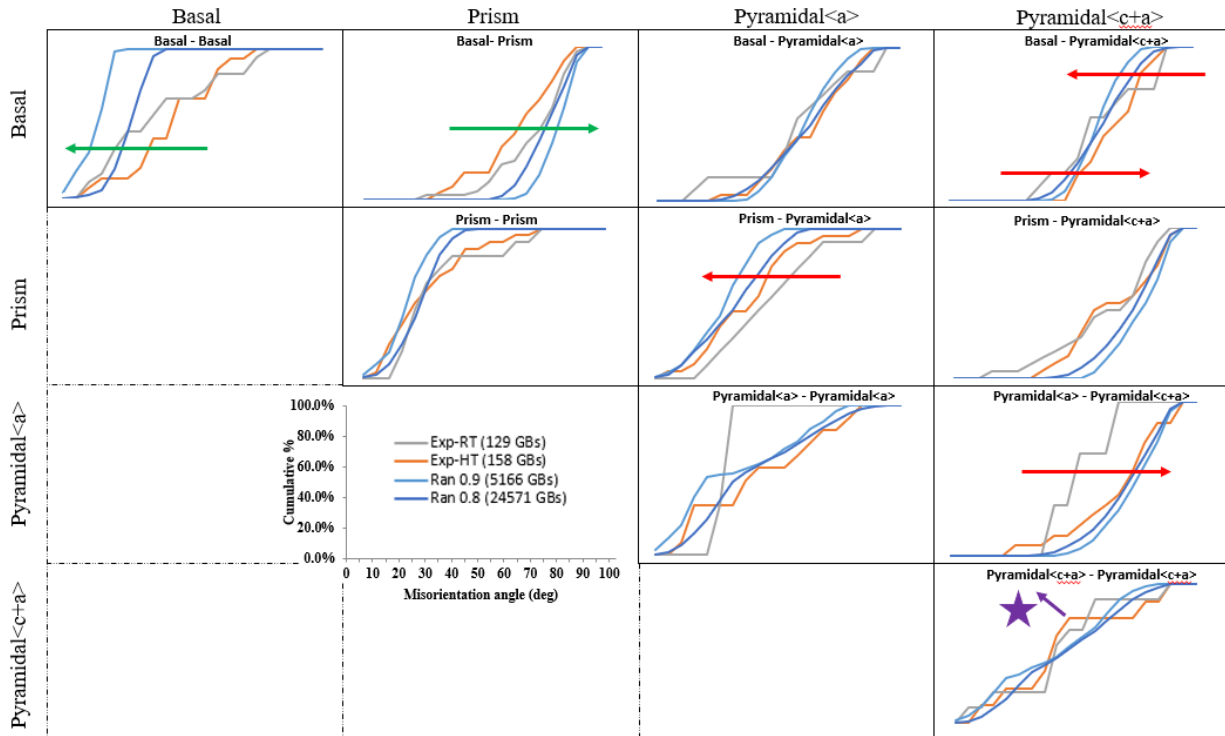


Figure 5.5: Misorientation angle cumulative percentages for Ti525 and randomly generated data sets separated by type of slip system observed in the grains. Pyramidal slip is behaving counter-intuitively with respect to more restrictive conditions.

It is important to note that the experimental data does have a 3 times random texture, while the randomly generated data has a true to random texture. This difference could account for the behavior contrary to the hypothesis in Figure 5.5. In general, pyramidal slip behaves counter-intuitively with respect to more restrictive conditions.

Figure 5.6 presents the overall Ti525 statistics for the type of slip system observed in the data compared to the two randomly generated data sets. It is hypothesized that the room temperature data would have more restrictive slip transfer conditions than the high temperature data set due to the higher ease of movement of dislocations by climb in the high temperature experimental data set. Basal-basal slip and basal-prism slip transfer have a higher number of observations at room temperature than elevated temperature, which could be related to the ease

of these slip systems. The variance in the relative activity of different combinations of slip systems may reflect different temperature dependence on the critical resolved shear stress for the four families of slip systems. The randomly generated data sets have a larger percentage shown in the pyramidal<a> to pyramidal<c+a> and pyramidal<c+a> to pyramidal<c+a> categories, but there are few experimental observations of these slip systems. The experimental data shows a large percentage with basal to prism slip while the random data sets have low percentages for this category.

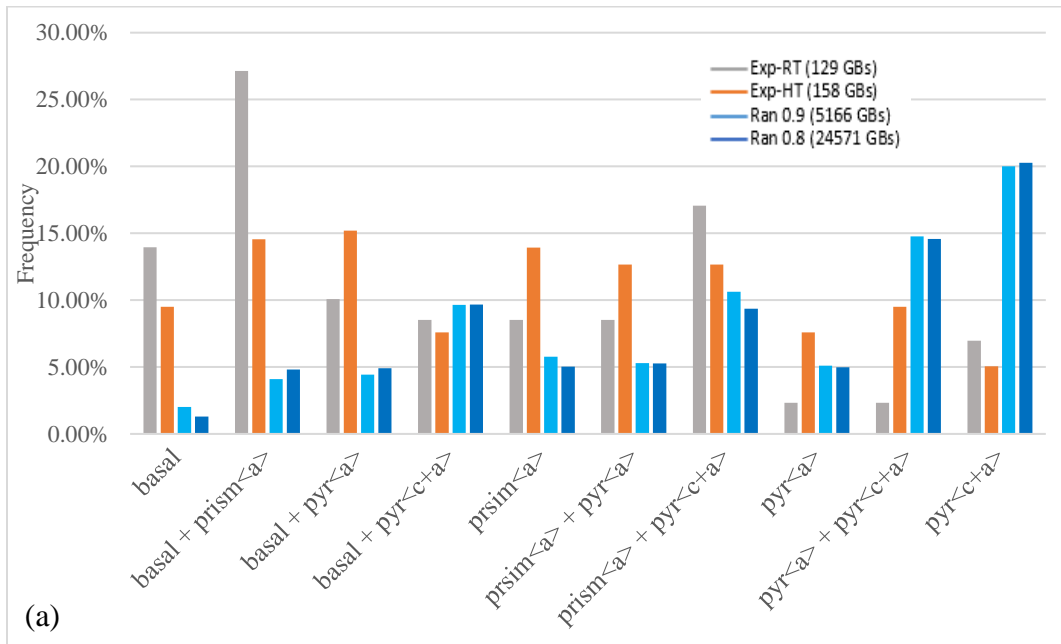


Figure 5.6: Overall Ti525 statistics in comparison to a random population. Random population data sets have a high frequency for pyramidal<c+a> to pyramidal<c+a> where experimental results are low for the same category.

Figure 5.7 shows the same data, but the frequencies are represented as half-circles. The larger the area of the half-circle, the higher the frequency for that slip system pair. In comparing the two data sets, the randomly generated data favors the lower right-hand corner, while the experimental data favors the upper left-hand corner. The randomly generated data have a large

frequency of slip system pairs including a pyramidal plane, and no distinction about the critical resolved shear stress, which could account for the large values for pyramidal  $\langle c+a \rangle$  slip systems.

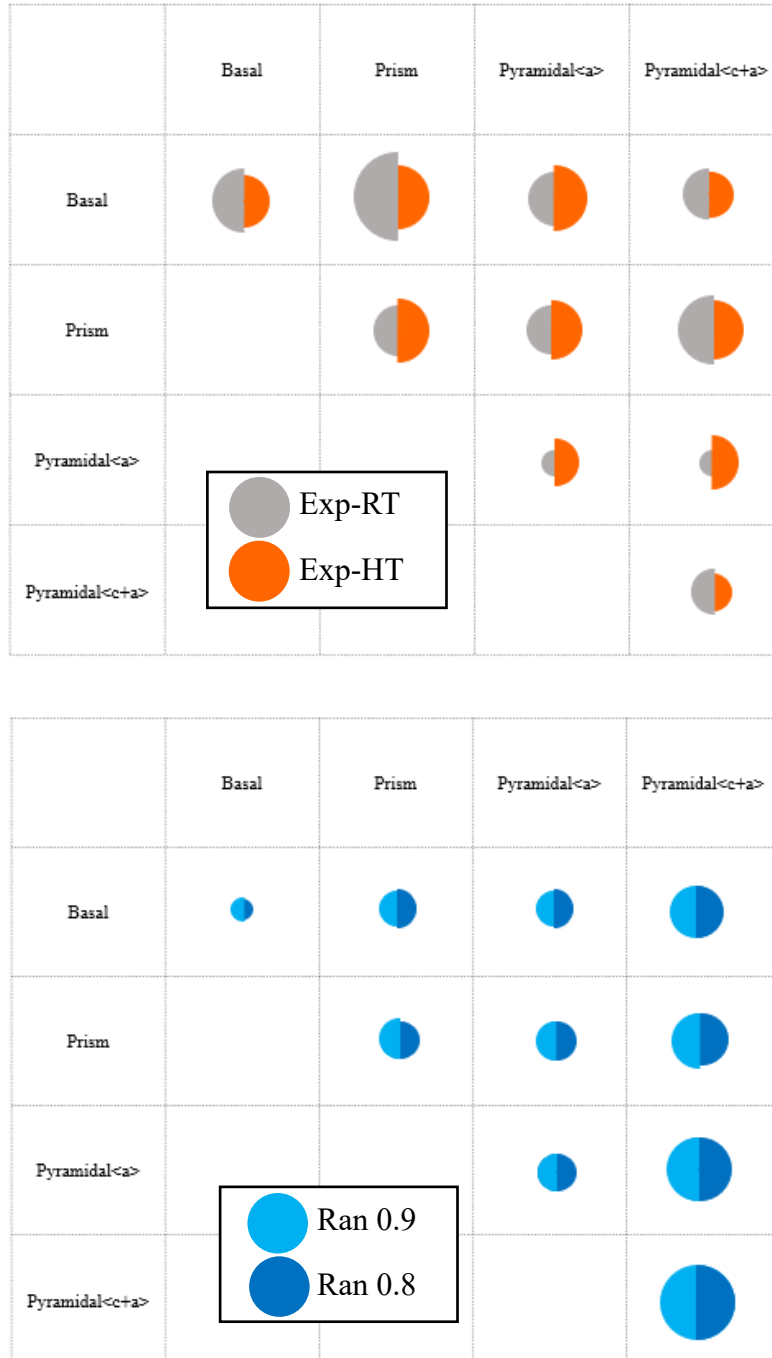


Figure 5.7: Relative frequency of data represented as half-circles. Larger area half-circle represents a higher frequency. (a) Comparison of experimental Ti525 at room temperature and high temperature. (b) Comparison of randomly generated data sets

Another analysis was done with the randomly generated data, to find the most likely slip system pair that would be present in the grain pairs. To determine the most likely slip system pair, a factor was calculated as follows:

$$factor = \frac{m'}{\Delta b} * SF_{LG} * SF_{RG} \quad (5)$$

The slip system pair with the highest factor for each orientation pair was deemed the slip system pair to most likely be present and facilitate slip.

Figure 5.8 (a) shows the frequency of each slip system pair represented by relative area of a circle. There is a larger frequency associated with the right side of the chart, especially the pyramidal<c+a> slip system. The multiplicity of the pyramidal<c+a> plane gives a significant advantage to slip transfer possibilities. To compensate for this, the Schmid factor for the pyramidal<c+a> slip system was halved, which would simulate a higher CRSS for this specific slip plane, and shown in Figure 5.8 (b). Reducing the likelihood for <c+a> slip caused the generated data to have a similar distribution to the experimental data, with basal to prism, and prism to pyramidal slip system pairs having a large frequency, and a smaller frequency in the lower right-hand corner of the chart in both sets. This shows that the factor in Equation 5 captures the overall phenomena that is observed experimentally.

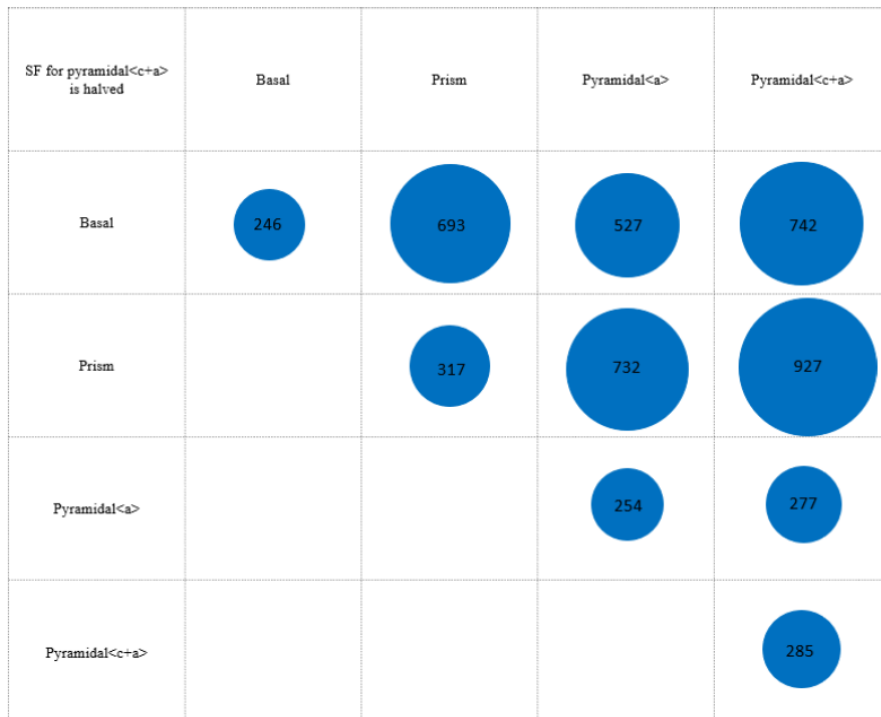
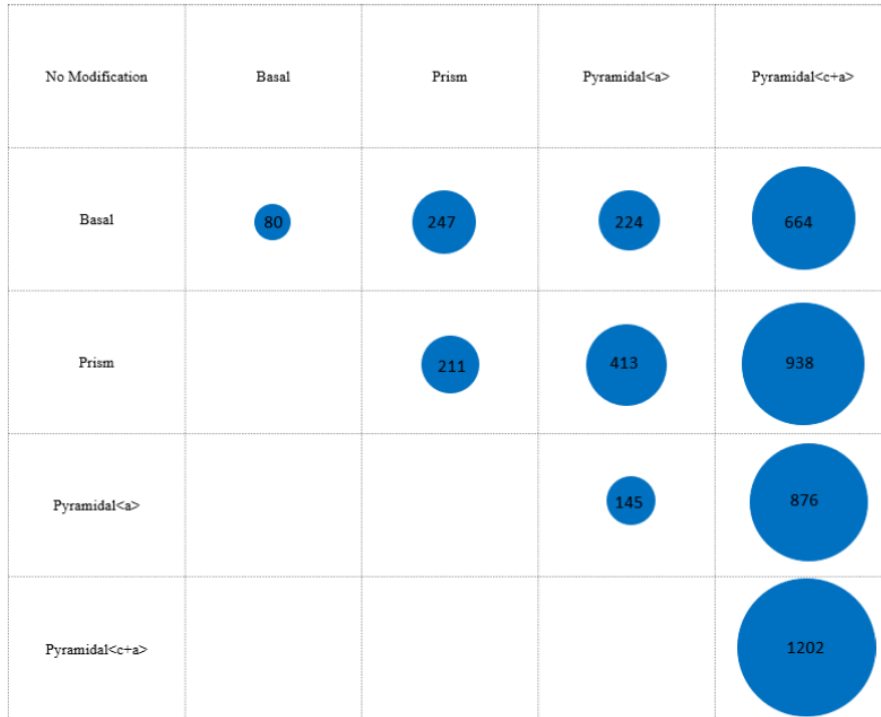


Figure 5.8: Randomly generated orientation pairs with the most likely slip systems present that facilitates slip across the grain boundaries. (a) Unmodified Schmid factors. (b) Schmid factor for pyramidal<c+a> is halved. A high frequency is present in slip system pairs with pyramidal slip systems in both cases.

## Chapter 6: Summary and conclusions

### 6.1 Summary

This thesis describes the method and results of a study of Ti-5Al-2.5Sn deformation behavior focusing on slip transfer across grain boundaries at two different temperatures (296K and 728K). The study investigates “slip transfer” conditions across grain boundaries and builds upon work done by Hongmei Li. The results are compared to a similar study that was done with pure aluminum by R. Alizadeh. In comparing the titanium results to an aluminum sample, some trends are similar, such as favorable slip transfer of the same slip system family at low misorientations. Details associated with geometrical constraints of more slip systems in the hexagonal crystal structure, but few facile ones, versus face centered cubic crystal structure in aluminum. These results show that slip transfer is much more commonly accomplished in the Ti-5Al-2.5Sn deformation in and room and to a greater extent at high temperatures, which provides a basis for installing slip transfer criteria into CPFEM modeling of the alloy.

### 6.2 Conclusions

1. “Slip transfer” data is more prevalent than “no slip transfer” data at misorientation angles  $< 30^\circ$ . At these low misorientation angles, slip traces are categorized as “slip transfer” more than being categorized as “no slip transfer” at both 296K and 728K.
2. There is a decreasing trend of  $m'$  “slip transfer” traces with increasing misorientation below  $20^\circ$  for both Al and Ti525. Many “slip transfer” cases occur at high misorientations in Titanium.
3. Literature suggests that high  $m'$  and low  $\Delta b$  enables slip transfer. This hypothesis was found true in Ti525. Room temperature Ti525 and room temperature Aluminum show a similar behavior in  $m'$  vs.  $\Delta b$ .

4. Considering both the Schmid factor *vs. m'*, and *m' vs. Δb*, geometrical constraints for “slip transfer” in hexagonal crystal structure are smaller than FCC.
5. Misorientation angles that favor a specific slip system pair (angles between slip systems are small) makes slip transfer easier and more prevalent.
6. In slip system pairs where there is no slip transfer, slip is not facilitated easily as the alignment of slip systems is low (angles between slip systems are generally large).
7. The basal + prism slip system pair is most common in Ti525. This relates to the low CRSS of basal and prism slip systems in Ti525.
8. Every type of slip system has a different kind of sensitivity with misorientation angle regarding the experimental data. This is partly due to the geometry of the slip systems, and partly unexplained.
9. Pyramidal slip behaves counter-intuitively with respect to high temperature and room temperature restrictiveness.
10. Using a random data set, the factor  $\frac{m'}{\Delta b} * SF_{LG} * SF_{RG}$  and penalizing the likelihood for <c+a> slip by a factor of two is able to capture the statistical trends similarly to the observed distribution of slip transfer observations.

### 6.3 Future work suggestions

1. A random generation of orientation pairs for the FCC crystal structure to observe if statistical trends are similar to that found in the Aluminum oligo-crystal experiments.
2. Investigate grain boundary sliding in correlation with the residual Burgers vector between two grains and the associated slip transfer in the high temperature Ti525 data. An atomic force microscope (AFM) or a profilometer could be used to identify the ledge height at the grain boundary.
3. A similar investigation with a different deformation mode, i.e. creep or compression testing to further the accuracy of CPFEM modeling by creating rules around slip transfer across grain boundaries.
4. The work of Line et al. could be analyzed with similar methods to determine the slip transfer relationships between high temperature (464K) and the room temperature (296K) aluminum oligo-crystal.

## **APPENDICIES**

## APPENDIX A: Matlab hexagonal orientation code (written by Thomas R. Bieler)

```

% HEXagonal orientation analysis by T.R. Bieler, November 22, 2010, updated 6 Nov 2018.
% No guarantees that it is 100% correct, but it seems so. If you use this for your work,
% it would be kind and ethical to acknowledge its use in published work.
clear; clc; % dbstop if error;
% Imported grains file requires Bunge Euler angles in columns 3:5, (x,y can be put in 1:2, for example)
% in as many rows as data set. Be wary about hidden assumptions;
% plotting uses x --> down, y right, so Euler angles are consistent with TSL maps,

a1=86.764;
b1=66.765;
c1=259.31;

%3,4,5 are Euler angles
Ang(1,:) = [1 0 a1+180 b1 c1];

ghkl = [ % for C3
-1 -1 2 8
0 -1 1 7
1 -2 1 8
0 -1 1 4];
dum = size(ghkl); ghklrows = dum(1,1);
dum = size(Ang); Angrows = dum(1,1);
% Stress tensor is defined; put the one you want in last positino, or make a new one.
ststens = [1 0 0 ; 0 0 0 ; 0 0 0]; LC = 'X'; % tension in X %
ststens = [0 0 0 ; 0 0 0 ; 0 0 1]; LC = 'Z'; % tension in Z %
ststens = [0 -1 0 ; -1 0 0 ; 0 0 0]; LC = '-XY'; % Shear in XY plane %
ststens = [0 1 0 ; 1 0 0 ; 0 0 0]; LC = '+XY'; % Shear in XY plane %
ststens = [0 0 0 ; 0 0 -1 ; 0 -1 0]; LC = '+XZ'; % Shear in XZ plane %
ststens = [1 0 0 ; 0 1 0 ; 0 0 0]; LC = 'BiXY'; % biaxial tension in X-Y %
ststens = [-1 0 0 ; 0 1 0 ; 0 0 0]; LC = 'PSC-XY'; % Plane Strain Compression in XY plane %
ststens = [0 0 0 ; 0 1 0 ; 0 0 0]; LC = 'Y'; % tension in Y %
theta = 0;
Rst = [cosd(theta) -sind(theta) 0; sind(theta) cosd(theta) 0; 0 0 1]; % rotates stress about Z axis
%Rst = [cosd(theta) 0 -sind(theta); 0 1 0; sind(theta) 0 cosd(theta)]; % rotates stress about Y axis
%Rst = [1 0 0; 0 cosd(theta) -sind(theta); 0 sind(theta) cosd(theta)]; % rotates stress about X axis
ststens_R = Rst*ststens*Rst'; % This rotates a desired stress tensor in the lab coord sys.
str2 = ststens_R*ststens_R';
ststens_mag = (str2(1,1)+str2(2,2)+str2(3,3))^0.5;
ststens_n = ststens_R/ststens_mag; % normalized stress tensor to get generalized Schmid factor
%
% Inverse pole figures can be drawn by setting values of ipfd; ipfd is
% inverse pole figure direction,
% iCTE is CTE direction, iEd is E direction, not checked recently, so bugs may exist.
stereo = 1; % plots stereographic projection, otherwise direct projection
ipfd = 2; %inverse pole figure direction (x,y,z, = 1,2,3) will plot points from a group
ihex = 1; % inverse pole figure for hexagonal crystal
iEd = ipfd; % plot magnitude of E in this direction as red (high) - blue (low)
% CTEd = ipfd; % plot magnitude of CTE in this direction as gray scale within symbol
nslphex=69;
% Slip sys: b p paa pya 1c+a 2c+a T1 T2 C2 C1 3c+a in first row, set 0 to skip, 1 to plot
sschoice = [1 1 0 1 1 0 1 1 1 1 0
1 4 7 10 16 28 34 40 46 52 58
3 6 9 15 27 33 39 55 51 57 69 ];
sscol = 1;
for isc = 1:1:nslphex
    pssf(isc) = sschoice(1,sscol);
    if isc == sschoice(3,sscol)
        sscol = sscol + 1;
    end
end
%
% This section allows the point of view of the unit cell to be changed.
Rotateview = [1 0 0 ; 0 1 0 ; 0 0 1];
iRotatev = 0; % Provide NUMBER of rotations

```

```

% rotation of observer from normal TSL point of view to another point of view (crystal stays put)
% This right hand rotation matrix has a 4th row which has in columns 2,3, the angle and axis of the rotation.
%Rotation(4,2:3,1) = [5,3]; % rotation to move axis to a tilted direction in the X-Y plane
%Rotation(4,2:3,1) = [-45,1]; % about the X axis to look through detector for DAXM
%Rotation(4,2:3,1) = [180,2]; % rotate viewpoint about vertical (x) axis + to view from above/right, - to view from above/left
Rotation(4,2:3,1) = [90,2]; % +90 to view from below, -90 to view from above
% Build the Euler angle rotation matrix starting with identity
if iRotatev ~= 0
    LC = ['! rot !' LC];
    for i = 1:iRotatev
        rang = Rotation(4,2,i);
        if Rotation(4,3,i) == 3
            Rotation(1:3,1:3,i)=[cosd(rang),sind(rang),0;-sind(rang),cosd(rang),0;0,0,1];
        elseif Rotation(4,3,i) == 2
            Rotation(1:3,1:3,i)=[cosd(rang),0,sind(rang);0,1,0;-sind(rang),0,cosd(rang)];
        elseif Rotation(4,3,i) == 1
            Rotation(1:3,1:3,i)=[1,0,0;0,cosd(rang),sind(rang);0,-sind(rang),cosd(rang)];
        end
        Rotateview = Rotateview*Rotation(1:3,1:3,i);
    end
end
%
% Below, six points define plane, start point is start of Burgers vector b, 4th is end of b
% 1st to 2nd or 2nd to 3rd or 3rd to 4th cross product identifies plane normal
c_a=1.59; % 1.587 this is the last place for user input in this cell ...

slpsys = cell(4,nslphex);

O = [ 0 0 0 0]; % (I) (H)
A = [ 2 -1 -1 0]/3; % C ----- B
B = [ 1 1 -2 0]/3; % / \ / \
C = [-1 2 -1 0]/3; % / a2 / \
D = [-2 1 1 0]/3; % / \ / \
E = [-1 -1 2 0]/3; % (J)D ----- O(P)-a1-> A(G)
F = [ 1 -2 1 0]/3; % \ / \ /
P = [ 0 0 0 1]; % \ a3 \ /
G = [ 2 -1 -1 3]/3; % \ / \ /
H = [ 1 1 -2 3]/3; % E ----- F
I = [-1 2 -1 3]/3; % (K) (L)
J = [-2 1 1 3]/3; %
K = [-1 -1 2 3]/3; % where a1 = OA a2 = OC a3 = OE
L = [ 1 -2 1 3]/3; % DA || a1, FC || a2, BE || a3

% Slip system definitions set as of 1 Nov 2019 to be consistent with DAMASK
% Hex plane direction 1st and 4th point is Burgers vector
% basal <a>-glide:&Be Mg Re Ti; Re
slpsys{2,1} = [0 0 0 1; 2 -1 -1 0; D ; E ; F ; A ; B ; C ];
slpsys{2,2} = [0 0 0 1; -1 2 -1 0; F ; A ; B ; C ; D ; E ];
slpsys{2,3} = [0 0 0 1; -1 -1 2 0; B ; C ; D ; E ; F ; A ];
ibas = 1;
fbas = 3;
% prism <a>-glide:Ti Zr RE; Be Re Mg
slpsys{2,4} = [ 0 1 -1 0; 2 -1 -1 0; E ; E ; E ; F ; L ; K ];
slpsys{2,5} = [-1 0 1 0; -1 2 -1 0; A ; A ; A ; B ; H ; G ];
slpsys{2,6} = [ 1 -1 0 0; -1 -1 2 0; C ; C ; C ; D ; J ; I ];
iprs = 4;
fprs = 6;
% prism <aa>
slpsys{2,7} = [ 2 -1 -1 0; 0 1 -1 0; F ; F ; F ; B ; H ; L ];
slpsys{2,8} = [-1 2 -1 0; -1 0 1 0; B ; B ; B ; D ; J ; H ];
slpsys{2,9} = [-1 -1 2 0; 1 -1 0 0; D ; D ; D ; F ; L ; J ];
i2prs = 7;
f2prs = 9;
% pyramidal <a>-glide --*- CORRECTED --*-
slpsys{2,10} = [ 1 0 -1 1; -1 2 -1 0; E ; E ; E ; D ; I ; L ];
slpsys{2,11} = [ 0 1 -1 1; -2 1 1 0; F ; F ; F ; E ; J ; G ];
slpsys{2,12} = [-1 1 0 1; -1 -1 2 0; A ; A ; A ; F ; K ; H ];
slpsys{2,13} = [-1 0 1 1; 1 -2 1 0; B ; B ; B ; A ; L ; I ];
slpsys{2,14} = [ 0 -1 1 1; 2 -1 -1 0; C ; C ; C ; B ; G ; J ];
slpsys{2,15} = [ 1 -1 0 1; 1 1 -2 0; D ; D ; D ; C ; H ; K ];

```

```

ipyra = 10;
fpyra = 15;
% pyramidal <c+a>-glide;; all?
slpsys{2,16} = [ 1 0 -1 1; -2 1 1 3; A ; B ; I ; P ; L ; A ];
slpsys{2,17} = [ 1 0 -1 1; -1 -1 2 3; B ; B ; I ; P ; L ; A ];
slpsys{2,18} = [ 0 1 -1 1; -1 -1 2 3; B ; C ; J ; P ; G ; B ];
slpsys{2,19} = [ 0 1 -1 1; 1 -2 1 3; C ; C ; J ; P ; G ; B ];
slpsys{2,20} = [-1 1 0 1; 1 -2 1 3; C ; D ; K ; P ; H ; C ];
slpsys{2,21} = [-1 1 0 1; 2 -1 -1 3; D ; D ; K ; P ; H ; C ];
slpsys{2,22} = [-1 0 1 1; 2 -1 -1 3; D ; E ; L ; P ; I ; D ];
slpsys{2,23} = [-1 0 1 1; 1 1 -2 3; E ; E ; L ; P ; I ; D ];
slpsys{2,24} = [ 0 -1 1 1; 1 1 -2 3; E ; F ; G ; P ; J ; E ];
slpsys{2,25} = [ 0 -1 1 1; -1 2 -1 3; F ; F ; G ; P ; J ; E ];
slpsys{2,26} = [ 1 -1 0 1; -1 2 -1 3; F ; A ; H ; P ; K ; F ];
slpsys{2,27} = [ 1 -1 0 1; -2 1 1 3; A ; A ; H ; P ; K ; F ];
ipyrc = 16;
fpyrc = 27;
% pyramidal <c+a>-2nd order glide
slpsys{2,28} = [ 1 1 -2 2; -1 -1 2 3; (O+B)/2 ; C ; J ; (P+K)/2 ; L ; A ];
slpsys{2,29} = [-1 2 -1 2; 1 -2 1 3; (O+C)/2 ; D ; K ; (P+L)/2 ; G ; B ];
slpsys{2,30} = [-2 1 1 2; 2 -1 -1 3; (O+D)/2 ; E ; L ; (P+G)/2 ; H ; C ];
slpsys{2,31} = [-1 -1 2 2; 1 1 -2 3; (O+E)/2 ; F ; G ; (P+H)/2 ; I ; D ];
slpsys{2,32} = [ 1 -2 1 2; -1 2 -1 3; (O+F)/2 ; A ; H ; (P+I)/2 ; J ; E ];
slpsys{2,33} = [ 2 -1 -1 2; -2 1 1 3; (O+A)/2 ; B ; I ; (P+J)/2 ; K ; F ];
i2pyrc = 28;
f2pyrc = 33;
% *** Twin directions are opposite in Christian and Mahajan, and are not correcte to be consistent with them
% FROM Kocks SXHEX plane direction 1st and 4th point is Burgers vector, order of C1 differs from Kock's file
% {1012}<1011> T1 twins 0.17; -1.3 twins: all Twin Vector must go in the
% sense of shear, opposite C&M sense.
slpsys{2,34} = [ 1 0 -1 2; -1 0 1 1; A ; B ; J ; K ; K ; K ];
slpsys{2,35} = [ 0 1 -1 2; 0 -1 1 1; B ; C ; K ; L ; L ; L ];
slpsys{2,36} = [-1 1 0 2; 1 -1 0 1; C ; D ; L ; G ; G ; G ];
slpsys{2,37} = [-1 0 1 2; 1 0 -1 1; D ; E ; G ; H ; H ; H ];
slpsys{2,38} = [ 0 -1 1 2; 0 1 -1 1; E ; F ; H ; I ; I ; I ];
slpsys{2,39} = [ 1 -1 0 2; -1 1 0 1; F ; A ; I ; J ; J ; J ];
iT1 = 34;
fT1 = 39;
% {2111}<2116> T2 twins: 0.63; -0.4; Ti Zr Re RE]; Also does not follow C&M definition for shear direction
slpsys{2,40} = [ 1 1 -2 1; -1 -1 2 6; (O+B)/2 ; C ; (J+I)/2 ; P ; (L+G)/2 ; A ];
slpsys{2,41} = [-1 2 -1 1; 1 -2 1 6; (O+C)/2 ; D ; (K+J)/2 ; P ; (G+H)/2 ; B ];
slpsys{2,42} = [-2 1 1 1; 2 -1 -1 6; (O+D)/2 ; E ; (L+K)/2 ; P ; (H+I)/2 ; C ];
slpsys{2,43} = [-1 -1 2 1; 1 1 -2 6; (O+E)/2 ; F ; (G+L)/2 ; P ; (I+J)/2 ; D ];
slpsys{2,44} = [ 1 -2 1 1; -1 2 -1 6; (O+F)/2 ; A ; (H+G)/2 ; P ; (J+K)/2 ; E ];
slpsys{2,45} = [ 2 -1 -1 1; -2 1 1 6; (O+A)/2 ; B ; (I+H)/2 ; P ; (K+L)/2 ; F ];
iT2 = 40;
fT2 = 45;
% {1011}<101-2> C1 twins: 0.10; 1.1; Mg; Zr Ti]; agrees with C&M
slpsys{2,46} = [ 1 0 -1 1; 1 0 -1 -2; P ; L ; A ; (A+B)/2 ; B ; I ];
slpsys{2,47} = [ 0 1 -1 1; 0 1 -1 -2; P ; G ; B ; (B+C)/2 ; C ; J ];
slpsys{2,48} = [-1 1 0 1; -1 1 0 -2; P ; H ; C ; (C+D)/2 ; D ; K ];
slpsys{2,49} = [-1 0 1 1; -1 0 1 -2; P ; I ; D ; (D+E)/2 ; E ; L ];
slpsys{2,50} = [ 0 -1 1 1; 0 -1 1 -2; P ; J ; E ; (E+F)/2 ; F ; G ];
slpsys{2,51} = [ 1 -1 0 1; 1 -1 0 -2; P ; K ; F ; (F+A)/2 ; A ; H ];
iC1 = 46;
fC1 = 51;
% {2112}<211-3> C2 twins;; 0.22; 1.2 Ti Zr Re]; agrees with C&M
slpsys{2,52} = [ 1 1 -2 2; 1 1 -2 -3; (K+P)/2 ; L ; A ; (A+C)/2 ; C ; J ];
slpsys{2,53} = [-1 2 -1 2; -1 2 -1 -3; (L+P)/2 ; G ; B ; (B+D)/2 ; D ; K ];
slpsys{2,54} = [-2 1 1 2; -2 1 1 -3; (G+P)/2 ; H ; C ; (C+E)/2 ; E ; L ];
slpsys{2,55} = [-1 -1 2 2; -1 -1 2 -3; (H+P)/2 ; I ; D ; (D+F)/2 ; F ; G ];
slpsys{2,56} = [ 1 -2 1 2; 1 -2 1 -3; (I+P)/2 ; J ; E ; (E+A)/2 ; A ; H ];
slpsys{2,57} = [ 2 -1 -1 2; 2 -1 -1 -3; (J+P)/2 ; K ; F ; (F+B)/2 ; B ; I ];
iC2 = 52;
fC2 = 57;

% <c+a>-3rd order glide;
slpsys{2,58} = [ 2 -1 -1 1; -1 2 -1 3; F ; (K+L)/2 ; P ; P ; (I+H)/2 ; B ];
slpsys{2,59} = [ 2 -1 -1 1; -1 -1 2 3; B ; (I+H)/2 ; P ; P ; (K+L)/2 ; F ];
slpsys{2,60} = [ 1 1 -2 1; -2 1 1 3; A ; (L+G)/2 ; P ; P ; (J+I)/2 ; C ];

```

```

slpsys{2,61} = [ 1 1 -2 1; 1 -2 1 3; C ; (J+I)/2 ; P ; P ; (L+G)/2 ; A ];
slpsys{2,62} = [-1 2 -1 1; -1 -1 2 3; B ; (G+H)/2 ; P ; P ; (K+J)/2 ; D ];
slpsys{2,63} = [-1 2 -1 1; 2 -1 -1 3; D ; (K+J)/2 ; P ; P ; (G+H)/2 ; B ];
slpsys{2,64} = [-2 1 1 1; 1 -2 1 3; C ; (H+I)/2 ; P ; P ; (L+K)/2 ; E ];
slpsys{2,65} = [-2 1 1 1; 1 1 -2 3; E ; (L+K)/2 ; P ; P ; (H+I)/2 ; C ];
slpsys{2,66} = [-1 -1 2 1; 2 -1 -1 3; D ; (I+J)/2 ; P ; P ; (G+L)/2 ; F ];
slpsys{2,67} = [-1 -1 2 1; -1 2 -1 3; F ; (G+L)/2 ; P ; P ; (I+J)/2 ; D ];
slpsys{2,68} = [ 1 -2 1 1; 1 1 -2 3; E ; (J+K)/2 ; P ; P ; (H+G)/2 ; A ];
slpsys{2,69} = [ 1 -2 1 1; -2 1 1 3; A ; (H+G)/2 ; P ; P ; (J+K)/2 ; E ];
i3pyrc = 58;
f3pyrc = 69;

% cell 3 = Cartesian slip system unit vectors, cell 4 = Schmid matrix %
for gg = 1:1:ghklrows
    ghklC(gg,:) = [ghkl(gg,1), (ghkl(gg,1)+2*ghkl(gg,2))/sqrt(3), ghkl(gg,4)/c_a]; %plane normal in cartesian
    unit_ghklC(gg,:) = ghklC(gg,:)/norm(ghklC(gg,:));
end

for isc=1:1:nslphex; % isc is slip system counter
    n = [slpsys{2,isc}(1,1), (slpsys{2,isc}(1,1)+2*slpsys{2,isc}(1,2))/sqrt(3), slpsys{2,isc}(1,4)/c_a]; %plane normal in cartesian
    m = [3*slpsys{2,isc}(2,1)/2, (slpsys{2,isc}(2,1)+2*slpsys{2,isc}(2,2))*sqrt(3)/2, slpsys{2,isc}(2,4)*c_a]; % slip direction in cartesian
    p1 = [3*slpsys{2,isc}(3,1)/2, (slpsys{2,isc}(3,1)+2*slpsys{2,isc}(3,2))*sqrt(3)/2, slpsys{2,isc}(3,4)*c_a]; % point 1
    p2 = [3*slpsys{2,isc}(4,1)/2, (slpsys{2,isc}(4,1)+2*slpsys{2,isc}(4,2))*sqrt(3)/2, slpsys{2,isc}(4,4)*c_a]; % point 2
    p3 = [3*slpsys{2,isc}(5,1)/2, (slpsys{2,isc}(5,1)+2*slpsys{2,isc}(5,2))*sqrt(3)/2, slpsys{2,isc}(5,4)*c_a]; % point 3
    p4 = [3*slpsys{2,isc}(6,1)/2, (slpsys{2,isc}(6,1)+2*slpsys{2,isc}(6,2))*sqrt(3)/2, slpsys{2,isc}(6,4)*c_a]; % point 4
    p5 = [3*slpsys{2,isc}(7,1)/2, (slpsys{2,isc}(7,1)+2*slpsys{2,isc}(7,2))*sqrt(3)/2, slpsys{2,isc}(7,4)*c_a]; % point 5
    p6 = [3*slpsys{2,isc}(8,1)/2, (slpsys{2,isc}(8,1)+2*slpsys{2,isc}(8,2))*sqrt(3)/2, slpsys{2,isc}(8,4)*c_a]; % point 6
    mag_m = (m(1,1)^2+m(1,2)^2+m(1,3)^2)^0.5;
    mag_n = (n(1,1)^2+n(1,2)^2+n(1,3)^2)^0.5;
    unit_m = m/mag_m;
    unit_n = n/mag_n;
    dot0(isc,1) = unit_m*unit_n;
    slpsys{1,isc} = isc;
    slpsys{3,isc} = [unit_n;unit_m;p1;p2;p3;p4;p5;p6]; % normal in first row, direction in next row, points in next 6 rows
    slpsys{4,isc} = 0.5*(unit_m*unit_n + unit_n*unit_m); % Schmid matrix
    unit_tau(isc,:) = [isc, cross(unit_m, unit_n)]; % edge dislocation line direction tau unit vectors are generated
    % if linedir(isc,2)<0
    %     linedir(isc,:) = -1.*linedir(isc,:);
    % end
end
sortlinedir = sortrows(unit_tau,[-2,-3,-4]);

Schm_f_ss = zeros(nslphex,11,Angrows);
Schm_labvecA = zeros(nslphex+1,33);
sortmv = zeros(nslphex+1,33,Angrows);
xic = zeros(nslphex,3,ghklrows);
xicg = zeros(nslphex,3,ghklrows);
xirg = zeros(nslphex,3,ghklrows);
xig = zeros(nslphex,3,ghklrows);
for gg = 1:1:ghklrows
    for isc=1:1:nslphex;
        xic(isc,1:3,gg) = cross(unit_tau(isc,2:4),unit_ghklC(gg,:)); % Streak direction vector in crystal frame, not normalized!
        % xi(isc,1:3,isc) = xi(isc,1:3,gg) / norm(xi(isc,1:3,gg));
    end
end

% code to set up inverse pole figure and labeling, probably has some inconsistencies

sij = [0.9581 -0.4623 -0.1893 0.698 2.1413 2.8408]/100; % for Ti from Simmons and Wang in units of 1/GPa
Elow = 83.2; Ehigh = 145.5; % Elastic Ccontants of Nb from Simmons and Wang for Ti
CTE = [15.4 15.4 30.6]; % this is for Sn, not a cubic material ... such as this inconsistency

f = figure('Position', [0,0,500,500]); movegui(f,'northwest'); set(gcf, 'Color', [1 1 1]); hold on;
hold on; axis square; xmax = 0;
if c_a ~= 1
    trideg = 45;
    if ihex == 1
        trideg = 30;
    end
    angle = 0:1:trideg;

```

```

xang = cosd(angle); yang = sind(angle);
borderx = [0 xang 0]; bordery = [0 yang 0]; xmax = 1.02;
axis([0 xmax 0 xmax]), % TickDir, 'out' ???
plot(borderx,bordery,'k-');

edgecolor = [0,0,1]; % perimeter of plotting symbol
if ipfd == 2
    edgecolor = [.9,.9,0];
end
if ipfd == 1
    edgecolor = [1,0,0];
end
for p = 0:.05:1 % plot inverse pole figure gray scale symbols
    plot(.03+p*xmax*.7,.95*xmax,'o','LineWidth',4,'MarkerEdgeColor',[1 1-p],...
        'MarkerFaceColor',[1 1 1],'MarkerSize',8)
    if c_a ~= 1
        plot(.03+p*xmax*.7,.85*xmax,'o','LineWidth',1,'MarkerEdgeColor',[p p p],...
            'MarkerFaceColor',[p p p],'MarkerSize',6)
    end
end
text(0.02,.9*xmax,'E direction, yellow (low) --> magenta (high)');
if c_a ~= 1
    text(0.02,.8*xmax,'CTE direction, black(low) --> white(high)');
end
if stereo == 0
    text(0.02,.7*xmax,'Z projection, not stereographic');
else
    text(0.02,.7*xmax,'Stereographic projection');
end
text(0.02,.5*xmax,['IPF direction ',num2str(ipfd)]);
text(0.02,.6*xmax,['c/a ratio ',num2str(c_a)]);

% Generate orientation matrices for each orientation in Ang
R45 = [1,0,0;0,cosd(45),-sind(45);0,sind(45),cosd(45)]; % Rotation of 45 deg about X axis
% %
for iAng=1:1:Angrows; % 1;%4; %2; %
    phidA = Ang(iAng,3:5);
    phidA(1) = phidA(1); %; +180% **** Rotating euler angles (e.g. to correct for 180 rotation)
    if phidA(1)>360
        phidA(1) = phidA(1)-360;
    end
    if phidA(1)<0
        phidA(1) = phidA(1)+360;
    end
    phisA = phidA*pi/180; %Compute Bunge orientation matrix g
    gphi1=[cos(phisA(1,1)),sin(phisA(1,1)),0;-sin(phisA(1,1)),cos(phisA(1,1)),0;0,0,1];
    gPhi=[1,0,0;0,cos(phisA(1,2)),sin(phisA(1,2));0,-sin(phisA(1,2)),cos(phisA(1,2))];
    gphi2=[cos(phisA(1,3)),sin(phisA(1,3)),0;-sin(phisA(1,3)),cos(phisA(1,3)),0;0,0,1];
    gA=gphi2*gPhi*gphi1; gAR = gA*Rotateview; % to rotate point of view in plot
    g(:,:,iAng)=gA; R(:,:,iAng)=gA';
    gsgTA = gA*ststens_n*gA'; %rotated stress tensor
    basalY(iAng,1) = abs(gA(3,2));

    for i = 1:1:3
        CTEm(:,i) = gA(:,i).*CTE';
    end
    for i = 1:1:3 % This gives the CTE in the x (1), y (2), z (3) directions

        e1 = sij(1)*(gA(1,i)^4 + gA(2,i)^4) + sij(4)*gA(3,i)^4;
        e2 = (2*sij(2) + sij(6))*(gA(1,i)^2 * gA(2,i)^2);
        e3 = (2*sij(3) + sij(5))*gA(3,i)^2 * (gA(1,i)^2 + gA(2,i)^2);
        EA(iAng,i)=1./(e1+e2+e3);
    end

    Eb = (EA(iAng,iEd)-Elow)/(Ehigh-Elow);
    pv = gA(:,ipfd); pv = abs(pv);
    if c_a == 1
        x(1) = median(pv);
        x(2) = min(pv);
    end

```

```

x(3) = max(pv);
else
x(1) = max(pv(1),pv(2));
x(2) = min(pv(1),pv(2));
x(3) = pv(3);
end
if ihex == 1
ang = atand(x(2)/x(1));
if ang > 30 % tangent of 30 deg
nang = 30-(ang - 30);
radius = (x(1)^2+x(2)^2)^.5;
x(1) = cosd(nang)*radius;
x(2) = sind(nang)*radius;
end
end
if stereo == 1
plot(x(1)/(1+x(3)), x(2)/(1+x(3)),'o','LineWidth',2,'MarkerEdgeColor',...
edgcolor,'MarkerFaceColor',[1 1-Eb Eb],'MarkerSize',14)
text(x(1)/(1+x(3)), x(2)/(1+x(3))+.037,num2str(iAng))
else
plot(x(1),x(2),'o','LineWidth',1,'MarkerEdgeColor',edgcolor,...
'MarkerFaceColor',[1 1-Eb Eb],'MarkerSize',8)
text(x(1),x(2)+.037,num2str(iAng))
end

for isc=1:1:nslphex
Sf=0.;
for i=1:1:3
for j=1:1:3 % Compute Schmid Factor, slpsys{4 = Schmid matrix}
Sf=Sf+gsgTA(i,j)*slpsys{4,isc}(i,j);
end
end
if isc >= 46 && Sf <0
Sf = 0.001 * Sf; % this is to prevent anti-twin shears from being seriously considered later
end
rot_nA = slpsys{3,isc}(1,:)*gAR;
rot_bA = slpsys{3,isc}(2,:)*gAR;
rot_p1 = slpsys{3,isc}(3,:)*gAR;
rot_p2 = slpsys{3,isc}(4,:)*gAR;
rot_p3 = slpsys{3,isc}(5,:)*gAR;
rot_p4 = slpsys{3,isc}(6,:)*gAR;
rot_p5 = slpsys{3,isc}(7,:)*gAR;
rot_p6 = slpsys{3,isc}(8,:)*gAR;
rot_tA = cross(rot_bA',rot_nA);
% This variable has slip system number, Schmid Factor, plane and Burgers in sample coord syst, and hkl,uvw
Schm_f_ss(isc,1:11,iAng)=[isc, Sf, abs(Sf), slpsys{2,isc}(1,:),slpsys{2,isc}(2,:)];
% Schmid factors (1-3), rotated plane normal (4-6), Computed rotated Burgers vector (7-9),
% , plane trace on Z surface (10-12) Computed rotated position vectors to points p1-p4 (13-24)
% 1 2 3 4-6 7-9 10-12
Schm_labvecA(isc,:) = [isc, Sf, abs(Sf), rot_nA, rot_bA, cross(rot_nA',[0,0,1]),...
rot_p1, rot_p2, rot_p3, rot_p4, rot_p5, rot_p6, rot_tA];
end% 13-15 16-18 19-21 22-24 25-27 28-30 31-33
%
% sortmv contains list from high to low Schmid factor, with associated infomation to draw slip system in unit cell
% useful plotting unit cell vectors will sort to bottom row
Schm_labvecA(nslphex+1,:) = [0 1 -1 [1 0 0]*gAR [0 1 0]*gAR [0 0 1]*gAR 0 0 0 0 0 0 0 0 0 0 0 0 0 0 0 0 0 0]; % 33 columns
sortmv(:,iAng) = sortrows(Schm_labvecA,-3);

if iAng == 1 % Rotated xi (streak) vectors
for gg = 1:1:ghklrows
ghklg(gg,1:3) = unit_ghklC(gg,:)*gAR;
for isc=1:1:nslphex;
xicg(isc,1:3,gg) = xic(isc,1:3,gg) * gA; % streak direction vector, rotated to sample coordinates
xirg(isc,1:3,gg) = cross(Schm_labvecA(isc,31:33),ghklg(gg,1:3)); % streak direction vector, from rotated sample coordinates
xig(isc,1:3,gg) = xirg(isc,1:3,gg) * R45; % rotated streak vector rotated from sample to detector coordinate system defined by R45
end
end
end
end
end

```

```

% plot the image of unit cell, slip vectors, planes, plane normals, and plane traces
% Then choose what row (orientation) to analyze,
% and set iAng to this orientation (row), and run this second cell.  X down and Y to right!!!
iAng = 1;
ptpl = 1; % 0 = don't plot plane traces,
ptss = 2; % 0 just the unit cell, and 1 slip planes, 2 and directions, 3 and plane normals, 4 directions only,
pta123o = 1; % 1 = a1 a2 a3 coordinates and origin (open circle),
nplots = nslphex; %48; %1; % number of slip sorted systems to plot
% no further user input below here

% Dashed lines give plane traces, (colors in groups based on slip
% families) Shorter plane traces imply that the slip plane is nearly
% parallel to page, longer traces imply that the plane is highly inclined.
% dotted red, green, blue lines give the x,y,z edges of unit cell.
% Turquoise/Teal line shows Burgers vector direction, with direction
% away from the ball end (--!->) adjusted for the sign of the Schmid factor <--!->).
% Slip plane is shaded light when the plane normal has out-of-page
% component, darker when into the page.

% Strategy: First extract useful vectors from slip system information to draw the hexagonal prisms
% positions in sortmv p1:13-15 p2:16-18 p3:19-21 p4:22-24 p5:25-27 p6:28-30
% positions in pln p1:4-6 p2:7-9 p3:10-12 p4:13-15 p5:16-18 p6:18-21
for isc = 1:1:nplots
    if sortmv(isc,1,iAng) == 1; % locate the two basal planes
        pln(1,4:21) = sortmv(isc,13:30,iAng); % bottom basal plane
        pln(2,4:21) = sortmv(isc,13:30,iAng); % top basal plane
        rotc = sortmv(isc,4:6,iAng)*c_a; % basal plane normal * c/a
        for j = 4:3:19
            pln(2,j:j+2) = pln(1,j:j+2) + rotc; % move top plane up by a unit of c
        end
        a1 = sortmv(isc,7:9,iAng); % locate a1 using SS1
    elseif sortmv(isc,1,iAng) == 2;
        a2 = sortmv(isc,7:9,iAng); % locate a2 using SS2
    elseif sortmv(isc,1,iAng) == 3;
        a3 = sortmv(isc,7:9,iAng); % locate a3 using SS3
    end
end
for isc = 1:1:nplots;
    if sortmv(isc,1,iAng) == 4; % locate two prism planes on opposite sides using SS4
        pln(3,4:21) = sortmv(isc,13:30,iAng);
        for j = 13:3:28
            pln(4,j-9:j-7) = sortmv(isc,j:j+2,iAng) + a2 - a3;
        end
    elseif sortmv(isc,1,iAng) == 5; % locate two prism planes on opposite sides using SS5
        pln(5,4:21) = sortmv(isc,13:30,iAng);
        for j = 13:3:28
            pln(6,j-9:j-7) = sortmv(isc,j:j+2,iAng) + a3 - a1;
        end
    elseif sortmv(isc,1,iAng) == 6; % locate two prism planes on opposite sides using SS6
        pln(7,4:21) = sortmv(isc,13:30,iAng);
        for j = 13:3:28
            pln(8,j-9:j-7) = sortmv(isc,j:j+2,iAng) + a1 - a2;
        end
    end
end
end
for j = 1:1:2 % Find z elevation of basal planes
    for k = 1:1:3
        pln(j,k) = (pln(j,3+k)+pln(j,6+k)+pln(j,9+k)+pln(j,12+k)+pln(j,15+k)+pln(j,18+k))/6;
    end
end
center = (pln(1,1:3)+pln(2,1:3))/2;
for j = 3:1:8 % Find z elevation of prism planes
    pln(j,3) = (pln(j,12)+pln(j,15)+pln(j,18)+pln(j,21))/4;
end
sortpln = sortrows(pln,-3);
minx = 0; miny = 0; minz = 0; maxx = 0; maxy = 0; maxz = 0;
for j = 1:1:8 % assemble vectors for plotting faces of hex prism
    prsxplt(j,1:7) = [sortpln(j,4) sortpln(j,7) sortpln(j,10) sortpln(j,13) sortpln(j,16) sortpln(j,19) sortpln(j,4)];
    minx = min(minx,min(prsxplt(j,:))); maxx = max(maxx,max(prsxplt(j,:)));
end

```

```

prsyplt(j,1:7) = [sortpln(j,5) sortpln(j,8) sortpln(j,11) sortpln(j,14) sortpln(j,17) sortpln(j,20) sortpln(j,5)];
miny = min(miny,min(prsyplt(j,:))); maxy = max(maxy,max(prsyplt(j,:)));
prszplt(j,1:7) = [sortpln(j,6) sortpln(j,9) sortpln(j,12) sortpln(j,15) sortpln(j,18) sortpln(j,21) sortpln(j,6)];
minz = min(minz,min(prszplt(j,:))); maxz = max(maxz,max(prszplt(j,:)));
end

sscol = 1; %decide if want to plot unit cells for this slip system
ipl = -8; % Strategy: Next, start isc loop for plotting slip systems
ipc = 0; % plot counter
for isc = 1:1:nplots
    ssn = sortmv(isc,1,iAng); % slip system number
    if pssf(ssn) == 1
        ipc = ipc + 1;
        if ipl-ipc == -9 % eight plots on a page
            f = figure('Position', [0,0,1050,525]); movegui(f,'northwest'); set(gcf, 'Color', [1 1 1]); hold on;
            ipl=ipl+8;
        end
        subplot(2,4,ipc-ipl)
        hold on
        sp1 = sortmv(isc,13:15,iAng); % beginning of Burgers vector
        sp2 = sortmv(isc,16:18,iAng); % extract plotted points on perimeter of the slip plane
        sp3 = sortmv(isc,19:21,iAng);
        sp4 = sortmv(isc,22:24,iAng);
        sp5 = sortmv(isc,25:27,iAng);
        sp6 = sortmv(isc,28:30,iAng);
        spx = [sp1(1) sp2(1) sp3(1) sp4(1) sp5(1) sp6(1) sp1(1)];
        spy = [sp1(2) sp2(2) sp3(2) sp4(2) sp5(2) sp6(2) sp1(2)];
        Sf = sortmv(isc,2,iAng); % Schmid factor
        Sfs = 1;
        if Sf < 0
            Sfs = -1;
        end;
        n = [0 0 0 sortmv(isc,4:6,iAng)]; % plane normal
        b = [sp1 sp4]; % p1+sortmv(isc,7:9,iAng); % Burgers vector
        nvec = sortmv(isc,4:6,iAng);
        bvec = sortmv(isc,7:9,iAng);
        pt = sortmv(isc,10:12,iAng); % plane trace
        minx = min(minx, sp1(1)+n(4));
        maxx = max(maxx, sp1(1)+n(4)); % find appropriate range of x and y for plot
        miny = min(miny, sp1(2)+n(5));
        maxy = max(maxy, sp1(2)+n(5));
        midx = (minx+maxx)/2;
        midy = (miny+maxy)/2;
        del = 2;

% These plots will match TSL with X down !!!! Plotting starts...
axis square
set(gca, 'ycolor', 'w'); set(gca, 'xcolor', 'w'); % make axes white for ease in later arranging.
axis([midy-del midy+del -midx-del -midx+del])
if pta123o > 0
    if Ang(iAng,4) < 90 % make the 3 coordinate axes visible below slip planes
        plot([0 a1(2)],-[0 a1(1)], ':', 'Linewidth',3,'Color',[1 0 .2]);% plot x = red
        plot([0 a2(2)],-[0 a2(1)], ':', 'Linewidth',3,'Color',[.6 .8 0]);% plot y = green-gold
        plot([0 a3(2)],-[0 a3(1)], ':', 'Linewidth',3,'Color',[0 0 1]);% plot z = blue
    end
end
if ipl-ipc == -1
end
if ptss > 0 && ptss < 4 % plot slip planes
    if sortmv(isc,6,iAng) > 0 % is k component of slip plane normal positive or negative?
        fill(spy,-spx, [.8 .8 .65]) % slip plane filled warm gray

    else % slip plane filled cool gray if normal has neg z component
        fill(spy,-spx, [.65 .65 .7])
    % plot([n(2) n(5)], -[n(1) n(4)], 'Linewidth',3, 'Color', [.65 .65 .7]);
    end
    if n(6) > 0
        pncolor = [0 0 0]; % positive plane normal color
    else
        pncolor = [.5 .5 .5]; % negative plane normal color
    end
end

```

```

end
end % plane is plotted
if ptss == 2 || ptss == 4 % plot Burgers vectors
    if sortmv(isc,6,iAng) > 0
        Bvcolor = [0 .7 .7];
        if ssn >= 55
            Bvcolor = [.1 .6 0];
        end
        if ssn >= 43 && ssn < 55
            Bvcolor = [1 .6 0];
        end
    else
        Bvcolor = [0 1 1];
        if ssn >= 55
            Bvcolor = [.3 .9 0];
        end
        if ssn >= 43 && ssn < 55
            Bvcolor = [1 .8 0];
        end
    end
    Sfs = 1;
    if ssn < 43 % will reverse the sign of Schmid factor for dislocations
        end
    if Sf > 0 % plot Burgers vector direction
        if ssn >= 43 % this is for twins - the Burgers vector length is shown to be 1/2 of the usual length in the unit cell
            plot(b(2),-b(1),'.','MarkerSize', 24, 'Color', Bvcolor)
            plot([b(2) (b(2)+b(5))/2],[-(b(1) (b(1)+b(4))/2)],'Linewidth',4,'Color',Bvcolor)
        else
            plot(b(2),-b(1),'.','MarkerSize', 24, 'Color', Bvcolor)
            plot([b(2) b(5)],-[b(1) b(4)],'Linewidth',4,'Color',Bvcolor)
        end
        % quiver(p1(1),p1(2),dp(1),dp(2),0,'Linewidth',2,'Color',Bvcolor)
    end
    else % plot Burgers vector in opposite direction
        if ssn >= 43 % this is for twins - the Burgers vector length is shown to be 1/2 of the usual length in the unit cell
            plot(b(2),-b(1),'.','MarkerSize', 24, 'Color', Bvcolor)
            plot([b(2) (2*b(2)+b(5))/3],[-(b(1) (2*b(1)+b(4))/3)],'Linewidth',4,'Color',Bvcolor)
        else
            plot(b(5),-b(4),'.','MarkerSize', 24, 'Color', Bvcolor)
            plot([b(5) b(2)],-[b(4) b(1)],'Linewidth',4,'Color',Bvcolor)
        end
        % quiver(p2(1),p2(2),-dp(1),-dp(2),0,'Linewidth',4,'Color',Bvcolor)
    end
end
if ptss ==3
    plot([b(2) (b(2)+n(5))],[-(b(1) (b(1)+n(4)))],'Linewidth',4,'Color',pncolor)
end
end % Burgers vector is plotted
for j = 1:1:4 % plot the 4 top most surface prisms of the hex cell that have the highest z elevation
    plot(prsyplt(j,:),-prsxplt(j,:), 'Linewidth',2,'Color',[.0 .0 .0]);
end
if pta123o > 0
    if Ang(iAng,4) >= 90 % make the 3 coordinate axes visible above slip planes
        plot([0 a1(2)],-[0 a1(1)], ' ','Linewidth',3,'Color',[1 0 .3]);% plot x = red
        plot([0 a2(2)],-[0 a2(1)], ' ','Linewidth',3,'Color',[.5 .6 0]);% plot y = green-gold
        plot([0 a3(2)],-[0 a3(1)], ' ','Linewidth',3,'Color',[0 0 1]);% plot z = blue
    end
end
if ptpl == 1 % plot plane traces
    if ssn >= 55 % compression twin plane traces green
        plot([-pt(2) pt(2)],-[-pt(1) pt(1)],'-','Linewidth',3,'Color',[.2 .8 0])
    elseif ssn > 42 && ssn < 55 % extension twin plane traces orange
        plot([-pt(2) pt(2)],-[-pt(1) pt(1)],'-','Linewidth',3,'Color',[1 .6 0])
    elseif ssn > 12 && ssn < 43 % <c+a> plane traces green-gold
        plot([-pt(2) pt(2)],-[-pt(1) pt(1)],'-','Linewidth',3,'Color',[.95 .85 0])
    elseif ssn < 13 && ssn > 6 % pyr <a> green
        plot([-pt(2) pt(2)],-[-pt(1) pt(1)],'-','Linewidth',3,'Color',[0 .9 .5])
    elseif ssn < 7 && ssn > 3 % prism <a> red
        plot([-pt(2) pt(2)],-[-pt(1) pt(1)],'-','Linewidth',3,'Color',[1 .2 0])
    else % {medium slip systems} blue
        plot([-pt(2) pt(2)],-[-pt(1) pt(1)],'-','Linewidth',3,'Color',[0 0 1])
    end
end %----> NOTE that Schmid factor vector is plotted in correct direction,

```

```

end % plot plane traces
if pta123o == 1 % plot coordinate axes
    plot(0,0,'ko');
end
%----> Burgers vector is labeled and plotted with consistently signed b vector direction.
if ptss >= 1
    title(['ssn' num2str(ssn) ' n' mat2str(slpsys{2,ssn}(1,:)) mat2str(Sfs*slpsys{2,ssn}(2,:)) 'b'],...
    [mat2str(sortmv(isc,4:6,iAng),3), mat2str(sortmv(isc,7:9,iAng),3)],...
    ['Eulers = ', mat2str(Ang(iAng,3:5),3)],...
    ['c-axis = ', mat2str(sortmv(nslphex+1,10:12,iAng),3)],...
    [LC ' Or-' num2str(iAng) ' m' num2str(isc) ' = ' num2str(Sfs*Sf, 3) ]
    ])
end
end
end
end

```

## APPENDIX B: Matlab MPR hexagonal grain pair analysis code (written by Thomas R. Bieler)

```
% T.R. Bieler - m' Schmid and fip calculator, 4 June-14 1 July 2013 with input from Adam L Pilchak
% contains pieces from prior codes that are probably right, but no guarantees, use at your own risk.
% Written and used in Matlab release R2009b, and R2016a,
% substantially revised in 2018 during sabbatical at IMDEA Materiales
%
% Sources for these ideas are discussed in
% Bieler et al. Int. J. Plasticity 25(9), 1655–1683, 2009, and
% Kumar et al. J. Engineering and Materials Technology 130, 021012, 2008
% Bieler et al. Current Opinion in Solid State and Materials Science 18(4) 2014 212-226
% and related prior work.

% Important note - Euler angle computation coordinate system is not
% necessarily consistent with any other coordinate system. To obtain
% consistent results to make slip planes and Burgers vectors come out
% right, we pre-rotate acquired data by 180deg in first Euler angle so that
% the Euler angle coordinate system has X down and Y right. Plotting is
% done with this perspective in mind. If your raw data is not pre-rotated
% then setting hkl = 1 and adjusting first Euler angle when computing g
% below is necessary.

% Input data are default type 2 grains file and reconstructed grain boundary files from TSL
% The reconstructed boundary file does not contain phase ID, so the grain
% file is also needed, and it is the primary source.

% This code expects phase ID to be 1 = hex, 2 = BCC, 3 = FCC, 4 = BCT (Sn).
% If your Phase ID is different, then some adjustments need to be made -
% probably easiest if you copy information in column 10 of IDgr and put it in
% column 11, and then transform it to the phase number needed in this code in column 10.

% To run on particular boundary with two orientations, put values into IDGR
% with estimates of relative grain center positions, and skip the file input in the next block
% [_ 25 13] is maximum Sf in single slip in Z
clc; clear;

IDgr = [1 8.0421 89.3031 354.1300 10 10 60.2 0.364 1.3 0 1 % 40.6+180 8.5 296 159.4, 8.8, 203.7, 36 IDgr = [1 0 0 0 354.27
88.49 352.07 60.2 0.364 0 0 1 % 40.6+180 8.5 296 159.4, 8.8, 203.7, 37
2 2.6823 101.5918 354.2043 15 4 60.2 0.364 1.3 0 1] % 270.6, 14.3, 96

delx = IDgr(2,5) - IDgr(1,5); dely = IDgr(2,6) - IDgr(1,6);
mid = [(IDgr(2,5)+IDgr(1,5)) (IDgr(2,6)+IDgr(1,6))]*.5; gbvec = [0 1;-1 0]*[delx;dely]*.5;
x1 = mid(1,1)+gbvec(1,1); y1 = mid(1,2)+gbvec(2,1); x2 = mid(1,1)-gbvec(1,1); y2 = mid(1,2)-gbvec(2,1);
trang = atand( -(y2-y1) / (x2-x1) );
if trang < 0
    trang = trang + 180;
end
RBdyn = [ 1 2 3 4 5 6 (delx^2+dely^2)^.5 trang x1 y1 x2 y2 2 1]
% Y goes down; length, angle, x1 y1 x2 y2 right grain #, left grain #
fnameRCB = 'just_one_pair_of_points_RB.txt';
% The code reads #(1), orientation(2:4), grain center(5,6), phase ID(10) from IDgr, and
% grain boundary inclination from horizontal(8) and segment position(9:12) and right, left grain #s (13,14)
% are read from the reconstructed grain boundary file

% If you want to enter your own data to explore using this code, you will want to populate the above
% two variables in the same way as Grain ID and Reconstructed Boundary files are, as follows:
% In IDgr, Column 1 is grain number, columns 2-4 are Bunge Euler angles with X down and Y to the right
% columns 5 and 6 contain x and y positions of the data points (normally grain center in Grains file)
% In RBdy, in in row 1 (which is boundary #1) euler angles for the two grains identified in columns 13 and 14
% are provided in columns 1-6. column 7 is grain boundary length, column 8 (H in excel), is the angle from the horizontal
% to the apparent grain boundary direction e.g. 90deg if you want a vertical boundary. columns 9-12 have start and
% end positions of the grain boundary. In columns 13 and 14 (J&K) put the
% right,left grain numbers on either side of boundary 1 in that order (yes, the right one first).

%%
```

```

clc; clear;

GF2HeaderLines = 16; % 11 for single phase, 12 for two phase
RCBHeaderLines = 11; % total number of header lines for the Reconstructed boundary file
fnameGF2 = 'C:\Users\chels\Desktop\Titanium\Tension\Ti525_#10_EBSD Scans\Ti525_10_GF.txt'; GF2HeaderLines = 17;
fnameRCB = 'C:\Users\chels\Desktop\Titanium\Tension\Ti525_#10_EBSD Scans\Ti525_10_RB.txt'; RCBHeaderLines = 11;
GF2HeaderLines = 12;
RCBHeaderLines = 8;
fileID = fopen(fnameGF2)
dataGF = importdata(fnameGF2, '', GF2HeaderLines)
IDgr = dataGF.data;
fileID = fopen(fnameRCB)
dataRB = importdata(fnameRCB, '', RCBHeaderLines)
RBdyn = dataRB.data;
fclose('all')
fnlengthRCB = length(fnameRCB); chr=char(fnameRCB);

%%
Sfthr = 0.2; % higher schmid tolerance value used to limit serach for high m' values
SflimL = 0.0; % lower schmid tolerance value used to limit filling out table
mpthr = 0.75; % threshold value for considering m' values to be meaningful
hkl = 1; % flag used to decide whether to adjust first euler angle for various reasons... see below

nslphex = 39; c_a_hex = 1.59; % 1.587 for pure Ti ... not turning on compression twinning in Hexagonal
nslpbcc = 24; c_a_bcc = 1.0; % could differ for metastable phases... not turning on 123 slip
nslpfcc = 12; c_a_fcc = 1.0; % ~1.02 for TiAl% For FCC, it is 18 if cube slip is included.
nslpbct = 32; c_a_bct = 0.5456; % for Sn
nslp = [nslphex, nslpbcc, nslpfcc, nslpbct]; % number of slip systems used for phases 1, 2, 3, 4
c_a = [c_a_hex, c_a_bcc, c_a_fcc, c_a_bct];

% If your data is SINGLE PHASE, then you must put the correct phase number into the variable one_ss, HERE
one_ss = 1; % e.g. , the if statement below will set phase = 1 for Hex, 2 for BCC(3 for FCC) in IDgr file column 10:
numPhases = max(IDgr(:,10)); % check the number of phases in the dataset
if numPhases > 0 && (chr(fnlengthRCB-4) == 'B' || chr(fnlengthRCB-4) == 'b')
    % do nothing
else % for a grain boundary trace, need to set IDGR to one_ss
    IDgr(:,10) = one_ss; % single phase, ---!!! set to 1 for HEX or 2 for BCC above !!!---
    for i = 1:1:4 % else if it's two phase, do nothing, if phase 1 is hex, 2 is bcc.
        if i ~= one_ss
            nslp(i) = 0;
        end
    end
end

% Stress tensor is defined using TSL convensions with x down !!! put the one you want last
sigma = [0,0,0; 0,1,0; 0,0,0];
nsten = 1;
for i = 1:1:nsten
    str2 = sigma(:,i)*sigma(:,i)';
    ststens_mag = (str2(1,1)+str2(2,2)+str2(3,3))^5;
    sigma_n(:,i) = sigma(:,i)/ststens_mag; % normalized stress tensor to get generalized Schmid factor
    sigma_v(:,i) = [sigma(1,1) sigma(2,2) sigma(3,3)]'; % vectorized version of trace
end

dIDgr = size(IDgr); % This is a default type 2 grain file, both are needed.
dRBdyn = size(RBdyn); % This is a reconstructed grain boundary file
good = 0;
if dRBdyn(1,2) == 21;
    for ii = 1:1:dRBdyn(1,1)
        end
    else
        RBdy = RBdyn;
    end
dRBdy = size(RBdy);

% E(X,Y,Z) will be calculated from [S11 S12 S13 S33 S44 S66] in 1/GPa;
% hexagonal stiffness chosen:
sij(1,:) = [0.9581 -0.4623 -0.1893 0.698 2.1413 2.408]/100; % for Ti from Simmons and Wang in units of 1/GPa

```

```

% cubic stiffness chosen:
sij(2,:) = [0.6862 -0.2581 -0.2581 0.6862 1.2123 1.2123]/100; % for Ta from Simmons and Wang in units of 1/GPa
% disp(E(X,Y,Z) in GPa; S11 S12 S13 S33 S44 S66 210 Rayne, J.A. and B.S. Chandrasekhar,
% Elastic Ccontants of beta tin from 4.2K to 300K, Phys Rev. 118, 1545-49, 1960
sij(4,:) = [4.3627 -3.3893 -0.394 1.4501 4.5393 4.1667]/100; % for Sn in units of 1/GPa
% Ti-6Al, Ti-15Cr, alpha/beta in Ti6242 from J. Kim and S.I. Rokhlin, J. Acoust. Soc. Am. 126-6 dec 2009

```

```

%% % Set up vectors useful for plotting unit cells with slip systems

```

```

O = [0 0 0 0]; % (I) (H)
A = [2 -1 -1 0]/3; % C ----- B
B = [1 1 -2 0]/3; % / \ / \
C = [-1 2 -1 0]/3; % / a2 / \
D = [-2 1 1 0]/3; % / \ / \
E = [-1 -1 2 0]/3; % (J)D ----- O(P)-a1-> A(G) --> x
F = [1 -2 1 0]/3; % \ / \ /
P = [0 0 0 1]; % \ a3 \ /
G = [2 -1 -1 3]/3; % \ / \ /
H = [1 1 -2 3]/3; % E ----- F
I = [-1 2 -1 3]/3; % (K) (L)
J = [-2 1 1 3]/3; %
K = [-1 -1 2 3]/3; % where a1 = OA a2 = OC a3 = OE
L = [1 -2 1 3]/3; % DA || a1, FC || a2, BE || a3

```

```

% Slip system definitions set as of 1 Nov 2019 to be consistent with DAMASK

```

```

% Hex plane direction 1st and 4th point is Burgers vector

```

```

% basal <a>-glide:&Be Mg Re Ti; Re

```

```

sshex(:,1) = [0 0 0 1; 2 -1 -1 0; D; E; F; A; B; C];

```

```

sshex(:,2) = [0 0 0 1; -1 2 -1 0; F; A; B; C; D; E];

```

```

sshex(:,3) = [0 0 0 1; -1 -1 2 0; B; C; D; E; F; A];

```

```

ibas = 1;

```

```

fbas = 3;

```

```

% prism <a>-glide:Ti Zr RE; Be Re Mg

```

```

sshex(:,4) = [0 1 -1 0; 2 -1 -1 0; E; E; E; F; L; K];

```

```

sshex(:,5) = [-1 0 1 0; -1 2 -1 0; A; A; A; B; H; G];

```

```

sshex(:,6) = [1 -1 0 0; -1 -1 2 0; C; C; C; D; J; I];

```

```

iprs = 4;

```

```

fprs = 6;

```

```

% prism <aa>

```

```

sshex(:,7) = [2 -1 -1 0; 0 1 -1 0; F; F; F; B; H; L];

```

```

sshex(:,8) = [-1 2 -1 0; -1 0 1 0; B; B; B; D; J; H];

```

```

sshex(:,9) = [-1 -1 2 0; 1 -1 0 0; D; D; D; F; L; J];

```

```

i2prs = 7;

```

```

f2prs = 9;

```

```

% pyramidal <a>-glide --*-- CORRECTED --*--

```

```

sshex(:,10) = [1 0 -1 1; -1 2 -1 0; E; E; E; D; I; L];

```

```

sshex(:,11) = [0 1 -1 1; -2 1 1 0; F; F; F; E; J; G];

```

```

sshex(:,12) = [-1 1 0 1; -1 -1 2 0; A; A; A; F; K; H];

```

```

sshex(:,13) = [-1 0 1 1; 1 -2 1 0; B; B; B; A; L; I];

```

```

sshex(:,14) = [0 -1 1 1; 2 -1 -1 0; C; C; C; B; G; J];

```

```

sshex(:,15) = [1 -1 0 1; 1 1 -2 0; D; D; D; C; H; K];

```

```

ipyra = 10;

```

```

fpyra = 15;

```

```

% pyramidal <c+a>-glide:: all?

```

```

sshex(:,16) = [1 0 -1 1; -2 1 1 3; A; B; I; P; L; A];

```

```

sshex(:,17) = [1 0 -1 1; -1 -1 2 3; B; B; I; P; L; A];

```

```

sshex(:,18) = [0 1 -1 1; -1 -1 2 3; B; C; J; P; G; B];

```

```

sshex(:,19) = [0 1 -1 1; 1 -2 1 3; C; C; J; P; G; B];

```

```

sshex(:,20) = [-1 1 0 1; 1 -2 1 3; C; D; K; P; H; C];

```

```

sshex(:,21) = [-1 1 0 1; 2 -1 -1 3; D; D; K; P; H; C];

```

```

sshex(:,22) = [-1 0 1 1; 2 -1 -1 3; D; E; L; P; I; D];

```

```

sshex(:,23) = [-1 0 1 1; 1 1 -2 3; E; E; L; P; I; D];

```

```

sshex(:,24) = [0 -1 1 1; 1 1 -2 3; E; F; G; P; J; E];

```

```

sshex(:,25) = [0 -1 1 1; -1 2 -1 3; F; F; G; P; J; E];

```

```

sshex(:,26) = [1 -1 0 1; -1 2 -1 3; F; A; H; P; K; F];

```

```

sshex(:,27) = [1 -1 0 1; -2 1 1 3; A; A; H; P; K; F];

```

```

ipyrc = 16;

```

```

fpyrc = 27;

```

```

% pyramidal <c+a>-2nd order glide
sshex(:,28) = [ 1 1 -2 2; -1 -1 2 3; (O+B)/2 ; C ; J ; (P+K)/2 ; L ; A];
sshex(:,29) = [-1 2 -1 2; 1 -2 1 3; (O+C)/2 ; D ; K ; (P+L)/2 ; G ; B];
sshex(:,30) = [-2 1 1 2; 2 -1 -1 3; (O+D)/2 ; E ; L ; (P+G)/2 ; H ; C];
sshex(:,31) = [-1 -1 2 2; 1 1 -2 3; (O+E)/2 ; F ; G ; (P+H)/2 ; I ; D];
sshex(:,32) = [ 1 -2 1 2; -1 2 -1 3; (O+F)/2 ; A ; H ; (P+I)/2 ; J ; E];
sshex(:,33) = [ 2 -1 -1 2; -2 1 1 3; (O+A)/2 ; B ; I ; (P+J)/2 ; K ; F];
i2pyrc = 28;
f2pyrc = 33;
% *** Twin directions are opposite in Christian and Mahajan, and are not correct to be consistent with them
% FROM Kocks SXHEX plane direction 1st and 4th point is Burgers vector, order of C1 differs from Kock's file
% {1012}<1011> T1 twins 0.17; -1.3 twins: all Twin Vector must go in the
% sense of shear, opposite C&M sense.
sshex(:,34) = [ 1 0 -1 2; -1 0 1 1; A ; B ; J ; K ; K ; K ];
sshex(:,35) = [ 0 1 -1 2; 0 -1 1 1; B ; C ; K ; L ; L ; L ];
sshex(:,36) = [-1 1 0 2; 1 -1 0 1; C ; D ; L ; G ; G ; G ];
sshex(:,37) = [-1 0 1 2; 1 0 -1 1; D ; E ; G ; H ; H ; H ];
sshex(:,38) = [ 0 -1 1 2; 0 1 -1 1; E ; F ; H ; I ; I ; I ];
sshex(:,39) = [ 1 -1 0 2; -1 1 0 1; F ; A ; I ; J ; J ; J ];
iT1 = 34;
fT1 = 39;
% {2111}<2116> T2 twins: 0.63; -0.4; Ti Zr Re RE]; Also does not follow C&M definition for shear direction
sshex(:,40) = [ 1 1 -2 1; -1 -1 2 6; (O+B)/2 ; C ; (J+I)/2 ; P ; (L+G)/2 ; A];
sshex(:,41) = [-1 2 -1 1; 1 -2 1 6; (O+C)/2 ; D ; (K+J)/2 ; P ; (G+H)/2 ; B];
sshex(:,42) = [-2 1 1 1; 2 -1 -1 6; (O+D)/2 ; E ; (L+K)/2 ; P ; (H+I)/2 ; C];
sshex(:,43) = [-1 -1 2 1; 1 1 -2 6; (O+E)/2 ; F ; (G+L)/2 ; P ; (I+J)/2 ; D];
sshex(:,44) = [ 1 -2 1 1; -1 2 -1 6; (O+F)/2 ; A ; (H+G)/2 ; P ; (J+K)/2 ; E];
sshex(:,45) = [ 2 -1 -1 1; -2 1 1 6; (O+A)/2 ; B ; (I+H)/2 ; P ; (K+L)/2 ; F];
iT2 = 40;
fT2 = 45;
% {1011}<101-2> C1 twins: 0.10; 1.1; Mg; Zr Ti]; agrees with C&M
sshex(:,46) = [ 1 0 -1 1; 1 0 -1 -2; P ; L ; A ; (A+B)/2 ; B ; I];
sshex(:,47) = [ 0 1 -1 1; 0 1 -1 -2; P ; G ; B ; (B+C)/2 ; C ; J];
sshex(:,48) = [-1 1 0 1; -1 1 0 -2; P ; H ; C ; (C+D)/2 ; D ; K];
sshex(:,49) = [-1 0 1 1; -1 0 1 -2; P ; I ; D ; (D+E)/2 ; E ; L];
sshex(:,50) = [ 0 -1 1 1; 0 -1 1 -2; P ; J ; E ; (E+F)/2 ; F ; G];
sshex(:,51) = [ 1 -1 0 1; 1 -1 0 -2; P ; K ; F ; (F+A)/2 ; A ; H];
iC1 = 46;
fC1 = 51;
% {2112}<211-3> C2 twins: 0.22; 1.2 Ti Zr Re]; agrees with C&M
sshex(:,52) = [ 1 1 -2 2; 1 1 -2 -3; (K+P)/2 ; L ; A ; (A+C)/2 ; C ; J];
sshex(:,53) = [-1 2 -1 2; -1 2 -1 -3; (L+P)/2 ; G ; B ; (B+D)/2 ; D ; K];
sshex(:,54) = [-2 1 1 2; -2 1 1 -3; (G+P)/2 ; H ; C ; (C+E)/2 ; E ; L];
sshex(:,55) = [-1 -1 2 2; -1 -1 2 -3; (H+P)/2 ; I ; D ; (D+F)/2 ; F ; G];
sshex(:,56) = [ 1 -2 1 2; 1 -2 1 -3; (I+P)/2 ; J ; E ; (E+A)/2 ; A ; H];
sshex(:,57) = [ 2 -1 -1 2; 2 -1 -1 -3; (J+P)/2 ; K ; F ; (F+B)/2 ; B ; I];
iC2 = 52;
fC2 = 57;

mns1p = max(nslp);
ss = zeros(8,3,mns1p,4);

for i=1:1:mns1p % Change n & m to unit vector,
if i <= nslphex
n=[sshex(1,1,i) (sshex(1,2,i)*2+sshex(1,1,i))/3^0.5 sshex(1,4,i)/c_a_hex]; % Plane normal /c_a_hex
m=[sshex(2,1,i)*1.5 3^0.5/2*(sshex(2,2,i)*2+sshex(2,1,i)) sshex(2,4,i)*c_a_hex]; % Slip direction *c_a_hex
ss(1,:,i,1) = n/norm(n); % alpha plane
ss(2,:,i,1) = m/norm(m); % alpha direction PHASE 1 is HEX
ss(3,:,i,1) = [3*sshex(3,1,i)/2, (sshex(3,1,i)+2*sshex(3,2,i))*sqrt(3)/2, sshex(3,4,i)*c_a_hex]; % hpoint 1
ss(4,:,i,1) = [3*sshex(4,1,i)/2, (sshex(4,1,i)+2*sshex(4,2,i))*sqrt(3)/2, sshex(4,4,i)*c_a_hex]; % hpoint 2
ss(5,:,i,1) = [3*sshex(5,1,i)/2, (sshex(5,1,i)+2*sshex(5,2,i))*sqrt(3)/2, sshex(5,4,i)*c_a_hex]; % hpoint 3
ss(6,:,i,1) = [3*sshex(6,1,i)/2, (sshex(6,1,i)+2*sshex(6,2,i))*sqrt(3)/2, sshex(6,4,i)*c_a_hex]; % hpoint 4
ss(7,:,i,1) = [3*sshex(7,1,i)/2, (sshex(7,1,i)+2*sshex(7,2,i))*sqrt(3)/2, sshex(7,4,i)*c_a_hex]; % hpoint 5
ss(8,:,i,1) = [3*sshex(8,1,i)/2, (sshex(8,1,i)+2*sshex(8,2,i))*sqrt(3)/2, sshex(8,4,i)*c_a_hex]; % hpoint 6
end

if i <= nslpbcc
n = [ssbcc(1,1,i),ssbcc(1,2,i),ssbcc(1,3,i)/c_a_bcc]; % slightly tetragonal has c/a < 1.0
m = [ssbcc(2,1,i),ssbcc(2,2,i),ssbcc(2,3,i)*c_a_bcc];
ss(1,:,i,2) = n/norm(n); % bcc plane PHASE 2 is BCC

```

```

ss(2,:;i,2) = m/norm(m); % bcc direction
ss(3,:;i,2) = [ssbcc(3,1,i),ssbcc(3,2,i),ssbcc(3,3,i)*c_a_bcc]; % point 1
ss(4,:;i,2) = [ssbcc(4,1,i),ssbcc(4,2,i),ssbcc(4,3,i)*c_a_bcc]; % point 2
ss(5,:;i,2) = [ssbcc(5,1,i),ssbcc(5,2,i),ssbcc(5,3,i)*c_a_bcc]; % point 3
ss(6,:;i,2) = [ssbcc(6,1,i),ssbcc(6,2,i),ssbcc(6,3,i)*c_a_bcc]; % point 4
ss(7,:;i,2) = [ssbcc(7,1,i),ssbcc(7,2,i),ssbcc(7,3,i)*c_a_bcc]; % point 5
ss(8,:;i,2) = [ssbcc(8,1,i),ssbcc(8,2,i),ssbcc(8,3,i)*c_a_bcc]; % point 6
end

if i <= nslpfcc
n = [ssfcc(1,1,i),ssfcc(1,2,i),ssfcc(1,3,i)/c_a_fcc]; % slightly tetragonal has c/a < 1.0
m = [ssfcc(2,1,i),ssfcc(2,2,i),ssfcc(2,3,i)*c_a_fcc];
ss(1,:;i,3) = n/norm(n); % fcc plane PHASE 3 is FCC
ss(2,:;i,3) = m/norm(m); % fcc direction
ss(3,:;i,3) = [ssfcc(3,1,i),ssfcc(3,2,i),ssfcc(3,3,i)*c_a_fcc]; % point 1
ss(4,:;i,3) = [ssfcc(4,1,i),ssfcc(4,2,i),ssfcc(4,3,i)*c_a_fcc]; % point 2
ss(5,:;i,3) = [ssfcc(5,1,i),ssfcc(5,2,i),ssfcc(5,3,i)*c_a_fcc]; % point 3
ss(6,:;i,3) = [ssfcc(6,1,i),ssfcc(6,2,i),ssfcc(6,3,i)*c_a_fcc]; % point 4
ss(7,:;i,3) = [ssfcc(7,1,i),ssfcc(7,2,i),ssfcc(7,3,i)*c_a_fcc]; % point 5
ss(8,:;i,3) = [ssfcc(8,1,i),ssfcc(8,2,i),ssfcc(8,3,i)*c_a_fcc]; % point 6
end

if i <= nslpbct
n = [ssbct(1,1,i),ssbct(1,2,i),ssbct(1,3,i)/c_a_bct];
m = [ssbct(2,1,i),ssbct(2,2,i),ssbct(2,3,i)*c_a_bct];
ss(1,:;i,4) = n/norm(n); % bct plane PHASE 4 is BCT
ss(2,:;i,4) = m/norm(m); % bct direction
ss(3,:;i,4) = [ssbct(3,1,i),ssbct(3,2,i),ssbct(3,3,i)*c_a_bct]; % point 1
ss(4,:;i,4) = [ssbct(4,1,i),ssbct(4,2,i),ssbct(4,3,i)*c_a_bct]; % point 2
ss(5,:;i,4) = [ssbct(5,1,i),ssbct(5,2,i),ssbct(5,3,i)*c_a_bct]; % point 3
ss(6,:;i,4) = [ssbct(6,1,i),ssbct(6,2,i),ssbct(6,3,i)*c_a_bct]; % point 4
ss(7,:;i,4) = [ssbct(7,1,i),ssbct(7,2,i),ssbct(7,3,i)*c_a_bct]; % point 5
ss(8,:;i,4) = [ssbct(8,1,i),ssbct(8,2,i),ssbct(8,3,i)*c_a_bct]; % point 6
end

end

%% Loop for grains to establish slip conditions for each grain

EY = zeros(int16(dIDgr(1,1)*1.1),3);
Sfplbv = zeros(mnslp+1,30);
sortmv = zeros(mnslp+1,30,int16(dIDgr(1,1)*1.1));
grcen = zeros(int16(dIDgr(1,1)*1.1));
listSf = zeros(8,dIDgr(1,1)); listss = zeros(8,dIDgr(1,1));
grcen(:,1) = -1; % that is a little bigger than needed because some grain numbers are skipped,
% and are thus marked with -1. Grains are processed by grain number, not array location
grmax = 0; ngcount = 0; fprintf('Numbers and vectors computed for Grain # ');
fnlengthRCB = length(fnameRCB); chr=char(fnameRCB);
Xr = [0;1;2;3];
for ng=1:1:dIDgr(1,1); % generalized Schmid factor calculation loop for each grain ng
if ng>ngcount+dIDgr/10;
ngcount=ngcount+dIDgr/10;
fprintf(' %d ',ng);
end
ig = IDgr(ng,1);
if ig > grmax
grmax = ig;
end
if ig > 0 % phase(1) grain center(2,3) eulers(4:6) grain ID
grcen(ig,1:7) = [IDgr(ng,10) IDgr(ng,5:6) IDgr(ng,2:4) IDgr(ng,1)];
phid = grcen(ig,4:6); % phid is Euler phi angles in degrees

ph = grcen(ig,1); % phase ID set

if hkl == 1
phid(1) = phid(1)+ 180 ; % + 180 or +90 to convert hkl to TSL software default
if phid(1)>360 % or +180 to modify TSL Euler angle coordinate system to have X down and Y right;
phid(1) = phid(1) - 360;

```

```

elseif phid(1) < 0
    phid(1) = phid(1) + 360;
end
end

g1=[cosd(phid(1)),sind(phid(1)),0; -sind(phid(1)),cosd(phid(1)),0; 0,0,1];
g2=[1,0,0; 0,cosd(phid(2)),sind(phid(2)); 0,-sind(phid(2)),cosd(phid(2))];
g3=[cosd(phid(3)),sind(phid(3)),0; -sind(phid(3)),cosd(phid(3)),0; 0,0,1];
g=g3*g2*g1;
if nsten == 1
    sigma_n(:,ig) = sigma_n(:,1);
    sigma_v(:,ig) = sigma_v(:,1);
end
gsgT = g*sigma_n(:,ig)*g'; %rotated stress tensor
green(ig,7:9) = [0 0 1]*g; %c-axis direction
green(ig,10:18) = [g(1,:) g(2,:) g(3,:)]; % Orientation matrix is stored

% calculate elastic modulus to find compliance mismatch in three principal directions (from Nye textbook on Anisotropy)
if ph == 5 % needs a different structure for the sij matrix - needs more terms, not working in this version.
elseif ph == 4
    for i = 1:1:3 % This gives the modulus in the x (1), y (2), z (3) directions (as looped by i)
        e1 = sij(ph,1)*(g(1,i)^4 + g(2,i)^4) + sij(ph,4)*g(3,i)^4;
        e2 = (2*sij(ph,2) + sij(ph,6))*(g(1,i)^2 * g(2,i)^2);
        e3 = (2*sij(ph,3) + sij(ph,5))*g(3,i)^2 * (g(1,i)^2 + g(2,i)^2);
        EY(ig,i)=1./(e1+e2+e3); % NOTE: slip system and plane information not installed in this version for Sn or TiAl
    end
elseif ph == 2 || ph == 3
    for i = 1:1:3
        EY(ig,i) = 1./(sij(ph,1) - 2*(sij(ph,1) - sij(ph,2) - sij(ph,5)/2) * ...
            (g(1,i)^2*g(2,i)^2 + g(2,i)^2*g(3,i)^2 + g(3,i)^2*g(1,i)^2) );
    end
elseif ph == 1
    for i = 1:1:3
        EY(ig,i) = 1./(sij(ph,1) * (1-g(3,i)^2)^2 + sij(ph,4) * g(3,i)^4 + ...
            (sij(ph,5) + 2*sij(ph,3))*(1-g(3,i)^2)*g(3,i)^2);
    end
end

for j=1:1:nslp(ph) % direction plane Sfplbv means Schmid factor, plane and Burgers vector (and points on plane)
    Sfplbv(j,1) = j; % m * sigma * n
    Sfplbv(j,2) = ss(2,:,j,ph)*gsgT*ss(1,:,j,ph); % generalized Schmid factor
    if ph == 1 && j>27 && Sfplbv(j,2)<0
        Sfplbv(j,2) = 0.001*Sfplbv(j,2); % this is to prevent anti-twin shears from being seriously considered later
    end
    Sfplbv(j,3) = abs(Sfplbv(j,2)); % abs(generalized schmid factor)
    Sfplbv(j,4:6) = g*ss(1,:,j,ph); % plane normal in lab coords
    Sfplbv(j,7:9) = g*ss(2,:,j,ph); % bv direction in lab coords
    Sfplbv(j,10:12) = cross(Sfplbv(j,4:6),[0,0,1]); % plane trace
    for k = 1:1:6
        is = 3*k+10;
        ie = is+2;
        Sfplbv(j,is:ie) = g*ss(k+2,:,j,ph); % plane plotting vectors from origin to points in cell, in lab coords
    end
end
% useful plotting for hexahedral tetragonal unit cell vectors that sort to bottom row
Sfplbv(mnslp+1,:) = [ph 1 -1 [1 0 0]*g [0 1 0]*g [0 0 1*c_a(ph)]*g 0 0 0 0 0 0 0 0 0 0 0 0]; % don't change g to g' here!
otherwise it may make incorrect cubic prisms
sortmv(:,ig) = sortrows(Sfplbv,-3); % Sort slip systems by Schimid factor
% find slope of first four slip systems; y-intercept is close to max Schmid factor
% XRank = [1 0; 1 1; 1 2; 1 3]; BL = XRank\YLSf; BR = XRank\YRSf;
YSf(1:4,1) = sortmv(1:4,3,ig); mdl = fitlm(Xr,YSf);
green(ig,19:21) = [mdl.Coefficients{1:2,{'Estimate'}}] mdl.Rsquared.Ordinary ];
listSf(1:8,ig) = sortmv(1:8,3,ig); listss(1:8,ig) = sortmv(1:8,1,ig);
end

end % ig > 0 check
end % ng loop
fprintf(' %d\n ', ng);

for ii = 1:1:dRBdy(1,1);
    gblist(ii,1) = ii;
end

```

```

end
% to modify gblist with a short list, paste desired list into this variable as column and delete remaining rows

%% Now start processing by grain boundary...
gbcount = 0;
BL = [0 0 0]; BR = [0 0 0];
gbnorm = zeros(dRBdy(1,1),3);
gbtrac = zeros(dRBdy(1,1),3);
damp = zeros(24,dRBdy(1,1));
mpr = zeros(mnslp+2,mnslp+2,dRBdy(1,1));
pln = zeros(mnslp+2,mnslp+2,dRBdy(1,1));
Bvd = zeros(mnslp+2,mnslp+2,dRBdy(1,1));
rbvm = zeros(mnslp+2,mnslp+2,dRBdy(1,1));
rbvec = zeros(mnslp+2,3,mnslp+2,dRBdy(1,1));
nbcoun = 0; fprintf('Computing grain boundary parameters for GB # ');
jk4max = 1; top3d3 = 0; top3d2 = 0; top3d1 = 0; top3d0 = 0;
gbcheck = sortrows(gblist,1);
while gbcount < length(gbcheck)
    gbcount = gbcount+1;
    gbnum = gbcheck(gbcount,1);
    % for gbnum = 1:1:dRBdy(1,1); %gbnum is grain boundary number, will calculate m' and other damage parameters
    if gbnum>nbcoun+dRBdy/10;
        nbcoun=nbcoun+dRBdy/10;
        fprintf(' %d ',gbnum);    % , jk4max
    end
    grL = RBdy(gbnum,13);    grR = RBdy(gbnum,14);
    % check and reset RBdy to 13 (left grain) and 14 (right grain)
    if grL > 0 && grR > 0 && grL <= grmax && grR <= grmax % dIDgr(1,1) && grR <= dIDgr(1,1)
        if grcen(grL,1) > 0 && grcen(grR,1) > 0 % this is to correct if left and right grains are wrong
            if grcen(grR,2)<grcen(grL,2)
                grR = RBdy(gbnum,13);    grL = RBdy(gbnum,14);
                RBdy(gbnum,13) = grL ; RBdy(gbnum,14) = grR ;
            end
        end

        jk = 1; % counter for the number of m' calculations made where Schmid factors are > low tolerance
        jk4 = 1; % counter for the number of m' calculations made where Schmid factors are > high tolerance
        mpmax = 0;    mploc = 0;
        dpsum = 0;    dpsum4 = 0;
        mpsum = 0;    mpsum4 = 0;
        damage = 0;    damage4 = 0;

        mpr(2,1,gbnum) = grL; mpr(1,2,gbnum) = grR; mpr(2,2,gbnum) = gbnum; % m-prime table label for grain numbers in mpr()

        if strcmp(num2str(sigma_v(:,ig)),num2str([1 0 0])) % stress axis || [100] (X)
            EgrL = EY(grL,1); EgrR = EY(grR,1);
        elseif strcmp(num2str(sigma_v(:,ig)),num2str([0 1 0])) % stress axis || [010] (Y)
            EgrL = EY(grL,2); EgrR = EY(grR,2);
        elseif strcmp(num2str(sigma_v(:,ig)),num2str([0 0 1])) % stress axis || [001] (Z)
            EgrL = EY(grL,3); EgrR = EY(grR,3);
        elseif trace(sigma_n(:,ig)) == 0 % Crude estimate of shear effects follows, may not be meaningful
            EgrL = EY(grL,3)*abs(sigma_n(1,2,ig)) + EY(grL,2)*abs(sigma_n(1,3,ig)) + EY(grL,1)*abs(sigma_n(2,3,ig));
            EgrR = EY(grR,3)*abs(sigma_n(1,2,ig)) + EY(grR,2)*abs(sigma_n(1,3,ig)) + EY(grR,1)*abs(sigma_n(2,3,ig));
        else
            fprintf('Can't calculate modulus for this stress state\r');
            EgrL = 1; EgrR = 1 % pause
        end
        Eratio = min(EgrL,EgrR)/max(EgrL,EgrR);    % always use Emin/Emax!

        F1A = zeros(1,mnslp); % F1 FIP, Simkin et al. 2003 for grain A
        % F14A = 0; % F1 FIP w/ restriction on Schmid factor value for grain A
        F1B = zeros(1,mnslp); % F1 FIP for grain B
        % F14B = 0; % F1 FIP w/ restriction on Schmid factor value for grain B
        F1 = 0; % F1 for grainA/grainB
        F14A = zeros(1,mnslp); % F14 for grainA (with restriction on Schmid factor value)
        F14B = zeros(1,mnslp);

        avgdp4 = .75; % These values indicate instances where values
        avgmp4 = .55; % of dm' or m' are too low to take seriously
        % RBdy(gbnum,1:6) = (180/pi).*RBdy(gbnum,1:6);

```

```

gbnorm(gbnum,:) = [cosd(RBdy(gbnum,8)) sind(RBdy(gbnum,8)) 0];
gbtrac(gbnum,:) = sigma_n(:,grL)*gbnorm(gbnum,:);

for k = 1:1:mnsplp % Build table of m' values for each grain pair
    SchmL = sortmv(k,2,grL); % Use the correctly signed version of Schmid factor in position 2
    mpr(k+2,1,gbnum) = sortmv(k,1,grL); mpr(k+2,2,gbnum) = abs(SchmL); % Schmid factor header grL is down (k goes with L)
    if abs(SchmL) > Sfthr
        kmax = k;
    end
    for j = 1:1:mnsplp % j goes across (with R grain in columns)
        SchmR = sortmv(j,2,grR); % Use the correctly signed version of Schmid factor in position 2
        if k == 1 && abs(SchmR) > Sfthr % find size of upper left corner of m' matrix for which Schmid factors are higher than threshold
            jmax = j;
        end
        mpr(1,j+2,gbnum) = sortmv(j,1,grR); mpr(2,j+2,gbnum) = abs(SchmR); % grL goes down, grR across, (j goes with R)
        if abs(SchmL) > SflimL && abs(SchmR) > SflimL
            mpl = sortmv(j,4:6,grR)*sortmv(k,4:6,grL); % plane This is a dot product
            mbv = sortmv(j,7:9,grR)*sortmv(k,7:9,grL)*sign(SchmL*SchmR); % direction This is a dot product
            mprime = mpl*mbv; % if the b directions are pointing similarly mb is positive
            mpr(k+2,j+2,gbnum) = mprime; pln(k+2,j+2,gbnum) = mpl; Bvd(k+2,j+2,gbnum) = mbv; % m', plane and Burgers vector table
            is filled in,
            rbva = sortmv(j,7:9,grR) - sortmv(k,7:9,grL); % store residual Burgers vector
            rbvb = sortmv(j,7:9,grR) + sortmv(k,7:9,grL); % store residual Burgers vector
            if norm(rbva) > norm(rbvb)
                rbv = rbvb;
            else
                rbv = rbva;
            end
            rbvm(k+2,j+2,gbnum) = norm(rbv);
            rbvec(k+2,1:3,j+2,gbnum) = rbv;

            % schmA
            F1A(k) = F1A(k)+abs(sortmv(k,3,grL)*dot(sortmv(k,7:9,grL)',sigma_v(:,ig))*dot(sortmv(k,7:9,grL)',sortmv(j,7:9,grR'))); % F1
            for grain A
            F1B(j) = F1B(j)+abs(sortmv(j,3,grR)*dot(sortmv(j,7:9,grR)',sigma_v(:,ig))*dot(sortmv(j,7:9,grR)',sortmv(k,7:9,grL'))); % F1 for
            grain B
            if mprime > mpthr % assumes no slip transfer (or damage) occurs if m' < m' threshold or when m' = 1
                dampar = mprime + 0.1; % pushes m' up by 0.1, so that 1 is worst case (i.e. m'=0.9 is most damaging condition).
                if dampar > 1
                    dampar = 2-dampar; % assume dampar < 1 means less likely to generate damage due to less slip transmission activity
                end
                dpsum = dpsum + dampar; % damage parameter only, for all slip systems where m' > mpthr
                mpsum = mpsum + abs(mprime); % m' only, for all slip systems where m' > mpthr
                damage = damage + dampar*max(abs(SchmL),abs(SchmR)); % damage parameter modified by schmid factor

                if (abs(SchmL) > Sfthr && abs(SchmR) > Sfthr) || abs(SchmL) < 0.001 || abs(SchmR) < 0.001 % latter condition is for twins,
                to enable seeing them later
                    % assumes that slip transfer happens only if Sf > 0.Sfthr and both have high schmid factor and capturing effect of anti-twin
                    himp4(jk4,gbnum) = [k j abs(mprime), mprime SchmL SchmR]; % location and values of high m' values for grain pair;
                    k(rows) is from left grain; j(columns) is from right grain
                    dpsum4 = dpsum4 + dampar; % running sum of slip system interactions that have Sf > 0.4
                    mpsum4 = mpsum4 + abs(mprime); % running sum of m' for slip system interactions that have Sf > Sfthr
                    damage4 = damage4 + dampar*max(abs(SchmL),abs(SchmR)); % damage parameter modified by schmid factor
                    if jk4 > jk4max
                        jk4max = jk4;
                    end
                    jk4 = jk4 + 1;
                    F14A(k) = F14A(k)+abs(sortmv(k,3,grL)*dot(sortmv(k,7:9,grL)',sigma_v(:,ig))*dot(sortmv(k,7:9,grL)',sortmv(j,7:9,grR')));
                    % F14 for grain A
                    F14B(j) = F14B(j)+abs(sortmv(j,3,grR)*dot(sortmv(j,7:9,grR)',sigma_v(:,ig))*dot(sortmv(j,7:9,grR)',sortmv(k,7:9,grL'))); %
                    F14 for grain B
                end
                if mpmax < abs(mprime) % record maximum m' value % and its location in matrix ?
                    mpmax = abs(mprime);
                end
                jk = jk + 1;
            end % of m' > mpthr if statement
        end % of if statement for values with schmid factors > SflimL
    end % slip system j loop for each B grain in pair
end % slip system k loop for each A grain in pair

```

```

% Variables evaluated above in the loops: dpsum mpsum jk4 dpsum4 mpsum4 F1 F14
gbodam = damage*abs(norm(gbtrac(gbnum,:))); % damage parameter modified by apparent GB inclination
gbodam4 = damage4*abs(norm(gbtrac(gbnum,:))); % damage parameter for high schmid modified by GB inclination
caxmis = (1-(grcen(grL,7:9)*grcen(grR,7:9))^2)^.5; % misorientation of c-axes (not meaningful for cubic)
avgdp = dpsum/(jk-1); % average value of dm'
avgmp = mpsum/(jk-1); % average value of m'
F1Asort = sort(F1A,'descend'); F1Bsort = sort(F1B,'descend');
F14Asort = sort(F14A,'descend'); F14Bsort = sort(F14B,'descend');
maxF1 = max(F1Asort(1),F1Bsort(1));
maxF14 = max(F14Asort(1),F14Bsort(1));
if jk4 > 1
    avgdp4 = dpsum4/(jk4-1); %average value of damage for slip systems with Sf > 0.4
    avgmp4 = mpsum4/(jk4-1); %average value of m' for slip systems with Sf > 0.4
end

jk6 = 0; jktop3or6 = 0; % counters for number of m' values to average later.
top3mpn = 0; top6mpn = 0; t3mpthr = 0; maxmpkj = 0; maxSfk = 0; maxSfj = 0; maxkjSfs = 0; Sfsum = 2;
pairsum = zeros(mnslp,mnslp); pairprod = zeros(mnslp,mnslp);
mpSflist = zeros(kmax*jmax:6); mpSfshlist = zeros(1,36); ikj = 1;
for k = 1:1:kmax % Rather than finding all m' values for Sf > tolH, look only for top 3 or top 6 Sf value pairs
    for j = 1:1:jmax % find sum of schmid factors for each element of mpr array and put in pairsum(), similarly for pairprod(uct)
        pairsum(k,j) = mpr(k+2,2,gbnum) + mpr(2,j+2,gbnum); pairprod(k,j) = mpr(k+2,2,gbnum) * mpr(2,j+2,gbnum);
        mpSflist(ikj,1:6) = [k j abs(mpr(k+2,2,gbnum)) abs(mpr(2,j+2,gbnum)) abs(mpr(k+2,j+2,gbnum)) rbvm(k+2,j+2,gbnum)];
        ikj = ikj + 1;
    end
end
sortmplist = sortrows(mpSflist,-5);
for ii = 1:1:6
    mpSfshlist(1,6*(ii-1)+1:6*ii) = sortmplist(ii,1:6);
end % parameters for max m' are in first row; k j Sf(kL) Sf(jR) m' rbvm
maxSfk = mpSfshlist(1,1); maxSfj = mpSfshlist(1,2); maxmpkj = mpSfshlist(1,5);
maxkjSfs = mpSfshlist(1,3)+mpSfshlist(1,4); maxkjSfp = mpSfshlist(1,3)*mpSfshlist(1,4);
maxkjsmp = maxkjSfs*maxmpkj; maxkjpmp = maxkjSfp*maxmpkj; maxmprbv = mpSfshlist(1,6);

while (jk6 < 6 || jktop3or6 < 3) && Sfsum > 0
    kjmax = [0 0 0 0];
    for k = 1:1:kmax % find location of highest pairsum (and product) in current pairsum array
        for j = 1:1:jmax
            if pairsum(k,j) > kjmax(1) % finds largest Spair value in current kmax x jmax Pairsum() array
                kjmax = [pairsum(k,j) k j pairprod(k,j)]; % identifies location k j of sum of Schmid factors
            end
        end
    end
    Sfsum = kjmax(1);
    mpchk = abs(mpr(kjmax(2)+2,kjmax(3)+2,gbnum)); % puts (next) m' into mpchk
    if jk6 < 6 && Sfsum > 0
        top6mpn = top6mpn + mpchk;
        pairsum(kjmax(2),kjmax(3)) = -1; % Now that the highest pairsum value is found and added to sum, make it unfindable
        jk6 = jk6 + 1;
        if jk6 == 3;
            top3mpn = top6mpn; % capture top 3 values in this variable
        end
    end
    if jktop3or6 < 3 && Sfsum > 0
        pairsum(kjmax(2),kjmax(3)) = pairsum(kjmax(2),kjmax(3)) -1; % mark position with -2 if inside this query
        if mpchk > mpthr
            t3mpthr = t3mpthr + mpchk; % more stringent criterion for m' only > mpthr used.
            jktop3or6 = jktop3or6 + 1;
            % [gbnum t3mpthr mpchk jktop3or6 maxkj]
        end
    end
end
top6mpn = top6mpn/jk6; % These average values of m' are without regard to magnitude of m'
if top3mpn > 0
    top3mpn = top3mpn/3;
else
    top3mpn = top6mpn;
end
if jktop3or6 == 3

```

```

t3mpthr = t3mpthr/jktop3or6;
top3d3 = top3d3 + 1;
elseif jktop3or6 == 2
t3mpthr = t3mpthr/jktop3or6;
top3d2 = top3d2 + 1;
elseif jktop3or6 == 1
t3mpthr = t3mpthr/jktop3or6;
top3d1 = top3d1 + 1;
elseif jktop3or6 == 0
t3mpthr = 0;
top3d0 = top3d0 + 1;
end
mpr(1,1,gbnum) = mpmax;

% GB#, left gr, right gr, angle/axis of misorientation, average of top 3 m' values in upper kj box, maximum m' in upper kjbox, corresponding
Schmid factor sum,
% product between Schmid factor sum and maximum m' value, row for k (left grain), column for j (right grain),
% left grain y-intercept, slope, and correlation coefficient, right grain y-intercept, slope, and correlation coefficient.
slpint = [-min(grcen(grL,20),grcen(grR,20)) -max(grcen(grL,20),grcen(grR,20))... % slope, intercept, and R^2 values for left and right
grains
max(grcen(grL,19),grcen(grR,19)), min(grcen(grL,19),grcen(grR,19)) grcen(grL,19:21) grcen(grR,19:21)];
mpmaxgrp = [t3mpthr maxmpkj maxkjsfs maxkjsmp maxkjsfp maxkjpmv maxmprbv maxSfk maxSfj];
tablepub(gbnum,:) = [gbnum grL grR RBdyn(gbnum, 7:10) mpmaxgrp slpint mpSfshlist];
damp(:,gbnum) = [maxSfk maxmpkj maxSfj dpsum damage gbodam caxmis dpsum4 damage4 gbodam4 avgdp avgdp4 avgmp avgmp4 ...
maxF1 maxF14 maxF1*Eratio maxF14*Eratio Eratio top3mpn top6mpn t3mpthr kmax jmax]; % this is a summary matrix used for
plotting
end % of if for grains with positive ID
end % of if for valid grain pair
end % of gbnum loop
gbcount = 1;
for ii = 1:length(tablepub)
if tablepub(ii,1) > 0
tablepubshort(gbcount,:) = tablepub(ii,:); gbcount = gbcount+1;
end
end
fprintf(' %d\n ', gbnum);
plotname = {' mp5k ', maxmpkj ', mp5j ', dm'sum ', m'dm'sum ', gbo*m'dm'sum ', cax-mis ', dm'sum4 ',...
' m'dm'4 ', gbo*dam4 ', norm dm" ', norm dm'4 ', norm m" ', norm m'4 ',...
' max(F1A,F1B) ', max(F14A,F14B) ', Emax(F1A,F1B) ', Emax(F14A,F14B) ', Eratio ', top3mpn', top6mpn', t3mpthr'};

%% Choose what to plot along the grain boundary map from variables 4-19 noted above
mpthr = mpthr; chsize = 16;
plist = [22 2]; % 13 14 11 12 15 16 17 18 19 20 21
for k = 1:length(plist); % 1:length(plist); % 4:4:4 %
plnx = plist(k);
if plnx == 13 || plnx == 14
bins = [.60 .64 .68 .72 .76 .80 .84 .88 .92 .96]; % for mp or mp4 or Eratio
elseif plnx == 11 || plnx == 12
bins = [.80 .82 .84 .86 .88 .90 .92 .94 .96 .98]; % for normp or normp4
elseif plnx == 7
bins = [0 0.156 0.309 0.454 0.588 0.707 0.809 0.891 0.951 0.988 1.000]; % for c-axis plot
% Corresponding degrees for bins above = [0 9 18 27 36 45 54 63 72 81 90]; % for c-axis plot
elseif plnx == 22 || plnx == 2
bins = mpthr:(1-mpthr)/10:1;
else
bins = linspace(min(nonzeros(damp(plnx,:))), max(damp(plnx,:)), 11); % auto bin size for anything
end
binsdat = bins; % temporary storage while setting up plot scale

max1 = max(RBdy(:,9)); % max x value for grR
max2 = max(RBdy(:,11)); % max x value for grL
maxx = max([max1; max2]);
may1 = max(RBdy(:,10)); % max y value for grR
may2 = max(RBdy(:,12)); % max y value for grL
maxy = max([may1; may2]);
f = figure('Position', [0,0,750,500]); movegui(f,'northwest'); set(gcf, 'Color', [1 1 1]); hold on;
% plot is based upon TV rastering, as given by TSL
axis([0 maxx*2 -maxy .15*maxy]); axis image; %equal;
set(gcf,'Color',[1,1,1]) % surrounding field is this color
text(maxx*-0.12, 0.11*maxy, 'm' , 'FontSize', chsize);

```

```

text(maxx*.004, 0.11*maxy, num2str(binsdat(1,1),'%4.3f'),'FontSize', chsize);
bins = [10 20 30 40 50 60 70 80 90 100]; % To set color key for boundaries
bcnt = 2;
for gbnnum = 1:1:100;
    wid = 10; widk = 2; % thickness for width bar
    if fix(gbnnum/10)<gbnnum/10 % tick marks for color bar
        wid = 2;
        if gbnnum > 90;
            wid = 4; widk=4;
        elseif gbnnum > 80;
            wid = 3; widk=3;
        end
    else
        text(maxx/100*(gbnnum-1)-maxx*0.03, 0.11*maxy, num2str(binsdat(1,bcnt),'%4.3f'),'FontSize', chsize); bcnt = bcnt + 1;
    end

    vec = gbnnum;
    if vec<bins(1); % [0.3 0.3 0.3] gray 0-bins(1)
        vRGB=[.3+.5*vec/bins(1) .3-.3*vec/bins(1) .3+.5*vec/bins(1)]; % gray -> purple
    elseif vec>=bins(1) && vec <bins(2); % [0.8 0.8 0.8] purple bins(1)-bins(2)
        vRGB=[.8-.8*(vec-bins(1))/(bins(2)-bins(1)) 0 .8-.1*(vec-bins(1))/(bins(2)-bins(1))]; % purple -> blue
    elseif vec>=bins(2) && vec <bins(3); % [0.0 0.7 0.7] blue bins(2)-bins(3)
        vRGB=[0 .9*(vec-bins(2))/(bins(3)-bins(2)) .7+.2*(vec-bins(2))/(bins(3)-bins(2))]; % blue -> turquoise
    elseif vec>=bins(3) && vec <bins(4); % [0.0 0.9 0.9] turquoise bins(3)-bins(4)
        vRGB=[.1*(vec-bins(3))/(bins(4)-bins(3)) .9-.4*(vec-bins(3))/(bins(4)-bins(3)) .9-.8*(vec-bins(3))/(bins(4)-bins(3))]; % turquoise -> dk
grn
    elseif vec>=bins(4) && vec <bins(5); % [0.1 0.5 0.0] dk grn bins(4)-bins(5)
        vRGB=[.1+.1*(vec-bins(4))/(bins(5)-bins(4)) .5+.4*(vec-bins(4))/(bins(5)-bins(4)) 0.0]; % dk grn -> green
    elseif vec>=bins(5) && vec <bins(6); % [0.2 0.9 0.0] green bins(5)-bins(6)
        vRGB=[.2+.7*(vec-bins(5))/(bins(6)-bins(5)) .9 0.0]; % green -> yellow
    elseif vec>=bins(6) && vec <bins(7); % [0.9 0.9 0.0] yellow bins(6)-bins(7)
        vRGB=[.9 .9-.3*(vec-bins(6))/(bins(7)-bins(6)) 0.0]; % yellow -> orange
    elseif vec>=bins(7) && vec <bins(8); % [0.9 0.6 0.0] orange bins(7)-bins(8)
        vRGB=[.9+.1*(vec-bins(7))/(bins(8)-bins(7)) .6-.6*(vec-bins(7))/(bins(8)-bins(7)) 0.0]; % orange -> red
    elseif vec>=bins(8) && vec <bins(9); % [1.0 0.0 0.0] red bins(8)-bins(9)
        vRGB=[1 .7*(vec-bins(8))/(bins(9)-bins(8)) .7*(vec-bins(8))/(bins(9)-bins(8))]; % red -> pink
    elseif vec>=bins(9) && vec <bins(10); % [1.0 0.7 0.7] pink bins(9)-bins(10)
        vRGB=[1-.4*(vec-bins(9))/(bins(10)-bins(9)) .7-.7*(vec-bins(9))/(bins(10)-bins(9)) .7-.4*(vec-bins(9))/(bins(10)-bins(9))]; % red ->
pink
    elseif vec > bins(10);
        vRGB = [.6 0.0 .2]; % [0.6 0.0 .3] mauve bins(9)
    end
plot(maxx/100*[gbnnum-1; gbnnum],[0.06*maxy; 0.06*maxy],[Linewidth',wid,'color',vRGB); % place color key x coordinate at suitable place...
end
bins = binsdat; % replacing the necessary bins parameters for plotting along grain boundaries
for gbnnum = 1:1:dRBdy(1,1); % Plot parameter values on grain boundaries
    if RBdy(gbnnum,13) > 0 && RBdy(gbnnum,14) > 0 && RBdy(gbnnum,13) <= grmax && RBdy(gbnnum,14) <= grmax
        % wid = (RBdy(iGB,16)-.95*minF1m)/(maxF1m-minF1m)*4;
        wid = 2;
        if damp(plnx,gbnnum) > bins(9)
            wid = 4;
        elseif damp(plnx,gbnnum) > bins(8)
            wid = 3;
        end
        kind = damp(1,gbnnum); jind = damp(1,gbnnum);
        kss = mpr(kind,1,gbnnum); jss = mpr(1,jind,gbnnum);
        if one_ss == 1 && kss < 7 && jss < 7
            linetype = '-.'; % dotted lines for hexagonal slip systems of basal and/or prism
        elseif one_ss == 1 && kss < 7 || one_ss == 1 && jss < 7
            linetype = '-.-.'; % dot dash lines for hexagonal slip systems if one ss is basal or prism
        else
            linetype = '-';
        end

        vec = damp(plnx,gbnnum);
        if vec<bins(1); % [0.3 0.3 0.3] gray 0-10
            vRGB=[.3+.5*vec/bins(1) .3-.3*vec/bins(1) .3+.5*vec/bins(1)]; % gray -> purple
        elseif vec>=bins(1) && vec <bins(2); % [0.8 0.8 0.8] purple 10-20
            vRGB=[.8-.8*(vec-bins(1))/(bins(2)-bins(1)) 0 .8-.1*(vec-bins(1))/(bins(2)-bins(1))]; % purple -> blue
        elseif vec>=bins(2) && vec <bins(3); % [0.0 0.7 0.7] blue 20-30

```

```

vRGB=[0. .9*(vec-bins(2))/(bins(3)-bins(2)) .7+.2*(vec-bins(2))/(bins(3)-bins(2))]; % blue -> turquoise
elseif vec>=bins(3) && vec <bins(4); % [0.9 .9] turquoise 30-40
vRGB=[.1*(vec-bins(3))/(bins(4)-bins(3)) .9-.4*(vec-bins(3))/(bins(4)-bins(3)) .9-.8*(vec-bins(3))/(bins(4)-bins(3))]; % turquoise ->
dk grn
elseif vec>=bins(4) && vec <bins(5); % [1.5 .0] dk grn 40-50
vRGB=[.1+.1*(vec-bins(4))/(bins(5)-bins(4)) .5+.4*(vec-bins(4))/(bins(5)-bins(4)) 0.]; % dk grn -> green
elseif vec>=bins(5) && vec <bins(6); % [2.9 .0] green 50-60
vRGB=[.2+.7*(vec-bins(5))/(bins(6)-bins(5)) .9 0.]; % green -> yellow
elseif vec>=bins(6) && vec <bins(7); % [9.9 .0] yellow 60-70
vRGB=[.9 .9-.3*(vec-bins(6))/(bins(7)-bins(6)) 0.]; % yellow -> orange
elseif vec>=bins(7) && vec <bins(8); % [9.6 .0] orange 70-80
vRGB=[.9+.1*(vec-bins(7))/(bins(8)-bins(7)) .6-.6*(vec-bins(7))/(bins(8)-bins(7)) 0.]; % orange -> red
elseif vec>=bins(8) && vec <bins(9); % [1.0 .0] red 80-90
vRGB=[1. .7*(vec-bins(8))/(bins(9)-bins(8)) .7*(vec-bins(8))/(bins(9)-bins(8))]; % red -> pink
elseif vec>=bins(9) && vec <bins(10); % [1.7 .7] pink bins(9)-bins(10)
vRGB=[1.-.4*(vec-bins(9))/(bins(10)-bins(9)) .7-.7*(vec-bins(9))/(bins(10)-bins(9)) .7-.4*(vec-bins(9))/(bins(10)-bins(9))]; % red ->
pink
elseif vec > bins(10);
vRGB = [.6 0. .2]; % [6 0.4] mauve bins(9)
end
plot([RBdy(gbnum,9);RBdy(gbnum,11)],[-RBdy(gbnum,10);-RBdy(gbnum,12)],linetype,'Linewidth',wid,'color',vRGB);
end
end
end % k for plist
set(gca,'FontSize',chsize);
xlabel('Position, microns');
ylabel('Position, microns');

%% plot grain numbers
chsize = 14;

for ng = 1:1:grmax
if grcen(ng,1) == 1 || grcen(ng,1) == 4
text(grcen(ng,2),-grcen(ng,3),int2str(ng),'color',[0 .5 1], 'FontWeight', 'bold','FontSize',chsize); % [ng grcen(ng,4:6)]
elseif grcen(ng,1) == 2
text(grcen(ng,2),-grcen(ng,3),int2str(ng),'color',[0 .5 0], 'FontWeight', 'bold','FontSize',chsize);
elseif grcen(ng,1) == 3
text(grcen(ng,2),-grcen(ng,3),int2str(ng),'color',[.8 0 0], 'FontWeight', 'bold','FontSize',chsize);
end
end

%% plot gb numbers

for gbnum = 1:1:dRBdy % plot grain boundary numbers
if RBdy(gbnum,13) > 0 && RBdy(gbnum,14) > 0 && RBdy(gbnum,13) <= grmax && RBdy(gbnum,14) <= grmax
text((2*RBdy(gbnum,9)+RBdy(gbnum,11))/3,-(2*RBdy(gbnum,10)+RBdy(gbnum,12))/3,...
int2str(gbnum), 'color',[0 0 .5], 'FontWeight', 'light','FontSize',chsize);
end
end

%% Plot of rotated grain around grain 1... (for single intial grain pair with file of rotated orientations)
clear m1; clear m2; clear m3; symbsize = 15;
colorvec = [0 .2 .7 ; 1 0 0 ; 1 .8 0 ; .7 0 .6 ; 0 .8 0 ; 0 1 1 ; .6 0 .2 ; 0 0 1 ; 1 .4 0 ];
for ii = 1:1:360
m1(ii,:) = mpr(3,3,ii) ;
m2(ii,:) = [mpr(3,4,ii) mpr(4,4,ii) mpr(4,3,ii) ];
m3(ii,:) = [mpr(3,5,ii) mpr(4,5,ii) mpr(5,5,ii) mpr(5,4,ii) mpr(5,3,ii) ];

m1s(ii,:) = round( symbsize * mpr(3,2,ii) * mpr(2,3,ii) + 1 ) ;

m2s(ii,:) = [round( symbsize*1.3 * mpr(3,2,ii) * mpr(2,4,ii) + 1 ) ...
round( symbsize*1.0 * mpr(4,2,ii) * mpr(2,4,ii) + 1 ) ...
round( symbsize*0.7 * mpr(4,2,ii) * mpr(2,3,ii) + 1 ) ];

m3s(ii,:) = [round( symbsize*1.3 * mpr(3,2,ii) * mpr(2,5,ii) + 1 ) ...
round( symbsize*1.3 * mpr(4,2,ii) * mpr(2,5,ii) + 1 ) ...
round( symbsize*1.0 * mpr(5,2,ii) * mpr(2,5,ii) + 1 ) ...
round( symbsize*0.7 * mpr(5,2,ii) * mpr(2,4,ii) + 1 ) ...
round( symbsize*0.7 * mpr(5,2,ii) * mpr(2,3,ii) + 1 ) ];

```

```

end
f = figure('Position', [0,0,800,600]); movegui(f,'northwest'); set(gcf, 'Color', [1 1 1]); hold on;

plot(m1,'LineWidth',3)
plot(m2,'-','LineWidth', 2)
plot(m3,':','LineWidth', 2)
legend('mp11', 'mp12', 'mp22', 'mp21', 'mp13', 'mp23', 'mp33', 'mp32', 'mp31', 'Location','southwest' );
ylabel('m prime value');
xlabel( [mat2str(grcen(1,4:6)) ' rotation incremented about Z axis of ' mat2str(grcen(2,4:6))] );
hold off;

f = figure('Position', [0,0,800,600]); movegui(f,'northwest'); set(gcf, 'Color', [1 1 1]); hold on;

for ii = 1:1:360
    plot(ii, m1(ii,1),'+', 'MarkerSize', m1s(ii,1), 'color',colorvec(1,:));
    for jj = 1:1:3
        plot(ii, m2(ii,jj),'o', 'MarkerSize', m2s(ii,jj), 'color',colorvec(jj+1,:));
    end
    for jj = 1:1:5
        plot(ii, m3(ii,jj),'^', 'MarkerSize', m3s(ii,jj), 'color',colorvec(jj+4,:));
    end
end
legend('mp11', 'mp12', 'mp22', 'mp21', 'mp13', 'mp23', 'mp33', 'mp32', 'mp31', 'Location','southwest' );
ylabel('m prime value (size = sum of SF)');
xlabel( [mat2str(grcen(1,4:6)) ' rotation incremented about Z axis of ' mat2str(grcen(2,4:6))] );
hold off;

%% Choose your favorite grain boundary -----

gbrnum = 276
mpr_cur = mpr(:,gbrnum); rbvm_cur = rbvm(:,gbrnum); rbvec_cur = rbvec(:,gbrnum); mplimit = .6
whiteannotation = 1; % make gb trace and axes white
ptpl = 1; % plots plane traces if = 1 Red dashed line in plot is perpendicular to the line connecting the centers of the two grains
prsxplt = zeros(8,7); % Black solid line in plot is the RC boundary segment orientation
prsyplt = zeros(8,7); % 13 and 14 lead to misplaced plane traces.
prszplt = zeros(8,7);
clear Sflist; clear sortSflist;
mp4gr = himp4(:,gbrnum);
sorthimp4 = sortrows(mp4gr,-4); % This sorts on basis of actual m' value
mplimit = min(mplimit, sorthimp4(1,4));
gbcen = [RBdy(gbrnum,11)+RBdy(gbrnum,9) RBdy(gbrnum,12)+RBdy(gbrnum,10)]/2;
v13cpes = [grcen(RBdy(gbrnum,13),2) grcen(RBdy(gbrnum,13),3)] - gbcen; % find vector from center of GB to grain center in raster coordinates
v14cpes = [grcen(RBdy(gbrnum,14),2) grcen(RBdy(gbrnum,14),3)] - gbcen;
v1314b = [(RBdy(gbrnum,12)-RBdy(gbrnum,10)) -(RBdy(gbrnum,11)-RBdy(gbrnum,9)) ]; % vector [dy,-dx] pointing perpendicular to GB
if v13cpes * v1314b < 0
    v1314b = -v1314b;
end
v1314bn = v1314b/norm(v1314b) % find unit vector pointing perpendicular to GB in raster coords

plabel = ['Sfthr k j : ' num2str(Sfthr,3) ' ' num2str(damp(23,gbrnum),2) ' ' num2str(damp(24,gbrnum),2) ' t3mpthr ' num2str(damp(22,gbrnum),3)];
g_gb_g = [num2str(RBdy(gbrnum,13)) ' ' mat2str(grcen(RBdy(gbrnum,13),7:9),4) ' ' num2str(gbrnum) ' ' mat2str(grcen(RBdy(gbrnum,14),7:9),4) ' '
num2str(RBdy(gbrnum,14)) ];
ipl = -6; imp = 0; % Strategy: Next, start isc loop for plotting slip systems
while sorthimp4(imp+1,4) >= mplimit
    imp = imp + 1;

    if sorthimp4(imp,1) ~ = 0 % evaluate only for recorded values (m'>.6)
        if ipl-imp== -7 % six plots on a page
            f = figure('Position', [0,0,1200,750]); movegui(f,'northwest'); set(gcf, 'Color', [1 1 1]); hold on;
            ipl=ipl+6;
        end
        subplot(2,3,imp-ipl); hold on; set(gcf, 'Color', [1 1 1]);
        if whiteannotation == 1
            set(gca, 'ycolor', 'w'); set(gca, 'xcolor', 'w'); % make axes white for ease in later arranging.
        else
            plot([0 1.5*cosd(RBdy(gbrnum,8))], [0 1.5*sind(RBdy(gbrnum,8))], '-k'); % plots gb from map from angle given in normal x-y space
        end
        Sfsum = 0;
        kind = sorthimp4(imp,1)+2; jind = sorthimp4(imp,2)+2;
        kss = mpr(kind,1,gbrnum); jss = mpr(1,jind,gbrnum);
    end
end

```

```

for igr = 13:1:14 % 1 i.e. first for the left grain in column 13, then the right grain in column 14 in checked Reconstructed Boundary file.
    grnum = RBdy(gbnum,igr);
    issr = sorthimp4(imp,igr-12); % ss rank # in gr13 issr is slip system Schmid factor order #
    if igr == 13
        del = v1314bn;
        cellcolor = [0 0 0]; % [.3 0 .5];          plot ([0 del(1)], -[0 del(2)])
    else % del is position vector from center of gb to 13 in raster coord system (ydown)
        del = -v1314bn;
        cellcolor = [0 0 0]; % [0.5 0 0];          plot ([0 del(1)], -[0 del(2)])
    end

% Plot the image of hexagonal unit cell, slip vectors, planes, plane normals, and plane traces
% Strategy: First extract useful vectors to draw the hexagonal prisms from slip system information
% positions in mvns p1:13-15 p2:16-18 p3:19-21 p4:22-24 p5:25-27 p6:28-30
% positions in hpln p1:4-6 p2:7-9 p3:10-12 p4:13-15 p5:16-18 p6:18-21
    for isc = 1:1:nslphex
        if sortmv(isc,1,grnum) == 1; % locate basal planes using SS1
            hpln(1,4:21) = sortmv(isc,13:30,grnum); % bottom basal plane
            hpln(2,4:21) = sortmv(isc,13:30,grnum); % top basal plane
            rotc = sortmv(isc,4:6,grnum)*c_a_hex; % basal plane normal * c/a
            for j = 4:3:19
                hpln(2,j:j+2) = hpln(1,j:j+2) + rotc; % move top plane up by a unit of c
            end
            a1 = sortmv(isc,7:9,grnum); % locate a1 using SS1
        elseif sortmv(isc,1,grnum) == 2;
            a2 = sortmv(isc,7:9,grnum); % locate a2 using SS2
        elseif sortmv(isc,1,grnum) == 3;
            a3 = sortmv(isc,7:9,grnum); % locate a3 using SS3
        end
    end
    for isc = 1:1:nslphex
        if sortmv(isc,1,grnum) == 4; % locate two prism planes on opposite sides using SS4
            hpln(3,4:21) = sortmv(isc,13:30,grnum);
            for j = 13:3:28
                hpln(4,j-9:j-7) = sortmv(isc,j:j+2,grnum) + a2 - a3;
            end
        elseif sortmv(isc,1,grnum) == 5; % locate two prism planes on opposite sides using SS5
            hpln(5,4:21) = sortmv(isc,13:30,grnum);
            for j = 13:3:28
                hpln(6,j-9:j-7) = sortmv(isc,j:j+2,grnum) + a3 - a1;
            end
        elseif sortmv(isc,1,grnum) == 6; % locate two prism planes on opposite sides using SS6
            hpln(7,4:21) = sortmv(isc,13:30,grnum);
            for j = 13:3:28
                hpln(8,j-9:j-7) = sortmv(isc,j:j+2,grnum) + a1 - a2;
            end
        end
    end

    for j = 1:1:2 % Find z elevation of basal planes
        for k = 1:1:3
            hpln(j,k) = (hpln(j,3+k)+hpln(j,6+k)+hpln(j,9+k)+hpln(j,12+k)+hpln(j,15+k)+hpln(j,18+k))/6;
        end
    end
    center = (hpln(1,1:3)+hpln(2,1:3))/2;
    for j = 3:1:8 % Find z elevation of prism planes
        hpln(j,3) = (hpln(j,12)+hpln(j,15)+hpln(j,18)+hpln(j,21))/4;
    end
    sortpln = sortrows(hpln,-3);

    minx = 0; miny = 0; minz = 0; maxx = 0; maxy = 0; maxz = 0;
    for j = 1:1:8 % assemble vectors for plotting faces of hex prism
        prsxplt(j,1:7) = [sortpln(j,4) sortpln(j,7) sortpln(j,10) sortpln(j,13) sortpln(j,16) sortpln(j,19) sortpln(j,4)];
        minx = min(minx,min(prsxplt(j,:))); maxx = max(maxx,max(prsxplt(j,:)));
        prsyplt(j,1:7) = [sortpln(j,5) sortpln(j,8) sortpln(j,11) sortpln(j,14) sortpln(j,17) sortpln(j,20) sortpln(j,5)];
        miny = min(miny,min(prsyplt(j,:))); maxy = max(maxy,max(prsyplt(j,:)));
        prszplt(j,1:7) = [sortpln(j,6) sortpln(j,9) sortpln(j,12) sortpln(j,15) sortpln(j,18) sortpln(j,21) sortpln(j,6)];
        minz = min(minz,min(prszplt(j,:))); maxz = max(maxz,max(prszplt(j,:)));
    end
end

```

```

sp1 = sortmv(issr,13:15,grnum);    % identify plotted points on the slip plane
sp2 = sortmv(issr,16:18,grnum);
sp3 = sortmv(issr,19:21,grnum);
sp4 = sortmv(issr,22:24,grnum);
sp5 = sortmv(issr,25:27,grnum);
sp6 = sortmv(issr,28:30,grnum);
spx = [sp1(1) sp2(1) sp3(1) sp4(1) sp5(1) sp6(1) sp1(1)];
spy = [sp1(2) sp2(2) sp3(2) sp4(2) sp5(2) sp6(2) sp1(2)];
ssn = sortmv(issr,1,grnum);      % slip system number
Sf = sortmv(issr,2,grnum);      % Schmid factor
Sfsum = Sfsum + abs(Sf);
n = [0 0 0 sortmv(issr,4:6,grnum)]; % plane normal
b = [sp1 sp4]; % p1+sortmv(issr,7:9,grnum)]; % Burgers vector
pt = sortmv(issr,10:12,grnum);  % plane trace
midx = (minx+maxx)/2;
midy = (miny+maxy)/2;
cellcenter = [midx midy];
dx =(1.6*del(2) - cellcenter(1)); % del is raster, cellcenter is TSL coords
dy =(1.6*del(1) - cellcenter(2)); % so not dy = del(2) - cellcenter(2);
[dx dy]; % diagnostic

% These plots will match TSL with X down !!!! Plotting starts
if green(grnum,5) < 90 % if PHI < 90, then make the 3 coordinate axes visible below slip planes
plot([0 a1(2)]+dy,-([0 a1(1)]+dx), 'r', 'Linewidth',3,'Color',[1 0 .2]);% plot x = red
plot([0 a2(2)]+dy,-([0 a2(1)]+dx), 'g', 'Linewidth',3,'Color',[.6 .8 0]);% plot y = green-gold
plot([0 a3(2)]+dy,-([0 a3(1)]+dx), 'b', 'Linewidth',3,'Color',[0 0 1]);% plot z = blue
end

if sortmv(issr,6,grnum)>0 % is k component of slip plane normal positive or negative?
fill(spy+dy,-(spx+dx), [.8 .8 .65]) % slip plane filled warm gray
% plot([n(2) n(5)], -[n(1) n(4)], 'Linewidth',3,'Color',[.8 .8 .65]);
else % slip plane filled cool gray if normal has neg z component
fill(spy+dy,-(spx+dx), [.65 .65 .7])
% plot([n(2) n(5)], -[n(1) n(4)], 'Linewidth',3,'Color',[.65 .65 .7]);
end
if sortmv(issr,6,grnum)>0
Bvcolor = [0 .7 .7];
if ssn >= iC1
Bvcolor = [1 .6 0];
end
if ssn >= iT1 && ssn <= fT2
Bvcolor = [1 .6 0];
end
else
Bvcolor = [0 1 1];
if ssn >= iC1
Bvcolor = [.3 .9 0];
end
if ssn >= iT1 && ssn <= fT2
Bvcolor = [1 .8 0];
end
end
Sfs = 1;
if ssn < iT1
Sfs = sign(Sf);
end
if Sf > 0 % plot Burgers vector direction
if ssn >= iT1 % this is for twins - the Burgers vector length is shown to be 1/2 of the usual length in the unit cell
plot(b(2)+dy,-(b(1)+dx), 'r', 'MarkerSize', 24, 'Color', Bvcolor)
plot([b(2) (b(2)+b(5))/2]+dy,-([b(1) (b(1)+b(4))/2]+dx), 'Linewidth',4,'Color',Bvcolor)
else
plot(b(2)+dy,-(b(1)+dx), 'r', 'MarkerSize', 24, 'Color', Bvcolor)
plot([b(2) b(5)]+dy,-([b(1) b(4)]+dx), 'Linewidth',4,'Color',Bvcolor)
end
else % plot Burgers vector in opposite direction
if ssn >= iT1 % this is for twins - the Burgers vector length is shown to be 1/2 of the usual length in the unit cell
plot(b(2)+dy,-(b(1)+dx), 'r', 'MarkerSize', 24, 'Color', Bvcolor)
plot([b(2) (2*b(2)+b(5))/3]+dy,-([b(1) (2*b(1)+b(4))/3]+dx), 'Linewidth',4,'Color',Bvcolor)
else
plot(b(5)+dy,-(b(4)+dx), 'r', 'MarkerSize', 24, 'Color', Bvcolor)
end
end

```

```

        plot([b(5) b(2)]+dy,-([b(4) b(1)]+dx),'Linewidth',4,'Color',Bvcolor)
    end
end

for j = 1:1:4 % plot the 4 top most surface prisms of the hex cell that have the highest z elevation
    plot(prsyplt(j:)+dy,-(prxpplt(j:)+dx), 'Linewidth', 2, 'Color', cellcolor);
end
if green(grnum,5) > 90 % if PHI < 90, make the 3 coordinate axes visible above slip planes
    plot([0 a1(2)]+dy,-([0 a1(1)]+dx), '-', 'Linewidth',3,'Color',[1 0 .2]);% plot x = red
    plot([0 a2(2)]+dy,-([0 a2(1)]+dx), '-', 'Linewidth',3,'Color',[.6 .8 0]);% plot y = green-gold
    plot([0 a3(2)]+dy,-([0 a3(1)]+dx), '-', 'Linewidth',3,'Color',[0 0 1]);% plot z = blue
end
if ptpl == 1
    if ssn >= iC1
        ptrcolor = [.2 .8 0]; % compression twin plane traces green
    elseif ssn >= iT1 && ssn <= fT2
        ptrcolor = [1 .6 0]; % extension twin plane traces orange
    elseif ssn > ipyr && ssn <= f2pyrc
        ptrcolor = [.95 .85 0]; % <c+a> plane traces green-gold
    elseif ssn <= fpyra && ssn >= ipyra
        ptrcolor = [0 .9 .5]; % pyr <a> green-blue
    elseif ssn <= f2prs && ssn >= iprs
        ptrcolor = [1 .2 0]; % prism <a,aa> red
    else
        ptrcolor = [0 0 1]; % basal <a> blue
    end
    %----> NOTE that Schmid factor vector is plotted in correct direction,
    plot([-pt(2) pt(2)]+dy, -([-pt(1) pt(1)]+dx),'--','Linewidth',3,'Color',ptrcolor)
end

if igr == 13
    line1 = ['L g' num2str(grnum) ' m' num2str(issr) ' = ' num2str(Sfs*Sf, 2) ' ss' num2str(ssn)...
            ' n' mat2str(sshex(1,,:),ssn) mat2str(Sfs*sshex(2,,:),ssn) ' b'];
    Sflist(imp,1:3) = [grnum ssn Sf];
end
if igr == 14
    title([line1] [' R g' num2str(grnum) ' m' num2str(issr) ' = ' num2str(Sfs*Sf, 2) ' ss' num2str(ssn)...
                ' n' mat2str(sshex(1,,:),ssn) mat2str(Sfs*sshex(2,,:),ssn) ' b'] [g_gb_g] [plabel ' m' = ' , num2str(sorthimp4(imp,4),3)]...
            ['rBvec = ' mat2str(rbvec(kind, :jind,gbnum),3) 'mag = ' num2str(rbvm_cur(kind,jind),3)] );
    Sflist(imp,4:6) = [grnum ssn Sf];
end
end % graincen for cubic or hex if (has middle else)
end % igr - grains 13 and 14

rbvgry = [max(0,1-rbvm_cur(kind,jind)) 0 0]%; / max(max((rbvm_cur)));
plot(0, 0, 'k+'); % gray scale of residual Burgers vector
plot([0 rbvec(kind,2,jind,gbnum)]*2, -[0 rbvec(kind,1,jind,gbnum)]*2, '-', 'Color', rbvgry, 'LineWidth', 2);
axis square;
axis([-3 3 -3 3]*1.5*(1.4-Sfsum)); % plot representation of grain boundary 1.2 for cubic, 1.4 for hex
Sflist(imp,7:9) = [imp Sfsum sorthimp4(imp,4)];
else
    fprintf('No slip system has Schmid factors > %4.2f for one of the two grains at GB %d %d\n', Sfthr, gbnum, imp)
end % if statement for continuing the loop for non-zero himp4 values
end % imp m' loop
sortSflist = sortrows(Sflist,-8); sortSfsize = size(sortSflist);

```

## APPENDIX C: Sample reconstructed boundary and grain files

### Sample reconstructed boundary file

# Header: Project1::post scan rotated cleaned cropped::All data::Grain Size 2/12/2020

#

# Column 1-3: right hand average orientation (phi1, PHI, phi2 in radians)

# Column 4-6: left hand average orientation (phi1, PHI, phi2 in radians)

# Column 7: Misorientation Angle

# Column 8-10: Misorientation Axis in Right Hand grain

# Column 11-13: Misorientation Axis in Left Hand grain

# Column 14: length (in microns)

# Column 15: trace angle (in degrees)

# Column 16-19: x,y coordinates of endpoints (in microns)

# Column 20-21: IDs of right hand and left hand grains

1.367	1.287	4.784	0.863	1.274	5.234	32.52	-18	14	-11	-18	14	-11	18.009	23.6	0.00	49.07	16.50	41.86	27	1
1.367	1.287	4.784	0.863	1.274	5.234	32.52	-18	14	-11	-18	14	-11	14.503	178.9	16.50	41.86	31.00	42.15	27	1
1.367	1.287	4.784	0.284	0.699	0.128	59.88	-9	14	1	-9	14	1	23.116	5.7	0.00	73.90	23.00	71.59	27	43
4.068	0.194	2.325	0.284	0.699	0.128	51.35	-11	4	-3	-11	4	-3	19.218	8.6	0.00	142.61	19.00	139.72	76	43
0.339	1.343	5.643	4.068	0.194	2.325	90.01	28	-1	-8	28	-1	-8	11.846	32.4	0.00	182.44	10.00	176.09	96	76
0.339	1.343	5.643	0.394	1.268	5.600	5.47	24	-11	7	24	-11	7	2.887	90.0	0.00	196.88	0.00	199.76	96	112

## Sample of grain file

# Header: Project1::post scan rotated cleaned cropped::All data::Grain Size 2/12/2020

#

# Partition Formula:

# Grain Tolerance Angle: 5.00

# Minimum Grain Size: 2

# Minimum Confidence Index: 0.00

# Multiple Rows Requirement: Off

# Column 1: Integer identifying grain

# Column 2-4: Average orientation (phi1, PHI, phi2) in degrees

# Column 5-6: Average Position (x, y) in microns

# Column 7: Average Image Quality (IQ)

# Column 8: Average Confidence Index (CI)

# Column 9: Average Fit (degrees)

# Column 10: An integer identifying the phase

# 1 - Titanium (Alpha)

# 2 - Titanium (Beta)

# Column 11: Edge grain (1) or interior grain (0)

1	49.464	72.992	299.89	18.911	20.765	234.9	0.470	0.80	1	1
2	105.059	4.763	247.52	54.452	3.723	216.5	0.623	1.06	1	1
3	199.783	57.925	157.96	81.238	12.249	176.8	0.539	1.18	1	1
4	190.524	86.037	166.98	93.086	3.490	222.9	0.515	1.05	1	1
5	59.181	67.583	287.44	108.472	27.021	183.5	0.497	0.93	1	1
6	138.098	80.576	209.67	129.297	6.448	303.9	0.565	0.94	1	1

## **BIBLIOGRAPHY**

## BIBLIOGRAPHY

Abuzaid W.Z, Sehitoglu H., Lambros J., 2016, Localisation of plastic strain at the microstructural level in Hastelloy X subjected to monotonic, fatigue, and creep loading: the role of grain boundaries and slip transmission, *Materials at High Temperatures*, Vol. 33 No. 4-5, pp. 384-400.

Alizadeh R., Peña-Ortega M., Bieler T.R., LLorca J., 2020, A criterion for slip transfer at grain boundaries in Al, *Scripta Materialia*, Vol. 178, pp. 408-412.

Aluminum 1100-O. Matweb.com, N.p, 2020, Web. 2 July 2020.

Bayerschen E., McBride A.T., Reddy B.D., Böhlke T., 2016, Review on slip transmission criteria in experiments and crystal plasticity models, *Material Science*, Vol. 52, pp. 2243-2258

Boyer R., 1996, An overview on the use of titanium in the aerospace industry, *Materials Science*

Bridier F., Villechaise P., and Mendez J., 2005, Analysis of the different slip systems activated by tension in a  $\alpha/\beta$  titanium alloy in relation with local crystallographic orientation, *Acta Materialia*, Vol. 53, No. 3, pp. 555-567.

Britton T.J., Wilkinson A.J., 2012, Stress fields and geometrically necessary dislocation density distributions near the head of a blocked slip band, *Acta Materialia*, Vol. 60, pp. 5773-5782.

Buchheit T.E., Carroll J.D., Clark B.G., Boyce B.L., 2015, Evaluating Deformation Induced Grain Orientation Change in a Polycrystal During In Situ Tensile Deformation using EBSD, *Microscopy and Microanalysis*, Vol. 21, pp. 969-984.

Ding R., Gong J., Wilkinson A.J., Jones I.P., 2015, A study of dislocation transmission through a grain boundary in hcp Ti-6Al using micro-cantilevers, *Acta Materialia*, Vol. 103, pp. 416-423.

Hémery S., Tromas C., Villechaise P., 2019, Slip-stimulated grain boundary sliding in Ti-6Al-4 V at room temperature, *Materialia*, Vol. 000, pp.100-189.

Li H., 2013, Analysis of the deformation behavior of the hexagonal close-packed alpha phase in titanium and titanium alloys [Doctor dissertation, Michigan State University].

Hull D., Bacon D.J., 2011, Introduction to dislocations, Fifth edition, Oxford, Butterworth-Heinemann.

Jackson A.G., 1991, Chapter 7: Slip Systems, Handbook of crystallography: for electron microscopists and others, pp.83-88.

Kacher J., Robertson I.M., 2014, In situ and tomographic analysis of dislocation/grain boundary interactions in  $\alpha$ -titanium, Philosophical Magazine, Vol. 94, No. 8, 814-829.

Kocks U.F., Tomé C.N., Wenk H.-R., 1998, Texture and Anisotropy, Cambridge, United Kingdom, Cambridge University Press and Engineering A, Vol. 213, No. 1-2, pp. 103-114.

Lee T.C., Robertson I.M., Birnbaum H.K., 1989, Prediction of slip transfer mechanisms across grain boundaries, Metallurgica, Vol. 23, pp. 799-803.

Li H., 2013, Analysis of the deformation behavior of the hexagonal close-packed alpha phase in titanium and titanium alloys, Michigan State University, PhD dissertation.

Linne M., Bieler T.R., Daly S., 2020, The Impact of Microstructure on the Relationship between Grain Boundary Sliding and Slip Transmission in High Purity Aluminum.

Luster J., Morris M.A., 1994, Compatibility of deformation in Two-Phase Ti-Al Alloys: Dependence on microstructure and orientation relationships, Metallurgical and Materials Transactions A, Vol. 26A, pp. 1745- 1756.

Matsuki K., Morita H., Yamada M., Murakami Y., 2013, Relative motion of grains during superplastic flow in an Al-9Zn-1 wt.% Mg alloy, Metal Science, Vol. 11, No. 5, pp. 156-163.

Palomares-García A.J., Pérez-Prado M.T., Molina-Aldareguia J.M., 2018, Slip transfer across c-TiAl lamellae in tension, Materials and Design, Vol. 146, pp. 81-95.

Peters M., Kumpfert J., Ward C.H., and Leyens, C., 2003, Titanium alloys for aerospace applications, Advanced Engineering Materials, Vol. 5, No. 6, pp. 419-427.

Sutton G., Biblarz O., 2017. Rocket Propulsion Elements, Ninth Edition, Ch. 10.

T.C. Lee, I.M. Robertson and H.K. Birnbaum, Prediction of Slip Transfer Mechanisms Across Grain Boundaries, Scripta Metall. 23, 799-803, 1989.

Ti-6Al-4V (Grade 5), Annealed. Matweb.com, N.p, 2020, Web. 2 July 2020.

Z. Shen, R. H. Wagoner and W. A. T. Clark, Dislocation and Grain Boundary Interactions In Metals, Acta metall. 36(12) 3231-3242, 1988.